ANTIBODIES IN CANCER THERAPY: NEW TARGETS, APPLICATIONS AND COMBINATION STRATEGIES

A Thesis

SUBMITTED TO THE FACULTY OF

UNIVERSITY OF MINNESOTA

BY

Vidhi Devendra Khanna

IN PARTIAL FULFILLMENT OF THE REQUIREMENTS

FOR THE DEGREE OF

DOCTOR OF PHILOSOPHY

Jayanth Panyam

Advisor

July, 2019

Acknowledgements

Five years in graduate school could not have gone by without the contributions of people surrounding me. I take this opportunity to thank them because none of this would be possible without each and every one of them. First, of course Dr. Jayanth Panyam - for his guidance, his encouragement and his unwavering confidence in me. I have yet to meet a more patient and understanding person as him.

My parents, my grandparents and Archit, for their constant love and support. This would have been a much harder journey without their daily words of encouragement. Thank you to Malhar, for believing in me when I didn't and because five years is a long time.

I am also extremely thankful to the Department of Pharmaceutics. Specifically, Katie James and Amanda Hokanson, for taking care of everything outside the lab. I still maintain that they have magical powers much beyond our understanding. Dr. William Elmquist, for being a ray of sunshine on a rainy day. My thesis committee for their time and input in my work.

I would like to thank past and present members of the Panyam lab, specifically Stephen Kalscheuer, Ameya Kirtane and Hyunjoon Kim - for teaching me everything I know in the lab, your patience and enthusiasm for science were a constant source of motivation for me. Ping Wang and Wenqui Zhang contributed a lot of their time and effort

to help me with my work and I could not be more grateful. I also want to thank Buddhadev Layek, for his ever-smiling nature and for having an answer to everything.

I am grateful that I had the chance to work with so many of Dr. Panyam's collaborators including: Dr. Da Yang, Dr. Wei-Zen Wei, Dr. Deepali Sachdev, Dr. David Ferguson and Dr. Markovic Svetomir. The core facilities at UMN have also been a constant source of information and much of our research would not be possible without them. Special thanks to Guillermo Marques at the University Imaging Centre, Brenda Koniar and Janae Diamond at RAR, Katalin Kovacs and Paula Overn at the Comparative Pathology Shared Resource, the flow cytometry core, the cytokine reference lab and Jim Fisher.

Finally, thank you to my friends – Neha, Bhatia, Ruia, Dhwani, Annapoorna, PD, Yuthika, Janu, Rachit, Surabhi, Darshini, Sonia, Kelsey and Navpreet – for always reminding me of life outside the lab.

Dedication

This thesis is dedicated to my parents, Aarti Khanna and Devendra Khanna, for their unconditional love and support.

Abstract

Over the last decade, antibodies have become an important component in the arsenal of cancer therapeutics. Their high-specificity, low-off target effects, desirable pharmacokinetics and high success rate are a few of the many attributes that make them amenable for development as drugs. The work presented here explores the targeting, mechanisms and use of antibody-based cancer therapy.

In the first chapter, we used a phage display-based cell panning procedure to develop two fully humanized antibodies, Tw1S4_6 and Tw1S4_AM6, that bind specifically to HSPG2/perlecan, a protein found to be overexpressed on tumor cells. Immunohistochemistry studies revealed high HSPG2 expression across various tumor sub-types including melanoma, bladder cancer, glioblastoma and ovarian cancer. There was significant correlation between high HSPG2 expression and poor survival in triple negative breast cancer, bladder and ovarian cancers. The data presented here points towards the relevance of HSPG2 as a novel target for not only triple negative breast cancer but other malignancies as well.

Based on its overexpression in different solid tumors, we evaluated HSPG2 as a therapeutic target in the second chapter. We observed significant tumor growth inhibition with Tw1S4_AM6 in the triple negative MDA-MB-231-LM2 breast cancer xenograft model. This efficacy was reduced in NSG mice, suggesting NK cell-mediated antibody dependent cellular cytotoxicity (ADCC) as a potential mechanism of action. *In vitro* studies

using human PBMCs confirmed induction of ADCC with anti-HSPG2 antibodies. In addition, conjugation of Tw1S4_AM6 on the surface of polymeric nanoparticles enabled increased tumor cell uptake of nanoparticles, suggesting Tw1S4_AM6 could be valuable as a targeting ligand for drug delivery systems.

There is a significant interest in designing therapeutic agents that can enhance ADCC and thereby improve clinical responses with approved antibodies. We have developed a suite of highly substituted imidazoquinolines, which activate TLR 7 and/or 8 and induce significantly higher levels of cytokines compared to the FDA-approved TLR7 agonist, imiquimod. In the third chapter, we evaluated our series of TLR7/8 agonists for their ability to improve ADCC. Our studies show that the second generation TLR 7/8 agonists induce robust pro-inflammatory cytokine secretion and activate NK cells. These agonists also enhanced ADCC *in vitro*. Finally, we found that these agonists significantly improved the anticancer efficacy of two monoclonal antibodies *in vivo.*

Thus, the work presented here encompasses the three critical aspects of antibody therapeutics: identifying the target, understanding their mechanisms, and leveraging these mechanisms to improve their efficacy.

Table of Contents

List of Figures

List of Abbreviations

522GGNPs	522-loaded, gas-generating PLGA nanoparticles
ADC	Antibody drug conjugate
ADCC	Antibody-dependent cellular cytotoxicity
ADCP	Antibody-dependent cellular phagocytosis
ANOVA	Analysis of variance
bFGF	Basic fibroblast growth factor
BM	Basement membrane
BSA	Bovine serum albumin
CD	Cluster of differentiation
CDC	Complement-dependent cytotoxicity
CDR	Complementarity determining region
C_{H1}, $C_{H3,}$ C_{H3}	Heavy chain constant domains 1, 2 and 3, respectively
C_L	Light chain constant domain
CTC	Circulating tumor cells
CTLA-4	Cytotoxic T-lymphocyte-associated protein 4
CXCL	Chemokine (C-X-C motif) ligand
CXCR3	C-X-C motif chemokine receptor 3
DC	Dendritic cells
DI water	De-ionized water
E:T	Effector : target

EGF	Epidermal growth factor
EGFR	Epidermal growth factor receptor
EMT	Epithelial to mesenchymal transformation
EpCAM	Epithelial cellular adhesion molecule
EPR	Enhanced permeability and retention
ER	Estrogen receptor
$F_{158.}$	Phenylalanine at position 158
Fab	Fragment antigen binding
FACS	Fluorescence activated cell sorting
FasL	FasL
FBS	Fetal bovine serum
Fc	Fragment crystalline
FcGR	Fcg receptor
FcRn	Neonatal Fc receptor
HER	Human epidermal growth factor receptor
HSPG2	Heparin sulfate proteoglycan 2 (Perlecan)
IFN	Interferon
IgA	Immunoglobulin A
IgD	Immunoglobulin D
IgE	Immunoglobulin E
IgG	Immunoglobulin G

IgM	Immunoglobulin M
IHC	Immunohistochemistry
IL	Interleukin
IM	Intramuscular
ITAM	Immunoreceptor tyrosine-based activation motifs
ITIM	Immunoreceptor tyrosine-based inhibition motifs
IV	Intravenous
MCAM	Melanoma cellular adhesion molecule
MEM	Minimum essential medium
MHCI	Major histocompatibility complex
NAT	Normal adjacent tissue
NK Cell	Natural killer cell
NSG	NOD *scid* gamma
PD-1	Programmed death protein 1
PD-L1	Programmed death ligand 1
PLA-PEG-Maleimide	Poly lactic acid – poly ethylene glycol – maleimide block co-polymer
PLGA	Poly(D,L-lactide-co-glycolide)
PBMC	Peripheral blood mononuclear cells
Poly I:C	Polyinosinic–polycytidylic acid
PR	Progesterone receptor

RBC	Red blood cells
RPMI	Roswell park memorial institute
SC	Subcutaneous
scFv	Single chain fragment variable
T-regs	Regulatory T cells
TLR	Toll-like receptor
TMDD	Target mediated drug disposition
TNBC	Triple negative breast cancer
TRAIL	TNF-related apoptosis-inducing ligand
V_{158}	Valine at position 158
VEGF	Vascular endothelial growth factor
V_L	Light chain variable domain

Chapter 1: Introduction

1.1. Introduction to Monoclonal Antibodies

The hypothesis that the immune system recognizes cancer cells as foreign has gained much traction in the past two decades.[1] In fact, a large fraction of the newer class of anti-cancer therapeutics are largely focused on modulating the immune system to improve recognition of cancer cells.[2] Following suit, antibodies have become a major focus for the development of new cancer therapeutics.[3] Over the past three decades, there has been a consistent increase in the number of monoclonal antibody products that have been approved.[4] Their stability, minimal toxicity (relative to cytotoxic drugs) and pharmacokinetic properties are some of the desirable attributes for pharmaceutical development.[5] The key properties of antibodies that enable their widespread application as immuno-therapeutics include their specificity and high affinity for the target antigen.[5,6] In addition, their clinical success is a definite motivation for further investment, considering that of the 130 drugs that have received breakthrough designation by the USFDA, 60 are some form of an antibody (as of December 31st, 2018; data accessed from US-FDA official website).

1.2. Development of Monoclonal Antibodies

The innate arm of the immune system is effective in defending the body against pathogens that are 'typical' in nature or those that have classical molecular patterns.

However, in order to fight a wide range of insults, the immune system also consists of an adaptive arm. B cells, a part of the adaptive immune system, recognize antigens through the B cell receptor.[7] Upon Helper T cell mediated stimulation, B cells secrete antibodies that are able to specifically bind to these foreign antigens. Circulating antibodies, also termed as immunoglobulins (IgGs)[7], are then able to eliminate antigens by two potential mechanisms: one involves directly binding to and neutralizing the antigen, and the other is to recruit innate immune components (complement proteins, NK cells, macrophages, and dendritic cells) that are able to eliminate the antigen from the system.[7] Thus, the idea behind the development of exogenous monoclonal antibodies is to enable the human body to recognize pathogens or tumor antigens that it may have missed.

B cells can develop antibodies to virtually any type of antigen, including pathogens as well as small molecules.[8] They secrete antibodies that bind to a vast variety of antigens. On average, a human has the ability to produce greater than 10^8 - 10^{10} different types of specific antibodies due to specialized processes of the immune system.[9] The hybridoma technology, developed by Kohler and Milstein, was an attempt to utilize these 'specialized processes' for the development of clinical therapeutics.[10] It involved immunizing animals (often mice or rabbits) repeatedly with an antigen of interest causing B cells to secrete antibodies specific to that antigen. Along with several following downstream processes, this technology provided researchers with the much-needed capability to artificially develop antibodies against specifically selected antigens. In addition, it also provided a means to produce large quantities of antibodies *in vitro*.[11] Kohler and Milstein were

awarded the 1994 Nobel Prize in Medicine/Physiology for their work in the development of hybridoma technology.[12] However, due to their non-human origin, hybridoma antibodies have had limited clinical success.[13] Mouse antibodies can cause significant immunogenicity and are unable to interact with other immune components when administered in humans.[14] These issues were addressed by the development of chimeric and humanized antibodies from hybridoma clones, that replaced portions of the mouse antibody sequence with human antibody sequences.[15] This led to the development of several tumor-targeted antibodies that have been clinically successful. The first chimeric monoclonal antibody approved for cancer treatment was Rituximab (Rituxan®)[16], an anti-human CD20 binding antibody with mouse and human sequences combined.[17]

Twenty four years after Kohler and Milstein received the Nobel prize for hybridoma work, Sir Gregory Winter and George Smith were awarded the Nobel Prize for phage display[18]. The technology has allowed scientists to develop fully-human antibodies against virtually any antigen of interest, *in vitro*. This method uses large, diverse libraries of bacteriophage (bacterial viruses) displaying antibody fragments on their surface for *in vitro* high-throughput screening of antibody fragments against the desired peptide/antigen. Sequential enrichment of antibody fragments that display specificity for the given target eventually leads to a manageable number of candidates that can be reformatted into fully human IgGs using modern molecular biology techniques. Adalimumab (Humira®)[19], the first approved monoclonal antibody developed using phage display, is used for the treatment of various auto-immune disorders.[20] It was approved in the US in 2002 and has

since topped the list of highest selling drugs in the US.[21] Phage display was a significant advancement over the hybridoma technology, that despite its success, suffered from several limitations such as being labor and time intensive. In addition to being an immensely useful tool in the development of antibodies, phage display can also be utilized for the discovery of novel targets.[22] Analogous to the use of tumor gene expression profiles to evaluate the presence of mutations or anomalous overexpression, phage display can be used to identify new targets in their native, physiological format. An example of such a procedure and the identification of a novel tumor antigen is discussed in chapter 2 of this thesis.

1.3. Antibody Structure and Classification

Antibodies can be classified into five different sub-classes based upon their structure. These include IgA, IgD, IgM, IgG and IgE.[6] Each sub-class has its own unique but complementary immune functions. The most abundant type of antibody in blood is IgG. It comprises 10-20% of the total plasma protein component and about 80-90% of the total plasma antibody component.[6,15] IgG is also the most extensively studied class of antibodies, representing more than 70% of all antibody based therapeutics.[23] From here on, any reference to antibodies (unless otherwise specified) will be made with respect to IgG antibodies. Each IgG molecule is a Y-shaped molecule (~150 kDa) consisting of four polypeptide chains, two identical heavy chains (~50 kDa each) and two identical light chains (~25 kDa each).[6] Two disulfide bonds link the two heavy chains together and one

disulfide bond, each, links the two heavy chain-light chain pairs together (Figure 1.1). In humans, there are five types of heavy chains (α, μ, γ, ε and δ) that determine the antibody classification of IgA, IgM, IgG, IgE and IgD, respectively. There are also two types of light chains classified as κ and λ.[6]

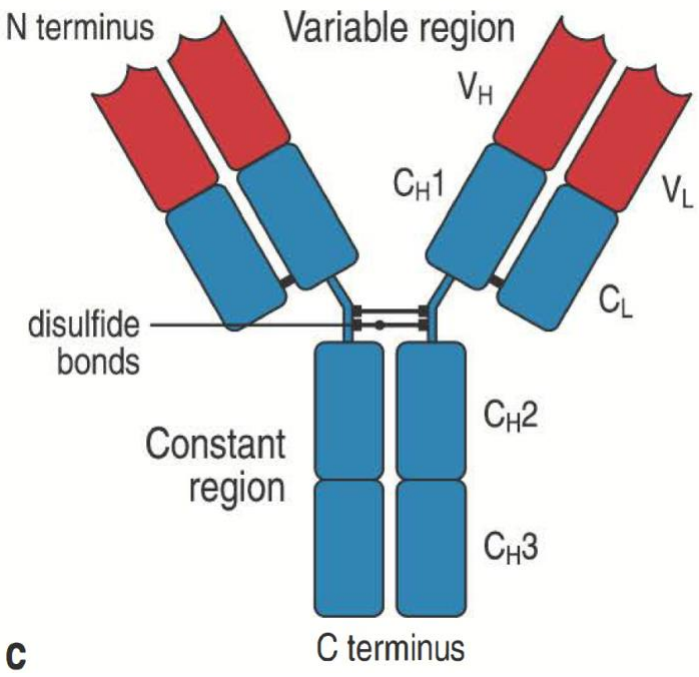

Figure 1.1: Structure of an IgG antibody. Image adapted from Janeway's Immunobiology[7]

Each light chain can be further sub-divided into the constant (C) domain and the variable (V) domain i.e., C_L and V_L, respectively. The heavy chain can be sub-divided into three constant domains and one variable domain i.e. C_{H1}, C_{H2}, C_{H3} and V_H, as well as an

additional hinge region between C_{H1} and C_{H2} (Figure 1.1).[7] Antibodies of classes other than IgG also have the same basic framework of heavy and light chains; however, variability in the heavy chain allows for different effector functions for different sub-classes.

Regions of an antibody can be grouped together structurally or functionally. Structurally, V_L and V_H are grouped together to form the variable region that is responsible for the expansive diversity observed in antigen binding.[7] More specifically, within each variable domain (V_H and V_L) are found three hypervariable regions or complementarity determining regions (CDRs) that allow for the highly diverse antigen binding.[24] Thus, each antibody can have six unique CDRs. Polypeptide chains outside the CDRs but within the variable domains are termed as 'framework'. On the other hand, the C_L and C_H regions are grouped together to form the constant region that varies only subtly, allowing for different effector functions.

Functionally, V_L, C_L and V_H, C_{H1} together form the 'fragment antigen binding' (Fab).[7] The presence of two Fab arms makes antibodies bivalent in nature i.e., they simultaneously bind to two antigen molecules, thus increasing the total strength of interaction through avidity.[6] On the other end, C_{H2} x2 and C_{H3} x2 together form the 'fragment crystalline' (Fc) portion of the antibody or the 'stem' of the antibody.[7]

Thus, an antibody can be thought to have two primary functions; the first to bind to a unique target antigen, and the second to bind to different components of the immune system. As the name suggests, the Fab arm of an antibody binds to the target antigen,

whereas the Fc region binds to different immune components and determines its effector function. The Fc region is also critical in terms of antibody pharmacokinetics, a property that is significantly different from that of traditional small molecule compounds and will be discussed in section 1.5. It is important to note here that, even though the Fab domains make antibodies unique and desirable for pharmaceutical development, the Fc domains are critical to antibody function and influence the outcome of therapeutic antibodies.

1.4. Antibodies of the IgG Isotype

IgG antibodies have subclasses, IgG1, IgG2, IgG3 and IgG4, based on the heavy chain structure.[25] The hinge region sequence and the number of disulfide bonds can vary among subclasses.[3] Despite these differences, IgG antibodies have closely related structures, with >90% similarity at the amino acid level.[26] The subtle structural differences, however, allow for differential function, such as antigen binding, formation of immune complexes and activation of effector functions. Thus, when designing antibodies *in vitro* as therapeutics or diagnostics, the selection of the isotype depends upon the desired *in vivo* function.

Within the four subclasses of IgGs, IgG1 has been used extensively for the development of antibody-based therapeutics. This is likely because when antibodies are designed for cancer therapy, they are required to have an 'active' role i.e., they are expected to interact with effector cells of the immune system (NK cells, macrophages, and DCs) and

recruit them against the target (tumor).[25] IgG1 and IgG3 antibodies have been characterized as having the most potent effector function among the IgG sub-classes, while IgG2 and IgG4 antibodies have been characterized as having minimal effector function. IgG3, however, has been largely excluded from developmental therapeutics, because it is more susceptible to proteolysis, leading to stability concerns. It also has a shorter half-life compared to IgG1 (endogenous IgG1 has a half-life of ~21 days, while endogenous IgG3 has a half-life of ~7 days).[26] Examples of successfully marketed IgG1 antibodies include trastuzumab (Herceptin®)[27] for the treatment of HER2 positive breast cancer and cetuximab (Erbitux®)[28] for the treatment of head and neck cancer and metastatic colorectal carcinoma.

More recently, the newer classes of anti-cancer therapeutics have 'blocking' functions, such as with checkpoint inhibitors. In such cases, the antibodies are required to have an 'inactive' isotype or antibodies that have a mechanism solely through their Fab arms, IgG2 and IgG4 can be a preferred choice.[25,26] Panitimumab (Vectibix®)[29], an anti-EGFR antibody approved for the treatment of metastatic colorectal carcinoma, is an IgG2 antibody. It acts by blocking the activation of EGFR receptors and thus does not require an 'active' isotype. Similarly, Pembrolizumab (Ketruda)[30], an anti-PD1 antibody for the treatment of metastatic melanoma (and other indications), is an IgG4 antibody. Pembrolizumab binds to PD-1 and prevents its interaction with PD-L1, thus once again requiring a 'blocking' isotype.[31]

Although broad generalizations in terms of active and inactive isotypes exist, the final decision is usually based on *in vivo* performance. This is often because pharmacokinetic parameters can take precedence. In such cases, antibody engineering can be undertaken to convert 'active' isotypes to an 'inactive' isotype or vice-versa.

1.5. Antibody Pharmacokinetics

As mentioned above, another key parameter that makes antibodies so desirable for clinical development is their favorable pharmacokinetic behavior. Antibodies are much larger than traditional chemotherapeutic agents (~700 Da v/s ~150kDa)[6] and thereby have distinct and often complex pharmacokinetic and pharmacodynamic properties. Some of the main attributes of antibody pharmacokinetics is discussed below.

1.5.1. Absorption

Antibodies are typically administered via the intravenous (IV) route. Pembrolizumab (Keytruda®)[30], ipilimumab (Yervoy®)[32], nivolumab (Opdivo®)[33], and rituximab (Rituxan®)[16] are some of the many FDA approved monoclonal antibodies given by IV infusion. However, IV administration requires active involvement of medical personnel and thus raises the cost of therapy. Thus, antibodies have also been explored for administration via subcutaneous (SC) and intramuscular (IM) injections.

Herceptin Hylecta®[34] is a specialized formulation of Trastuzumab along with hyaluronidase that has been approved for SC administration. Dupilumab (Dupixent®)[35] and Adalimumab (Humira®)[19] are also prescribed for SC administration. The major limitation with these routes is usually the maximum dose that can be administered. On average, the bioavailability of antibodies administered SC/IM is between 50-100%, and the time to maximum concentration in the plasma (T_{max}) varies between 2-8 days.[15,36,37] When antibodies are administered via extravascular routes i.e., via IM or SC injections, the two possible mechanisms of absorption are convection by lymphatic drainage and diffusion into blood vessels close to the site of administration. However, the large molecular size of antibodies results in poor diffusion rates. Since the lymphatics have a greater permeability to large molecules, it is expected that antibodies administered SC or IM are primarily absorbed by convective transport into the lymph vessels.[38,39]

When a small molecule is endocytosed into a cell, more often than not, it undergoes degradation in the lysosome.[40] Antibodies on the other hand are unique, because they have a 'salvage mechanism' that prevents degradation inside the lysosome. This mechanism is mediated by the neonatal Fc receptor (FcRn).[41] The FcRn receptor is expressed on endothelial cells, hepatocytes, intestinal macrophages, peripheral blood mononuclear cells and dendritic cells.[41] Antibodies bind to the FcRn receptor, through the Fc portion, in a pH dependent manner. At physiological pH (pH 7.4), antibodies undergo little binding; however, at the acidic pH of the lysosome (pH 5.5-6.5), binding is significant. Thus, when antibodies undergo endocytosis, for example in endothelial cells, they bind to the FcRn

receptor within the early endosome and are recycled back to the cell-surface, thus are 'salvaged'. Any unbound antibody will undergo proteolysis in the lysosome. Interaction with FcRn significantly affects antibody bioavailability and half-life. FcRn also plays a role in antibody absorption from SC/IM routes.[38] It is unclear whether the FcRn actively mediates antibody transport into the systemic circulation or simply prevents catabolism of the antibody at the site of injection.[15]

Despite the known absorption from SC and IM sites, very few antibodies in the clinic are administered via routes other than IV. This is likely to avoid higher cost of therapy associated with any reduction in bioavailability. In addition, there have also been higher concerns for immunogenicity through the IM/SC routes.[42]

1.5.2. Distribution

Distribution of antibodies depends upon their extravasation into tissues, distribution within the tissues, binding to target cells, endocytosis within target cells and clearance from tissues. The possible mechanisms operating in the distribution of antibodies from the vascular compartment to the extravascular compartment are passive diffusion, convection and active transcytosis.[6] Passive diffusion likely plays a minor role in antibody transport because of their large molecular size. For the most part, it is understood (through physiologically based pharmacokinetic models) that antibodies extravasate into tissues through convection, driven by the difference in pressure between the vascular compartment and the tissue.[43] In addition, the vascular pore size, tortuosity of the vessel and the number

of pores govern antibody convection across blood vessels.[15] Another possible mechanism for antibody distribution to tissues is through transcytosis. Transcytosis is possible through interaction of the antibody with the FcRn receptor. It has been shown *in vitro* that the FcRn receptor is able to mediate bidirectional transport of antibodies across membranes.[44,45] However, it is difficult to determine *in vivo* if either mechanism is dominant. Once inside the tumor, an antibody can distribute within the interstitial space through diffusion, convection and target binding.

It is interesting to note that antibody distribution can be quite different than small molecule distribution. Small molecules undergo relatively rapid diffusion, allowing rapid steady state equilibrium between plasma and different organs. Additionally, small molecules undergo clearance from well-perfused organs. As a result, the distribution of small molecules is independent of clearance i.e. clearance does not drive their distribution into tissues. On the other hand, antibodies primarily undergo clearance from organs that may not be in rapid equilibrium with the plasma. As a result, the distribution of antibodies is often driven by their clearance.

1.5.3. Elimination

The major routes of elimination for drug molecules are renal clearance (filtration), biliary secretion, and biotransformation (metabolism and catabolism).[6,15] Since antibodies are much larger in size than the renal filtration molecular weight cut-off of <50kDa, they do not undergo renal filtration. Biliary secretion also has very limited relevance for IgG

antibodies and thus bio-transformation is the major route, which may be target mediated or non-specific catabolism. Minor routes of antibody elimination include phagocytosis due to the formation of large immune complexes, and interaction with Fcγ receptors mediating endocytosis and catabolism.[6,15]

When antibodies bind to their target through the Fab domain, they undergo receptor mediated endocytosis. Once internalized into the target cells, antibodies often undergo catabolism inside the lysosome (in the absence of FcRn). This is a major pathway for distribution as well as elimination of monoclonal antibodies and has been termed as 'target mediated drug disposition', a saturable mechanism.

Antibodies can also undergo non-specific fluid phase endocytosis. This is a pathway primarily observed in the case of IgG circulating in plasma and undergoing endocytosis within endothelial cells.[15] However, the FcRn receptor 'salvages' a significant fraction (>90%) of IgGs that undergo non-specific endocytosis.[46] In fact, this mechanism also lends antibodies their unusually long half-lives, ranging from 2-3 days to up to 2-3 weeks.[6,41] The FcRn based salvage mechanism is also saturable, similar to any other receptor mediated mechanism. Thus, the average plasma concentration of endogenous antibodies can have a significant effect on the externally administered antibodies.[47] However, it may be worth noting that the typical IgG plasma concentration is about 10 mg/ml, and therapeutic antibodies are administered at doses that would change IgG concentrations by less than 2%.

An additional consideration for antibody clearance, distinct from small molecules, is immunogenicity. Any externally administered protein can be considered immunogenic, albeit to different extents.[42] The first generation of monoclonal antibodies, derived from rodents, were highly immunogenic, because they were recognized as foreign by the human immune system.[48] Second generation, chimeric antibodies attempted to work around immunogenicity by having a human Fc domain and murine Fab domains.[49] Currently, most antibodies in the clinic are either humanized (i.e., murine CDRs on human framework) or fully-human IgGs, and thus have significantly lower immunogenicity concerns due their structure *per se*.[50] However, there are still concerns for immunogenicity due to variable glycosylation patterns, unique post-translational modifications and issues as simple as aggregation. Unfortunately, the possibility of immune response due these factors is difficult to predict. The development of anti-drug antibodies can significantly affect the half-life of antibodies and must be taken into consideration, especially in cases where antibodies are administered in multiple doses.[51]

1.6. Antibodies as Therapeutics

With the advent of advanced hybridoma techniques and phage display, antibodies are being investigated for several different applications in research and in the clinic. In research, antibodies have become an indispensable reagent for various experimental techniques. However, for the purpose of this thesis, clinical application of antibodies is the

focus. Antibodies in the clinic have been utilized in versatile applications including, but not limited to, antibody-drug conjugates, diagnostic agents, targeting ligands and as therapeutics themselves. Here we will focus on the two classes that have been used as therapeutics for cancer therapy, antibody-drug conjugates and antibodies as therapeutics.

1.6.1. Antibody Drug Conjugates (ADCs)

ADCs are a special class of therapeutics that have gained significant attention in the past decade. The idea behind ADCs is to specifically delivery cytotoxic drugs to the tumor by leveraging a key property of antibodies i.e. specificity, and in turn sparing normal cells of toxicity. ADCs consist of a monoclonal antibody conjugated, via a linker, to an extremely potent drug.

Thus, ADCs have three components: antibody, linker and drug. Antibodies that are used to formulate ADCs are specific for antigens overexpressed (or solely expressed) on tumors.[52] The linker component is normally formulated to enable drug release once the ADC is endocytosed into the target cell i.e. cleavable at low pH of the lysosome or by enzymes in the lysosome. Finally, the drugs selected for the development of ADCs are sufficiently potent (IC50s usually in the sub-nanomolar range) such that administration of the free form raises concerns of toxicity.[52]

Currently, there are four FDA approved ADCs, including brentuximab vedotin (Adcetris®)[53] for the treatment of CD30 positive Hodgkin's lymphoma, ado-trastuzumab emtansine (Kadcycla®)[54] for the treatment of HER2 positive breast cancer, gemtuzumab

ozogamicin (Mylotarg®)[55] for the treatment of CD33 positive acute myeloid leukemia and inotuzumab ozogamicin (Besponsa®)[56] for the treatment of CD22 positive acute lymphoblastic leukemia.

1.6.2. Monoclonal Antibodies

The first monoclonal antibody was approved in 1986; muromonab, an anti-CD3 antibody to prevent kidney transplant rejections.[57] However, this mouse antibody had marginal efficacy and had limiting side-effects.[13,58] Presently, antibodies have significantly improved cancer therapy, demonstrated by the fact that among the top ten highest grossing drugs in 2018, six were monoclonal antibodies.[21] Monoclonal antibodies have found applications not only in cancer therapy but also in a variety of immune disorders, such as arthritis, psoriasis, ulcerative colitis, transplant rejection, and chronic inflammatory disorders. Moreover, antibody engineering techniques can almost allow the mechanism of action to be tailor-made for its application. The discussion here is limited to the antibodies used in the treatment of cancer.

1.7. Mechanisms of Monoclonal Antibodies

Antibodies used for cancer therapies have one of three broadly classified mechanisms of action.[5] The first involves direct antigen mediated activity, where binding of the antibody to its antigen leads to downstream signaling, prevents downstream

signaling or causes inactivation of the antigen. The second is checkpoint inhibition. In this case, antibodies bind to inhibitory receptors on key immune cells, thus preventing the inactivation of the immune system. The third mechanism involves binding to the target and recruitment of immune components such as NK cells, macrophages or the complement system to cause cytotoxicity. Each of these mechanisms is discussed below.

1.7.1. Direct antigen mediated activity

Binding of antibody to an antigen expressed on the tumor cell can cause receptor antagonist activity, leading to cell death. Antibody binding may also prevent downstream signaling that is critical for cell proliferation. The former mechanism has been observed for the anti-CD20 antibody Rituximab, which inhibits the p38 MAPK/STAT3/NF-kB/SP1/Bcl-2 pathway, the Src/Raf 1/MEK1/2/ ERK1/2/AP-1/Bcl-xL pathway, the NF-kB/Bcl-xL pathway, the AKT/Bcl-xL pathway and also causes re-distribution of the CD-20 receptor in lipid rafts, all of which lead to either apoptosis or chemo-sensitization.[59] The latter mechanism is often observed in cases of growth factor receptors, particularly of the human epidermal growth factor receptor (HER) family of receptors. These receptors are critical for the growth and rapid proliferation of tumor cells. The HER1 receptor (also known as epidermal growth factor receptor or EGFR) requires ligand binding for receptor dimerization and subsequent proliferation. EGFR is overexpressed on a wide variety of tumor types including colorectal carcinoma and head and neck cancer. Antibody therapeutics have been developed that bind to EGFR (cetuximab) and prevent ligand-receptor interaction as well as inhibit receptor dimerization.[60] The HER2 receptor, on the

other hand, has no identifiable ligand but does require receptor dimerization for downstream signaling.[61] HER2 is overexpressed in a specific sub-type of breast and ovarian cancers. Thus, trastuzumab, an anti-HER2 antibody, has been developed to prevent HER2 dimerization, leading to reduced cell proliferation.

1.7.2. Checkpoint inhibition

Checkpoint inhibitors are a specialized class of drugs that have gained significant traction in the past decade. Immune checkpoints are receptors of the immune system that normally function to prevent the immune system from attacking 'self' organs after an immune insult.[62] Unfortunately, certain tumors are able to leverage this mechanism to their advantage by engaging checkpoint receptors, resulting in a dampened immune response[62]. Checkpoint inhibitors are designed to bind to checkpoints and prevent their activation, thus maintaining the immune system consistently in 'fight mode'.[63] A number of antibodies have been developed as checkpoint inhibitors and have shown remarkable efficacy in cancer patients.

CTLA-4 is an inhibitory receptor expressed on T cells upon activation. Binding of CD80 and CD86 to CTLA-4 leads to inhibition of T cells.[63] Ipilimumab (Yervoy®)[32] is an anti-CTLA-4 antibody that has been developed to block this interaction leading to improved T cell activity against tumors. Similarly, PD-1 is another inhibitory receptor expressed on T cells.[63] Engagement of PD-1 by its ligands PD-L1 and PD-L2 leads to apoptosis of T cells. Antibodies, such as nivolumab (anti-PD-1 antibody)[33] and avelumab

(anti-PDL1 antibody),[64] have been developed to block this interaction. A noteworthy point is that nivolumab is an IgG4 antibody i.e., it has significantly lower effector function.[65] On the other hand, avelumab is an IgG1 antibody; i.e. an active isotype with active effector function.[66] The choice of isotype can be explained by the targets of the two antibodies (T cells and tumor, respectively).

1.7.3. Effector mechanisms

The most commonly observed mechanism of action for antibodies is the activation of effector mechanisms contributed by different components of the immune system. Immune cells, such as NK cells, monocytes, macrophages and granulocytes, have the ability to interact with antibodies through their Fc domain. Binding of an antibody to its target on the tumor cell and to an immune cell simultaneously leads to activation of the immune cell and consequent killing of the tumor cell. The most common cells that participate in this mechanism are the NK cells. Antibody-dependent cellular cytotoxicity (ADCC) is a term that can be used to describe cytotoxicity induced by a number of different cell types, as listed above.[7] However, for the purpose of this thesis, we will focus primarily on NK cell mediated ADCC.

Alternatively, activation of immune cells. such as macrophages. can also lead to tumor cell phagocytosis, termed as antibody-dependent cellular phagocytosis (ADCP).[67] Finally, non-cellular components of the immune system can also contribute to this mechanism. Some antibodies are able to bind to proteins of the immune system. known as

'complement proteins', triggering the complement cascade. This results in tumor cell death, termed as complement mediated cytotoxicity (CDC).[67] In the case of effector-based mechanisms, the target antigen is almost always expressed on the tumor cells. In fact, most antibodies that bind to a tumor antigen show some level of ADCC/CDC, despite having other mechanisms of action. Trastuzumab and cetuximab have both been shown to induce ADCC.[68,69] Rituximab on the other hand has been shown to have potent ADCC as well as CDC.[59]

As can be gauged from the previous sections, antibodies can act through different mechanisms. In fact, it is fairly common to observe antibodies in the clinic that have more than one distinct mechanism of action. For example, cetuximab prevents ligand (EGF) binding to the EGFR as well as EGFR receptor dimerization, thus 'starving' cancer cells of growth signals.[70] Cetuximab is also an extremely efficient mediator of ADCC[69] and CDC[71]. Another interesting but lesser known example is the anti-CTLA-4 antibody, ipilimumab. In addition to checkpoint inhibition, ipilimumab also activates ADCC, resulting in the death of regulatory T cells (Tregs).[72] Ipilimumab targets CTLA-4 that is overexpressed on Tregs and is therefore able to recruit NK cells against T-regs. This mechanism of ipilimumab significantly improves the effector T cell to regulatory T cell ratio in the tumor, leading to tumor rejection. Thus, with such varied mechanisms of action possible, it becomes critical to understand these mechanisms *in vitro* and *in vivo* for newly developed antibodies. This allows for the rational design of combination therapies. Chapter

3 of this thesis discusses the development of a novel antibody and the delineation of its mechanism of action.

1.8. Antibody Dependent Cellular Cytotoxicity (ADCC)

ADCC is a mechanism of action unique to antibodies and has become an integral part of developing cancer therapeutics. This section will deal with the various components involved in ADCC as well as the mechanism by which ADCC initiates tumor cell death.

1.8.1. NK Cells

NK cells are a part of the innate immune system and have now been accepted as key players in the anti-tumor immune response. At the core of NK cell activation (or inactivation) is the 'missing self' hypothesis. T-cells recognize their targets through MHC molecules. However, NK cells are wired to kill cells that (1) do not express MHC molecules or (2) express stress ligands.[73] Thus, unlike T-cells, NK cells do not require prior 'sensitization' to their target cells and are valuable players against the nascent stages of tumor development.[74] NK cell outcomes (i.e. activation or inactivation) are tightly regulated by the multitude of receptors expressed on their cell surface.

NK cells are characterized as being $CD3^-/CD56^+$ in humans and $CD3^-/CD49b^+$ (or $CD3^-/NK1.1^+$) in mice.[73] Another key receptor expressed on the surface of NK cells is the CD16a receptor (also known as FcγRIIIa)[73] that interacts with the Fc domain on antibodies

and will be discussed in further detail later in this chapter. The $CD3^-/CD56^+$ NK cells in the blood can be categorized into two populations based on the expression of CD16a. About 90% of NK cells in blood are $CD16^+/CD56^{dim}$ and form the 'cytotoxic population' mediating ADCC, whereas about 10% of NK cells are characterized as $CD16^-/CD56^{bright}$ and form the population secreting a majority of the cytokines.[73]

The major inhibitory receptors that are expressed on the NK cell surface are KIR, Ly49 and NKG2A; all function to detect self MHC Class I molecules on cell surfaces.[73] These inhibitory receptors prevent NK cells from killing healthy cells. They signal through immunoreceptor tyrosine-based inhibition motifs (ITIMs). In contrast, the major stimulatory receptors on the NK cell surface include NKG2D, NCRs, DNAM1 and CD16a.[73] These receptors (other than CD16a) function to recognize 'stress ligands' on the surface of cells, which are often found on rapidly proliferating, infected or transformed cells. CD16a is the key receptor in NK cell and antibody interactions. It is a potent stimulator of NK cell cytotoxicity and thus is key to ADCC. All stimulatory receptors signal through immunoreceptor tyrosine-based activation motifs (ITAMs). It must be noted though that the above mentioned receptors are only a few of the well-characterized receptors among many found on the NK cell surface.

At any given point, a number of different NK cell surface receptors can be engaged by their ligands. However, the outcome of NK cell activity is determined by the balance between activating and inhibitory receptors that are engaged.[73,75] Thus, in the case of antibodies, engagement of CD16a by the Fc domain of the antibody essentially 'tips' this

balance towards an activated phenotype, which then enables NK cells to attack the target cells. However, under normal circumstances, when there are more inhibitory receptors engaged, they are able to override the activating signals and NK cells remain inactivated.

1.8.2. Fcγ Receptors

Although FcγRIIIa has been described as the key receptor responsible for mediating ADCC, there are a number of other Fcγ receptors (FcγR) that can be involved in effector function. The human Fcγ family of receptors bind the IgG subclass antibodies and can be classified into FcγRI, FcγRII and FcγIII. FcγRII is further classified into FcγRIIa, FcγRIIb and FcγRIIc.[26] Similarly, FcγRIII is classified into FcγRIIIa and FcγRIIIb.[26] Each of these receptors not only have different functions but are also expressed on different cells types and have variable affinity towards the IgG Fc domain. FcγR can possess either activating tyrosine based motifs in their intracellular domains; i.e. ITAMs, or inhibitory tyrosine based motifs; i.e. ITIMs. FcγRI, FcγRIIa, FcγRIIc, and FcγRIIIa are all ITAM based receptors, whereas FcγRIIb is an ITIM based receptor.[26] A single NK cell can express both activating and inhibitory receptors that can potentially be simultaneously engaged; however, the delicate balance between the two decides the outcome of the immunological response.[76]

Among the various IgG isotypes, the difference in affinities for Fcγ[76] may explain why different isotypes are required for different functions i.e., ADCC v/s blocking antibodies v/s CDC, etc. It is understandable then that a broad generalization can be made

in terms of IgG affinities to the different Fcγ receptors - FcγRI> FcγRIIa> FcγRIIIa. However, it is important to note that FcγRI and FcγRII are not known to be expressed on the surface of NK cells, rather they are expressed on cells such as macrophages, monocytes, and dendritic cells.[77] Thus, FcγRIIIa is the key receptor for NK cell-mediated ADCC. FcγRIIb on the other hand is a lower affinity inhibitory receptor, primarily expressed on B cells and dendritic cells, and reduces ADCC outcome depending on the relative affinity of the antibody for FcRIIIa v/s FcγRIIb.[78]

In addition to the different isotypes of Fcγ receptors, certain Fcγ receptors also have polymorphisms in the normal human population, resulting in variable prognosis.[79] There are two isoforms possible for the gene encoding FcγRIIIa receptor that vary in the amino acid at position 158 i.e., V_{158} or F_{158}. The V_{158} has about five fold higher affinity for IgG1 than the F_{158}.[76] Patients with the V_{158} isoform respond considerably better to antibody therapeutics than patients with the F_{158} isoform.[80,81] Similar polymorphisms exist in the case of other Fcγ receptors as well that could influence the outcome of antibody therapeutics. Thus, it is critical to have a good understanding of the potential interactions of an antibody with the receptors during drug development.

1.8.3. Cell Killing

NK cells are described as 'large granular lymphocytes'.[7] Their cytoplasm contains lytic granules, also known as 'secretory lysosomes'. These granules contain a variety of proteolytic enzymes and death inducing molecules (perforin, Granzyme B, FasL, TRAIL,

etc.).[82] The point of contact between the target cell and the NK cell is termed as an 'activating immunological synapse' (synapses resulting in inhibition or regulation are termed as 'inhibitory immunological synapse' and 'regulatory immunological synapse', respectively).[82,83] Antibodies enable the formation of this synapse. Following contact with the target cell, activating receptors in the synapse are engaged by their respective ligands, leading to downstream activation of pathways causing lytic granules to localize at the immunological synapse. The lytic granules are then able to fuse with the cell membrane leading to a phenomenon termed as 'degranulation'.[82] Degranulation releases the proteolytic enzymes and death inducing proteins that cause target cell cytotoxicity. Perforin inserts itself into the cell membrane and forms pores in the target cell.[82] Granzyme B is then able to enter the target cell and induce apoptosis through caspase dependent and independent mechanisms.[82] In addition, FasL and TRAIL are death inducing proteins that, upon binding to their respective death receptors, are able to induce apoptosis.[82]

1.9. Parameters that affect ADCC

ADCC is a complex mechanism that involves a number of different components and thus is influenced by a myriad of factors. The key determinants of ADCC that need to be considered when designing therapeutic antibodies are discussed below.

1.9.1. Antibody Affinity

Antibody affinity may be defined either in the form of apparent affinity (also known as avidity) or intrinsic affinity. Intrinsic affinity refers to a monovalent interaction between

an antibody and a single antigen molecule and is often measured by methods that directly analyze the binding interactions. such as the rate of association and the rate of dissociation.[7,84] Examples of such analytical techniques include bio-layer interferometry and surface plasmon resonance. On the other hand, apparent affinity refers to the interaction between the antibody and antigen in a 'native' format.[7,84] In this case, because an antibody is bivalent in nature, the interaction itself is also bivalent and thus the apparent affinity is often much higher than the intrinsic affinity. Apparent affinity is measured via indirect techniques such as flow cytometry and ELISA. It has long been assumed that antibody affinity is a critical parameter determining ADCC; however, varying antibody affinities are usually observed across different antigen-antibody pairs, and thus a direct comparison is deemed inaccurate. In order to understand the practical implications of antibody affinity on ADCC, Tang et al[84] developed a panel of anti-HER2 antibodies with varying affinities and found that both intrinsic and apparent affinities play a critical role in ADCC.

The broad takeaway from the work of Tang et al[84] was that the key determinant of ADCC is the density of antibody molecules on the tumor cell surface: higher the concentration of antibody corresponds to greater ADCC. This was experimentally observed such that cell lines with high surface antigen concentration were dependent on higher apparent affinity rather than the intrinsic affinity i.e., antibodies with variable intrinsic affinities but similar apparent affinities showed similar cell kill in case of cell lines with high antigen density. In contrast, cell lines with lower antigen density were more

dependent on the intrinsic affinity i.e., antibodies with variable intrinsic affinities but similar apparent affinities showed variable cell kill in the case of cell lines with lower antigen density. Additionally, the group also observed that binding valency was a critical determinant for ADCC, with bivalent binding showing significantly better cell kill than monovalent binding. This is an interesting observation in light of the large number of bispecific antibodies that are currently under development, since most of these molecules have monovalent binding to the target antigen. In chapter 4 of this thesis, two antibodies that bind to the same target but show variable ADCC due to differences in affinity are discussed.

1.9.2. Antibody isotype and FcγR isotype

Antibodies (specifically IgGs) can be of four different isotypes, IgG1, IgG2, IgG3 and IgG4; each has a specialized yet complementary function in the immune system.[25,26] Their ability to perform these functions is dictated by their relative binding affinities to the various Fcγ receptors (i.e. FcγRI, FcγRIIa, FcγRIIb, FcγRIIIa, FcγRIIIb) and the C1 receptor. As discussed in section 1.8.2, the key receptors responsible for regulating ADCC are FcγRIIb (inhibitory) and FcγRIIIa (stimulatory). IgG1 antibodies bind with significantly higher affinity to FcγRIIIa, than to FcγRIIb. As a result, IgG1 antibodies are considered the most 'active' isoform i.e. they are considered to have the highest ADCC and CDC potential. Even though IgG3 antibodies have a similar binding profile as IgG1 antibodies and have significant ADCC potential, they have been largely excluded from

development. This is likely attributed to the fact that IgG3 antibodies are not considered to be as stable as IgG1s, and have a shorter half-life. On the other hand, IgG2 and IgG4 antibodies, have been considered as 'blocking' antibodies, since their binding affinities to the various FcγRs are ~one log order lower than those of IgG1 and IgG3.[76] IgG4 has been commonly utilized in the clinic for the development of checkpoint inhibitor antibodies, precisely because of this reason. Checkpoint inhibitor antibodies are required to bind to the target receptor and prevent native ligand binding. However, they are not always required to kill the target cell. An example of one such antibody is pembrolizumab. However, in light of the recent paper by Vargas et al[72], the solely 'blocking' function of checkpoint inhibitor antibodies may not be entirely accurate. Although, there are some stability concerns with IgG4 antibodies, due to their ability to exist in the half-Ig monovalent form *in vivo*.[25] This format, although desirable in the native immune system, may not be amenable for clinical development due to the unpredictable status of the drug molecule. However, pembrolizumab, an FDA approved IgG4 antibody, is one of the most successful monoclonal antibodies in the clinic.

1.9.3. Antigen density

Tang et al's paper[84] also shed light on the fact that higher antigen densities on the cell surface can promote ADCC, which essentially translates once again into 'higher the antibody density on the target cell surface, higher is the ADCC'. In fact, their work with apparent affinity v/s intrinsic affinities (discussed in section 1.9.1) also demonstrated the effect of antigen density. Cell lines with higher antigen density were less sensitive to

differences in intrinsic affinities and required lower antibody concentrations to achieve similar cell kill as opposed to cell lines with lower antigen density.

1.10. Limitations of ADCC

1.10.1. FcγR Polymorphisms

ADCC outcome is dictated by (1) the antibody and (2) the NK cells. The interaction between NK cells and the antibody is mediated via specialised Fcγ receptors, that have been described in section 1.8.2. The most important NK cell receptor responsible for mediating ADCC is the FcγRIIIa. This receptor is known to have polymorphisms in amino acid 158, resulting in three isoforms, the valine-valine isoform (VV), the phenylalanine-phenylalanine isoform (FF) and the valine-phenylalanine isoform (VF). The VV isoform (V_{158}) has about five-fold higher affinity for the constant domain of IgG1 antibodies than the FF isoform (F_{158}).[26,76] Consequently, it has been shown that patients with the V_{158} isoform respond significantly better to antibody therapy than those with the F_{158} isoform.[79] In fact, several *in vitro* studies have corrobrated this theory; ADCC is much higher in assays utilizing cells carrying the V_{158} isoform.[85] Cartron et al[80] found that patients with follicular non-Hodgkin‘s lymphoma responded significantly better to Rituximab monotherapy, if they exhibited the V_{158} isoform of the FcγRIIIa receptor. Similarly, Shimizu et al[86] reported differential responses of PBMCs (from HER2 positive breast cancer patients) to

Trastuzumab, depending upon the FcγRIIIa receptor isotype. Patients with the V_{158} isoform showed earlier enrichment of immune response related gene sets. They also showed downregulation of cytokine related gene sets that likely resulted in an improved anti-tumor response. However, there was a recent conflicting report that claimed a lack of correlation between FcγRIIIa receptor status and patient survival for trastuzumab[87]. Finally, metatastatic colorectal cancer patients with the FcγRIIIa V_{158} isoform also responded significantly better to cetuximab as opposed to patients with the FcγRIIIa F_{158} isoform.[81] On an average only between 7-25% of patients are known to have the V_{158} isoform[88,89,90], suggesting that only a minority ~20% of patients will respond robustly to antibody therapy.

1.10.2. Lack of NK cell infiltration in tumors

NK cells play a critical role in tumor immune-surveillance. They have the unique ability to recognize and kill tumor cells without the need for prior exposure (unlike T cells) or secondary signals.[74] T cells require the presence of MHC Class I molecules for the recognition of tumor cells. Thus, in order to evade T cell recognition, tumor cells have been known to downregulate MHC Class 1 molecule expression.[91] NK cells, on the other hand, gain a strong stimulatory signal due to the absence of MHC Class 1 molecules i.e. they recognize these cells as 'non-self' and proceed to eliminate them from the body.[92] This has been widely recognized by the research community and has led to the development of several NK cell-based cancer therapeutics.[73] Despite their promising cytotoxic abilities, however, NK cells have been shown to have limited infiltration in tumors. Histological

examination of several different tumor types has shown that NK cells are poor infiltrators. In colorectal carcinoma, Satiago et al[93] found that only 10-20% of 157 patients analyzed could be classified as having 'high NK cell infiltration'. Similarly, Ishigami et al[94] found that of the 146 gastric carcinoma patients analyzed, only ~27% showed high NK cell infiltration. In both of those examples, lower NK cell infiltration correlated with poor patient survival. Because ADCC requires simultaneous engagement of NK cells and tumor cells by the antibody, poor NK cell infiltration can result in poor antibody efficacy. Thus, mechanisms that enhance NK cell infiltration could potentially also enhance antibody efficacy.

1.10.3. Limited efficacy of ADCC

Finally, ADCC by itself can be quite limited in its efficacy. Cetuximab, for example, was only moderately effective as a single agent against colorectal carcinoma (improved the median survival by only 1.5 months[95]). In another study evaluating cetuximab in combination with platinum-based chemotherapy for head and neck cancer, the addition of cetuximab extended the median patient survival only by 2.7 months.[96] Of course, there are other monoclonal antibodies that have shown robust responses and efficacy in clinical trials; however more often than not, such antibodies have additional mechanisms of action other than ADCC. Thus, even though ADCC is a mechanism of action observed with a number of antibodies, there is still substantial scope for improvement. Specifically, there is a clear need for the development of combination therapeutics that can leverage the unique targeting ability observed with ADCC.

1.11. Monoclonal antibody combination strategies

The administration of monoclonal antibodies as anti-cancer therapeutics can be considered as a way of recruiting components of the immune system against the tumor, specifically NK cells in the case of ADCC. This is advantageous, because several groups have shown that recruiting NK cells to the tumor can also indirectly stimulate the adaptive immune system, leading to an antigen specific immune response.[97,98,99] However, ADCC by itself has several limitations. Several rational combination therapies have been explored for monoclonal antibodies, including chemotherapeutics and immune-stimulant molecules.

A majority of monoclonal antibodies are administered in combination with chemotherapeutic agents. Chemotherapeutics have been attractive molecules to combine with monoclonal antibody therapy, due to their long-standing use in cancer therapy. Moreover, there have been several reports that suggest chemotherapy sensitizes tumor cells to antibody mediated mechanisms.[100,101] In certain cases, the chemotherapeutic and the antibody may also act synergistically, such as targeting two different growth pathways. However, recently there have been contradictory reports that suggest combining chemotherapy with monoclonal antibodies may hinder adaptive immune response.[99]

There has been a gradual shift in the focus of combination therapy designs. More and more immune-stimulants are being considered in combination with monoclonal antibodies, simply because they are able to leverage the same mechanism of action.[102] An

important class of immune-stimulants being explored for this purpose are the toll-like receptor (TLR) agonists.[103] TLRs are specialized receptors, expressed on dendritic cells, that recognize classical or conserved features of microbes and thus are also known as pathogen recognition receptors. They play an important role in the development of adaptive immune response by stimulating dendritic cells to secrete cytokines that activate CD4 and CD8 T cells.[104] Specifically, TLR7 and TLR8 agonists have been widely explored as vaccine adjuvants due to these factors.[105] However, in addition to activating T cells, dendritic cells release cytokines that have the ability to activate NK cells. There have been several reports on the indirect activation of NK cells by TLR7/8 agonists that enable improved ADCC.[106–108] In chapter 4 of this thesis, the combination of TLR7/8 agonists with monoclonal antibodies to improve their anti-cancer efficacy is explored.

1.12. Specific Aims

The central aim of this thesis is to contribute to a fundamental new class of therapeutics in the clinic for cancer therapy, i.e. monoclonal antibodies. The work presented here examines monoclonal antibody therapeutics in terms of new targets, mechanisms and novel combination therapies.

1.12.1. Specific Aim 1: Evaluate HSPG2 as a novel target in metastatic triple negative breast cancer

Our work in chapter 2 is focused on evaluating HSPG2 as a target for metastatic triple negative breast cancer. We studied HSPG2 expression in human breast cancer tumor cell lines as well as in patient samples from the primary tumor and metastatic sites, in order to understand the contribution of HSPG2 to cancer progression. This was also extended to the correlation between HSPG2 expression and patient survival and to drug-resistant tumor models. An additional goal was to determine if HSPG2 was also relevant in other tumor types. Thus, we evaluated HSPG2 expression with respect to circulating tumor cells and patient survival in bladder cancer, ovarian cancer and melanoma.

1.12.2. Specific Aim 2: Identify the mechanism of action for anti-perlecan antibodies and evaluate drug delivery applications

Our lab developed two fully human anti-HSPG2 antibodies, which showed anti-cancer efficacy in an MDA-MB-231-LM2 breast cancer model, in nude mice. Our goal here was to understand the mechanism of action of anti-HPSG2 antibodies. In chapter 3, we describe the systematic *in vivo* and *in vitro* studies carried out to determine that ADCC is the major mechanism of action for anti-HSPG2 antibodies. Additionally, iwe also explore the use of anti-HSPG2 antibodies for drug delivery applications.

1.12.3. Specific Aim 3: Evaluate TLR7/8 agonists in combination with monoclonal antibody therapy

ADCC is a key mechanism of action for many antibodies. However, ADCC is often limited by poor NK cell infiltration, Fcγ receptor polymorphism, and low potency. TLR 7/8 agonists can improve ADCC through indirect NK cell activation. We initially encapsulated a bispecific TLR 7/8 agonist, 522**,** in nanoparticles (522GGNPs) and assessed ADCC with cetuximab. 522GGNPs significantly enhanced cetuximab mediated ADCC *in vitro* and improved the anti-cancer efficacy of cetuximab *in vivo* in an $EGFR^+$ A549 mouse tumor model. However, the combination treatment was only able to retard tumor growth. We then explored a panel of improved, higher-potency TLR7/8 agonists for their ability to enhance cetuximab mediated ADCC. Additionally, we conducted studies in a fully immunocompetent mouse model to characterize the immune response with the combination treatment.

Chapter 2: Perlecan (HSPG2) - a novel target in metastatic triple negative breast cancer

2.1. Introduction

Breast cancer is the most commonly occurring cancer in women, accounting for 30% of all cancers.[109] Consequently, there has been a lot of research dedicated to breast cancer, and the overall 5-year survival rates have improved remarkably from 75% in the 1970s to greater than 90% since 2007[110]. The 5-year survival for local breast cancer is 99% and for regional breast cancer is 85%. However, for women with metastatic disease, the 5-year survival rate drops sharply to just 27%[110]. Considering these statistics, it is clear that more research is required to improve the treatment outcomes for patients diagnosed with metastatic breast cancer.

Carcinomas, such as breast cancer, are epithelial in nature. They develop surrounded by the organ's basement membrane (BM)[111] and the presence of the BM is a significant limiting factor for tumor growth. In order to overcome this barrier, cancer cells undergo epithelial to mesenchymal transformation (EMT), which involves morphological changes in cancer cells that allow them to 'metastasize' from the primary tumor to secondary sites. EMT has been linked to acquiring not only a mesenchymal phenotype but also stem cell-like properties and drug resistance.[112] Our initial goal was to identify targetable metastatic markers, with the eventual goal of treating metastasis. We used scFv - based phage display to seek new extracellular targets in metastatic breast cancer.

As mentioned in section 1.2., phage display utilizes large, diverse libraries of bacteriophage (bacterial viruses) displaying antibody fragments (scFv) on their surface.

These libraries have diversities as high as $10^9 – 10^{12}$, thus allowing high-throughput screening against a desired target. Sequential screening steps lead to the isolation of scFv fragments that are selective for the intended target. We used an isogenic pair of cell lines – HMLE (a normal human mammillary epithelial cell line, "sink") and HMLE-Twist (a metastatic cell line derived from HMLE, "target")[112] – for an *in vitro* bio-panning procedure. This procedure led to the development of a full-length human IgG, Tw1S4_6 ($K_D \sim 1.8\mu M$).[113]

The experimental design for the development of Tw1S4_6 was such that there was no pre-set target antigen. The primary aim was to develop an antibody that binds specifically to HMLE-Twist, but not to HMLE, and in turn identify antigen(s) associated with metastasis. Target deconvolution revealed the target for Tw1S4_6 to be Heparin Sulfate Proteoglycan 2 (HSPG2), also known as perlecan. HSPG2 is a large, 400KDa basement membrane protein that is heavily glycosylated and plays an important role in tethering growth factors. There have been several previous reports demonstrating the involvement of HSPG2 in cancer progression[114,115,116,117], however there are limited reports on its expression or role in breast cancer.[118,119,120]

The work presented in this chapter is focused on evaluating HSPG2 as a marker for metastatic triple negative breast cancer using *in vitro* and *in vivo* models. We evaluated HSPG2 expression in cell lines, circulating tumor cells (CTCs), human breast cancer tissue microarrays as well as determined the correlation between HSPG2 expression and patient survival. Further, we also extended our analysis to different models of metastasis. Our

results suggested that not only is HSPG2 a relevant target in metastatic triple negative breast cancer but is also upregulated in other types of cancers such as melanoma, ovarian cancer and bladder cancer.

2.2. Methods

2.2.1. Materials

All cell culture supplies were obtained from Invitrogen (ThermoFisher Scientific, Waltham, MA) unless otherwise specified. All chemical supplies were purchased from Sigma-Aldrich (St. Louis, MO) unless otherwise specified. Fetal bovine serum (FBS) was purchased from Atlanta Biologicals (Flowery Branch, GA). FACs buffer refers to PBS (Life Technologies, CA) supplemented with 0.5% bovine serum albumin (BSA), 1mM EDTA and 0.1% sodium azide.

2.2.2. Cell Culture

MDA-MB-231-LM2 cells were a gift from Professor Deepali Sachdev at the University of Minnesota and have been previously described as being derived from lung metastasis developed upon intravenous injection of the parental MDA-MB-231 cells in mice. Cells were cultured in MEM supplemented with 10% FBS and antibiotics.

2.2.3. Tissue microarray immunohistochemistry

Human tissue microarrays (Catalog Numbers T088b, MET961) were purchased from USBiomax (Rockville,MD). Tw1S4_6 antibody was used for evaluation of HSPG2 expression. Standard immunohistochemistry was performed by the Comparative Pathology Shared Resource at the University of Minnesota. Images were captured on an inverted

Axiovert 40 CFL microscope at 10X magnification. Quantification of HSPG2 staining was carried out using ImageJ software (NIH).

2.2.4. HSPG2 Expression in tumor cell lines

HSPG2 and EGFR mRNA expression data was obtained from the Broad Institute's Cancer Cell Line Encyclopedia. The breast cancer cell lines were classified into sub-types based on Lehman et al[121] and Jian et al[122].

2.2.5. HSPG2 Expression and Survival Analysis

All survival analysis was conducted in collaboration with Dr. Da Yang at the University of Pittsburgh. To investigate the association between HSPG2 mRNA expression and breast cancer patient survival, we performed a log-rank test for pre-stratified patient groups by expression level. Patients were divided into three groups based on HSPG2 expression from high (first third), intermediate (second third) to low (last third) (n=1085). Since the grouping methods were arbitrary, univariate cox regression was applied to assess the overall association between HSPG2 expression and patient survival for each cancer type.

To investigate the association between mRNA HSPG2 expression and patient survival with triple-negative (ER-, PR-, HER2-) breast cancer (TNBC), log-rank test for pre-stratified patient groups was used. For analysis, patients (n = 298) were divided into three groups based on HSPG2 expression from high (first third), intermediate (second

third), low (last third). Univariate cox regression was applied to assess the overall association between HSPG2 expression and patient survival. All profiled patient samples and HSPG2 expression are from METABRIC.

2.2.6. Analysis of CTCs in Stage 4 melanoma patient samples

Stage 4 melanoma patient blood samples were obtained from Mayo Clinic (Rochester) from Dr. Markovic Svetomir's laboratory. The buffy coat was separated using Ficoll-Paque PLUS density gradient (GE Lifesciences, PA). The cells obtained were frozen at 10 million viable cells/ml in 10% DMSO + 90% FBS until further use. On the day of analysis, twenty million total cells of the buffy coat were thawed per patient sample. CD45 microbeads (Miltenyi Biotec, Germany) were used to deplete majority of the CD45 positive cells as per the company's protocol. The depleted samples were re-suspended in 0.5ml FACs buffer. Each sample was split into two halves, pre-treated with anti-human Fc block and stained with either Tw1S4_6 AF647, anti-EpCAM PE Cy-7, anti-CD45 FITC and anti-CD42b PE or with Tw1S4_6 AF647, anti-EpCAM PE Cy-7 and anti-MCAM PE for 1 hour at 4°C. All antibodies used were purchased from Miltenyi Biotec (Germany) or from eBiosciences (MA). MCAM is a melanoma CTC markers that has been used previously for CTC capture.[123] At the end of one hour, the cells were washed twice and fixed using 2% formaldehyde. 50,000 live cells were analyzed per sample by flow cytometry.

2.2.7. Analysis of CTCs in an Abraxane® resistant model

All experimental protocols using animals were reviewed and approved by University of Minnesota Institutional Animal Care and Use Committee (IACUC) and experiments were performed accordingly. MDA-MB-231-LM2 cells were trypsinized, resuspended in saline and mixed 1:1 (volume:volume) with matrigel (Corning, NY). One million live cells per 100μL were grafted subcutaneously in the fourth mamillary fat pad of Balb/c homozygous nude mice (Charles River Labs, MA or Jackson Labs, ME). Treatments were begun when the tumor volume, measured by Vernier calipers (Marathon) using the formula $V=(L^2xW)/2$ (L being the longer dimension), reached $100mm^3$. Abraxane® (Abraxis Biosciences, CA) was dosed at 40mg/kg equivalent of paclitaxel, every fourth day, for three doses. Mice were sacrificed when the average group volume reached either $300mm^3$ or $1000mm^3$. Blood was collected by cardiac stick into pre-treated EDTA tubes (BD Vacutainer, NJ) to prevent coagulation. The buffy coat was separated using Lymphoprep (Stemcell Technologies, BC Canada). RBCs were lysed using BD Pharm Lyse lysing buffer (BD Biosciences, CA) and the remaining sample was washed with flow buffer, pre-incubated with an anti-mouse Fc Block (Biolegend, CA) and stained with the following antibodies: Tw1S4_6 Alexa Fluor 647, anti-mouse CD45 PE (eBioscience, MA), anti-human EpCAM Pacific Blue (Biolegend, CA).

2.3. Results

2.3.1. HSPG2 expression increases with advancing tumor stage in human breast tumors

HSPG2 expression in human tumors had been previously examined in our lab using IHC[113], however, quantitative analysis was not performed. We observed that HSPG2 expression increased significantly with advancing tumor stage (Figure 2.1C, $P<0.05$, one-way ANOVA with multiple comparisons, statistical significance is based on comparison between NAT and metastatic sites). In addition, we also made an interesting observation that even though normal adjacent tissue (NAT) showed staining in the extracellular matrix (Figure 2.1A), the pattern of this staining was cellular in nature in tissues from metastatic sites (Figure 2.1B).

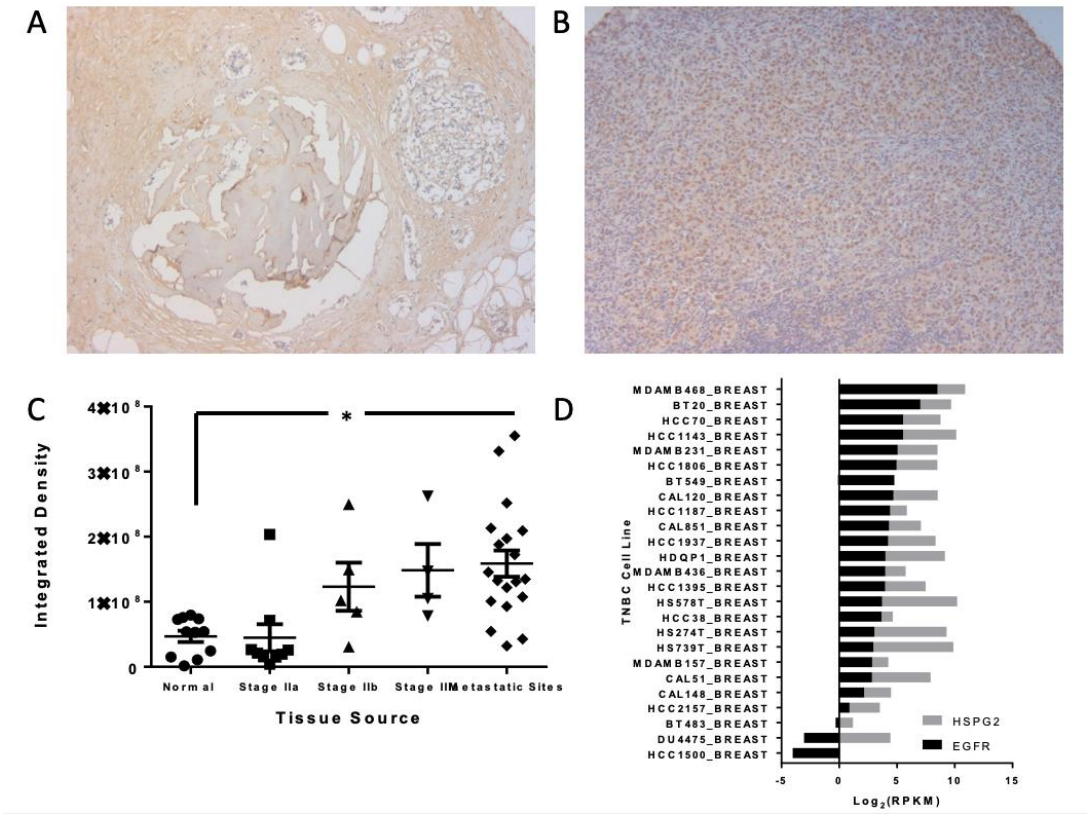

Figure 2.1: HSPG2 expression in human breast cancer tissue microarrays by IHC, mRNA expression in human TNBC cell lines. Representative IHC images (10X magnification) from **(A)** Normal adjacent tissue and **(B)** metastatic tissue. **(C)** HSPG2 expression quantified through Tw1S4_6 immunohistochemistry staining in human breast tumor tissue microarrays. HSPG2 expression increases with increasing tumor stage and is highest at the metastatic sites. (*P<0.05, one way ANOVA with multiple comparisons) **(D)** mRNA expression of HSPG2 and EGFR in TNBC cell lines (Broad Institute Cancel Cell Line Encyclopedia)

2.3.2. HSPG2 is overexpressed in human triple negative breast cancer cell lines

We utilized an open access online database of human tumor cell lines maintained by the Broad Institute of MIT & Harvard (Cancer Cell Line Encyclopedia, https://portals.broadinstitute.org/ccle) to examine HSPG2 expression at the mRNA level. We found significant HSPG2 expression in 22 out of 25 cell lines (Figure 2.1D). In most cases, HSPG2 expression was higher than EGFR, a commonly investigated therapeutic target for TNBC[124–126].

2.3.3. HSPG2 expression correlates with poor patient survival for TNBC

To determine whether there was an association between HSPG2 expression and disease prognosis, we conducted an analysis using the METABRIC database [PMID: 27161491] in collaboration with Dr. Da Yang at University of Pittsburgh. In the case of all breast cancer subtypes, there was no correlation between HSPG2 expression and patient survival ($P>0.05$, multi-group log-rank test) (Figure 2.2A). When the pre-stratified analysis was narrowed specifically to patients with TNBC, we observed a significant decrease in survival with higher HSPG2 expression in TNBC ($P<0.05$, multi-group log-rank test) (Figure 2.2B). A univariate cox regression analysis yielded a hazard ratio of 7.95 ($P<0.01$).

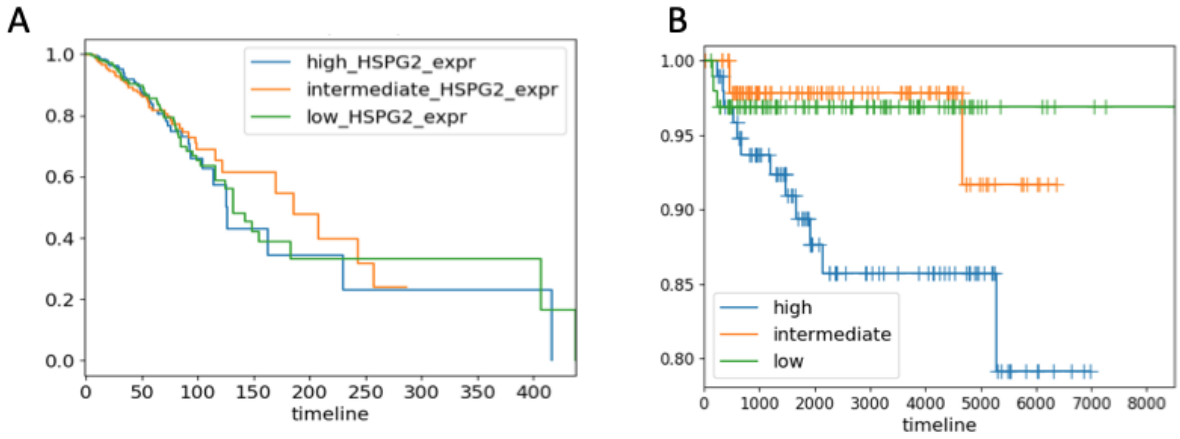

Figure 2.2: Survival analysis in bladder cancer patients based on HSPG2 expression **(A)** Survival analysis based on HSPG2 Expression. All patient and HSPG2 expression data were obtained from METABRIC. For patients with TNBC, high HSPG2 expression correlates with significantly poorer survival ($P<0.005$, multi-group log-rank test). **(B)** Survival analysis based on HSPG2 Expression. All patient, HSPG2 expression data were obtained from METABRIC. For patients with breast cancer and HSPG2 expression does not correlate with survival ($P>0.05$, multi-group log-rank test).

2.3.4. CTCs from an Abraxane® resistant tumor model have higher HSPG2 expression

To understand the clinical context of CTCs recognized by Tw1S4_6, we evaluated changes to this CTC population following treatment with Abraxane®[127], an albumin nanoparticle formulation of paclitaxel that is a key therapy option for metastatic TNBC patients who fail to respond to an initial taxane/anthracycline dosing regimen[128]. A dosing

schedule that promoted a brief remission prior to tumor rebound was used. In the chemotherapy naïve group (Fig 2.3A, Saline 1000), four of five mice had 5 or fewer Tw1S4_6 positive CTC's per 10^6 events analyzed (Figure 2.3B). Mice bearing size-matched, post-Abraxane® recurrent tumors had a significantly higher number of Tw1S4_6 positive CTCs (one-way ANOVA, non-parametric with multiple post-comparison tests, $P<0.05$), with several mice bearing 5- to 25-fold more Tw1S4_6^+ CTCs (Fig 2.3B). Enrichment of EMT marker expression in CTCs following chemotherapy has been a frequent clinical observation[129,130]. While more in-depth studies are needed, these results suggest that Tw1S4_6 could indeed be identifying a drug resistant, metastatically aggressive subset of CTCs.

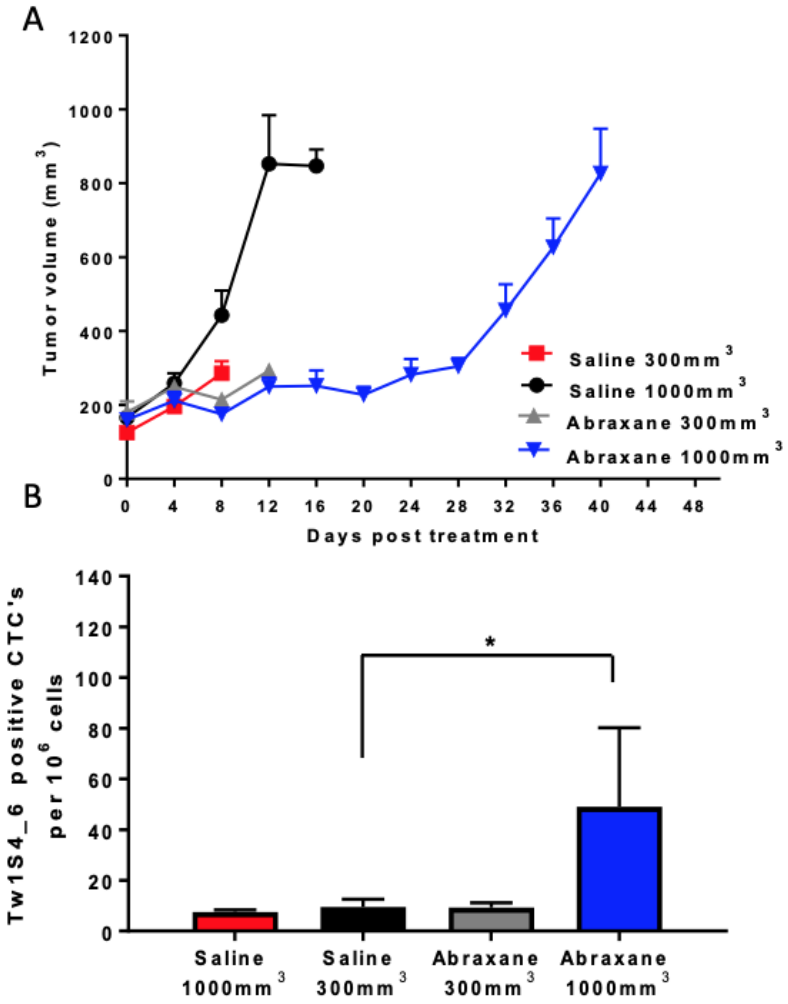

Figure 2.3: **(A)** Tumor volumes measured through the duration of the study. Mice from the two treatment groups (Saline or Abraxane) were sacrificed when the group average reached either 300mm^3 or 1000mm^3 (n=3-5 per group, per time point) **(B)** Number of Tw1S4 positive CTCs detected per million PBMCs analyzed by flow cytometry. Number of Tw1S4 positive events were significantly higher in the Abraxane treated group at a tumor volume of 1000mm^3 (one way ANOVA, non-parametric with multiple post-comparison tests, Saline 300mm^3 v/s Abraxane 1000mm^3 ,*P<0.05).

2.3.5. HSPG2 expression is observed in tissue samples from patients with bladder cancer and ovarian cancer

Considering that metastasis is a common occurrence in almost all types of cancers, we evaluated whether HSPG2 expression is also upregulated in other types of cancers. A previous report showed elevated HSPG2 expression in tumor tissues from glioblastoma patients.[116] Thus, we extended our analysis to bladder and ovarian cancers. We analyzed HSPG2 protein expression by IHC in human tumor samples. In bladder cancer, tissues of almost all stages showed consistently high expression of HSPG2 (Figure 2.4B). We did not observe a trend of increasing expression with increasing tumor stage as was in the case of triple negative breast cancer. In the case of ovarian cancer, we had a similar observation – the expression of HSPG2 was significantly higher ($P<0.05$ for all stages other than stage 4, one way ANOVA with multiple comparisons) than that in normal tissue (Figure 2.5B).

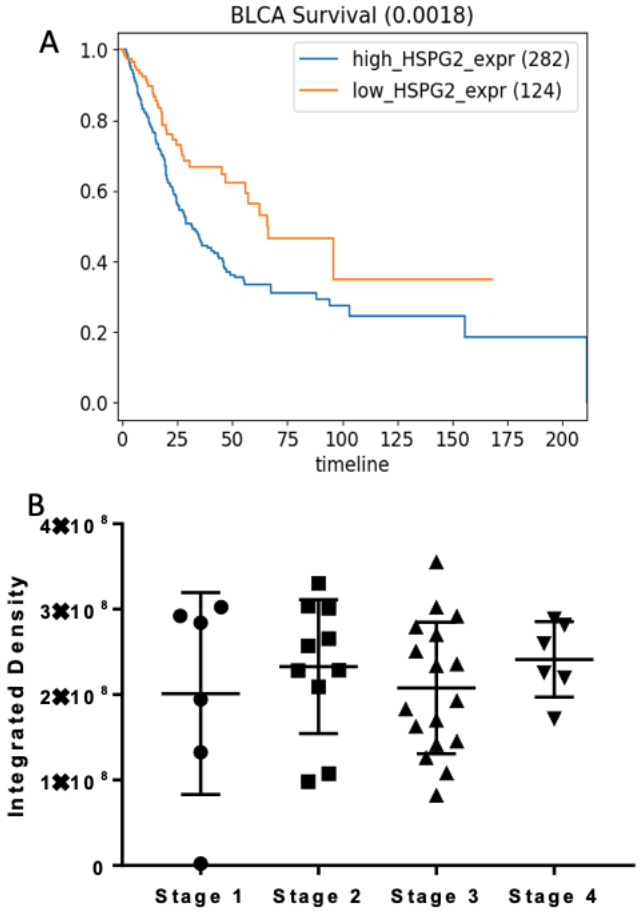

Figure 2.4: Survival analysis in bladder cancer patients based on HSPG2 expression **(A)** For patients with bladder cancer, high HSPG2 expression correlates with significantly poorer survival (P<0.005, paired log-rank test). **(B)** Quantified HSPG2 expression through Tw1S4_6 immunohistochemistry staining in human bladder tumor tissue microarrays (HBlaU066Su01, USBiomax)**.** HSPG2 expression is consistently high across all stages.

2.3.6. HSPG2 expression correlates with poor patient survival for bladder cancer and ovarian cancer

Similar to that for TNBC, we observed significantly greater survival ($p<0.05$) in bladder cancer patients with lower HSPG2 expression when we performed a log-rank test for pre-stratified patient groups by expression level (Figure 2.4A). Similar trends were also observed in ovarian cancer patients, where patients with lower HSPG2 expression tended to have better survival. (Figure 2.5A). Univariate cox regression analysis yielded hazard ratios of 1.29 ($P<0.001$) and 1.099 ($P>0.05$) for bladder and ovarian cancer respectively.

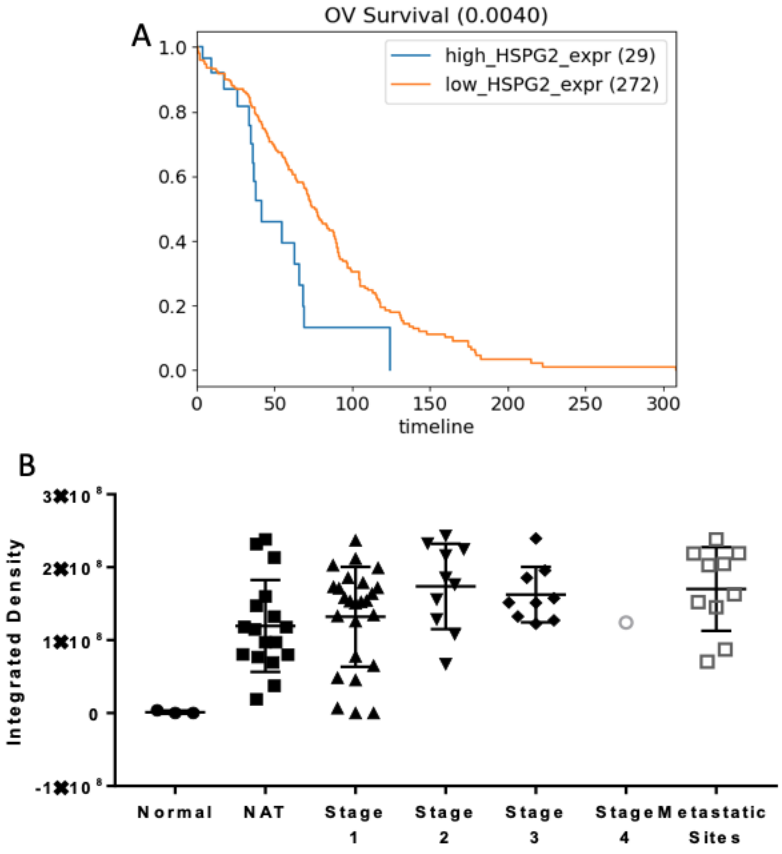

Figure 2.5: Survival analysis in ovarian cancer patients based on HSPG2 Expression **(A)** For patients with ovarian cancer, high HSPG2 expression correlates with significantly poorer survival (P<0.005, paired log-rank test). **(B)** Quantified HSPG2 expression through Tw1S4_6 immunohistochemistry staining in human ovarian tumor tissue microarray (OV1005b, US Biomax)**.** HSPG2 expression is consistently high across all stages, and significantly higher than normal ovarian tissue (P<0.05 for all stages other than stage 4, one-way ANOVA with multiple comparisons)

2.3.7. Melanoma patients have distinct sets of CTCs expressing HSPG2

For data presented in Figure 2.6A, the $CD45^-/CD42b^-$ population was gated and analyzed for expression of HSPG2 ($Tw1S4\_6^+$ staining) and EpCAM. The $Tw1S4\_6^+$ events were more numerous (ranging from 0-15 events) as opposed to the $EpCAM^+$ events (ranging from 0-2 events) (data not statistically significant). We observed no double positive events in any of the samples analyzed.

In order to confirm that we are indeed analyzing CTCs, we used a well-accepted marker for melanoma CTCs (MCAM) followed by analysis for Tw1S4_6 and EpCAM expression (Figure 2.6B). We found a definite overlap between both MCAM and Tw1S4_6, however the extent of overlap varied between patients. This points towards the inherent heterogeneity of CTCs, warranting the use of multiple markers. The results once again showed that $Tw1S4\_6^+$ events were significantly more numerous as opposed to $EpCAM^+$ events (Wilcoxon T-test, $P<0.05$).

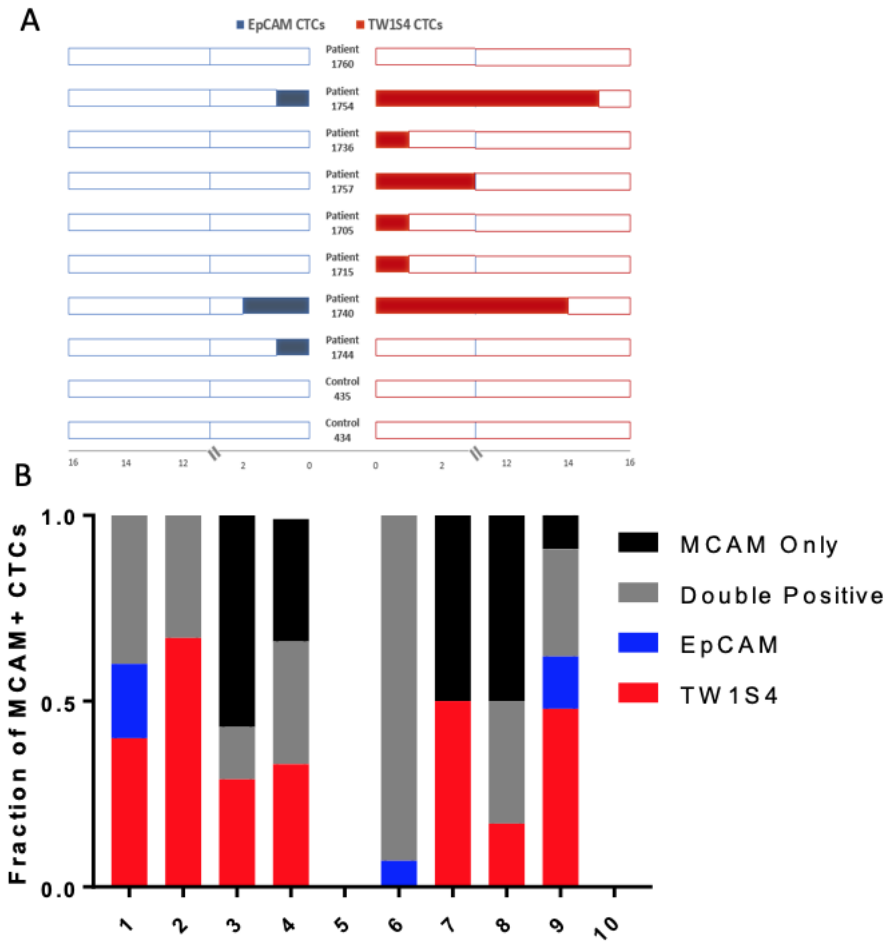

Figure 2.6: Analysis of CTCs from melanoma patients **(A)** Number of Tw1S4 positive or EpCAM positive CTCs detected per million PBMCs analyzed by flow cytometry. Number of Tw1S4 positive events range from 0-15 as compared to EpCAM positive events that range between 0-2. Data not statistically significant. **(B)** Fraction MCAM positive CTCs that are $Tw1S4^+$, $EpCAM^+$, $Tw1S4^+/EpCAM^+$ (double positive) or neither. A significantly higher fraction of $MCAM^+$ CTCs were $Tw1S4^+$, rather than $EpCAM^+$ (Wilcoxon T-test, $P<0.05$).

2.4. Discussion

The development of targeted therapeutics for specific breast cancer subtypes has led to the significantly improved survival rates observed at the early stages of this disease.[131] Trastuzumab (Herceptin®) is a classical example of a targeted therapeutic that has remarkably improved the outcome for patients presenting with $HER2^+$ breast cancer.[132] Unfortunately, such a targeted therapy is not available for TNBC. Patients presenting with TNBC must resort to traditional chemotherapeutic agents that are non-targeted and thus plagued with severe toxicities.[133] This is largely due to a lack in the identification of unique biomarkers for TNBC that can be leveraged for targeted therapy development. Metastatic TNBC presents a further complication resulting in poor outcomes.

In the drug discovery pipeline, a common approach is to look for anomalies at the genetic level of a disease, and utilize identified anomalies as molecular targets for drug development. However, at the genetic level, it is unlikely to be able to successfully predict the translated format of the protein. Most post-translational modifications such as phosphorylation, glycosylation, ubiquitination and bond formation, amongst others, go largely undetected. Thus, in order to successfully identify markers that are readily translatable into the clinic, it is critical to study a disease at the protein level, in its physiological state. Phage display is a powerful tool that can be utilized for this purpose.[20] We used scFv based phage display to develop antibodies targeted to metastasis, and in turn

discovered a protein – HSPG2 – that is overexpressed in metastatic triple negative breast cancer.

HSPG2 is a protein found in the extracellular matrix, and is critical for normal development.[134,135] In fact, in homozygous HSPG2 knock-out mice, most embryos die with pericardial bleeding by embryonic day 10.[134] When HSPG2 was knocked down in metastatic prostate cancer, it led to a reduction in VEGF and FGF mediated cell proliferation.[115] A similar study in colon cancer demonstrated a reduction in tumor growth when HSPG2 was knocked down.[117] Thus, the implication that HSPG2 is involved in the pathogenesis of tumors is not uncommon. Our work presented here was focused on understanding the relevance of HSPG2 in metastatic TNBC. We were also able to extend our analysis to other cancer types including melanoma, bladder cancer and ovarian cancer.

After an initial analysis of cancer cell lines from the Broad Institute's cancer cell line database, we found that a of majority of human TNBC cell lines were positive for HSPG2. In fact, a simultaneous analysis of EGFR in those cell lines revealed that HSPG2 expression was significantly higher in certain cases. There have been several reports suggesting the use of EGFR targeted therapies for the treatment of TNBC.[124–126,136,137] However considering this dataset, it would likely be more advantageous to target HSPG2 in specific patient subsets. Further, we analyzed HSPG2 expression directly in human tumor samples. Not only were the tissues HSPG2 positive but there was also a significant correlation between HSPG2 expression and cancer stage as well as between HSPG2 expression and patient survival. On the whole, our results suggested that not only is HSPG2

a relevant target in metastatic triple negative breast cancer but also that it is an indicator of poor prognosis. Previous studies from our lab have shown that HSPG2 is also expressed on circulating tumor cells (CTCs), which form the precursors of metastasis[113]. We found that a significantly higher number of CTCs from chemotherapy-resistant mice expressed HSPG2 as compared to the chemotherapy naïve mice, suggesting that HSPG2 is not only found on more aggressive tumor sub-types but is also indicative of drug resistance.

Considering the association of HSPG2 with metastatic TNBC, we (and others) have hypothesized that HSPG2 is likely involved in other tumor types that also undergo metastasis. Thus, we extended our work to include other types of cancer. We found that HSPG2 is expressed in human bladder cancer and ovarian cancer tissues and its expression correlated with poor patient survival. Additionally, in melanoma patients, specific sub-sets of CTCs were enriched with HSPG2. The expression of HSPG2 did not necessarily co-exist with commonly studied CTC markers, pointing to heterogeneity within CTCs. Further studies are required to determine the importance and consequences of $HSPG2^{+}$ CTCs.

It has been previously reported that growth factors such as bFGF and bind to HSPG2 (in addition to their own receptor) and can be made available to the growth factor receptors as and when required for development.[135,138,139] Hence, HSPG2 is also known as a "co-receptor". In essence, HSPG2 is able to hold a 'reserve' of growth factors that can be unleashed by the tumor as required. Further studies are required to understand whether this is an indirect mechanism of HSPG2 that is able to promote tumor growth or whether it is directly involved in tumor progression.

2.5. Conclusion

Phage display enabled the identification of HSPG2 as a novel marker for TNBC as well as bladder cancer, ovarian cancer and melanoma. This represents a potential new point of focus for developing new diagnostic and therapeutic approaches for metastatic disease.

Chapter 3: Applications and mechanisms of anti-HSPG2 antibodies

3.1. Introduction

HSPG2, an extracellular matrix glycoprotein, has been shown to be overexpressed in several different solid tumors.[113,114,117,140] The results of our experiments described in chapter 2 show that HSPG2 expression is closely associated with metastatic triple negative breast cancer. HSPG2 is normally present in the basement membrane and extracellular matrix of healthy tissues but is overexpressed on the surface of tumor cells as observed in our studies. Our studies show that HSPG2 is overexpressed in a number of different TNBC cell lines. We previously developed two human monoclonal antibodies against HSPG2 - Tw1S4_6 (intrinsic Kd ~ 1.8μM) and Tw1S4_AM6 (intrinsic Kd ~ 80nM) with the goal of targeting $HSPG2^{+}$ tumor cells.[113] The two antibodies, Tw1S4_AM6 in particular, demonstrated inhibition of tumor growth in an *in vivo* mouse model of metastatic TNBC. However, the mechanism of tumor growth inhibition with these antibodies was not established.

Antibodies may act via receptor mediated interactions, checkpoint inhibition or by recruiting immune cells against the tumor.[5] The studies discussed in this chapter were focused on understanding the mechanism of efficacy of anti-HSPG2 antibodies. Additionally, we also investigated the bio-distribution of the two antibodies. Our studies show that Tw1S4_AM6 works primarily through ADCC, with minimal involvement of other mechanisms.

Additionally, antibodies have found extensive application as targeting agents.[141,142] In the present study, we also investigated anti-HSPG2 antibodies for tumor-directed drug delivery. In a previously published study, we fabricated poly(D,L-lactide-co-glycolide) (PLGA) nanoparticles encapsulating paclitaxel as a model chemotherapeutic agent and surface functionalized them with the anti-HSPG2 antibodies.[143] These HSPG2 targeted nanoparticles showed promising efficacy in an *in vivo* model of TNBC.

3.2. Methods

3.2.1. Materials

All cell culture supplies were obtained from Invitrogen (Waltham, MA) or Corning (Tewksbury, MA), unless otherwise specified. Fetal bovine serum (FBS) was purchased from Atlanta Biologicals (Flowery Branch, GA). PLGA (50:50, 0.55-0.75Dl/g) was purchased from LACTEL Absorbable Polymers (Birmingham, AL). Polylactide-polyethylene glycol with terminal maleimide functionalization (PLA-PEG-Maleimide) (AI119) and PLGA-Rhodamine (AV011) were purchased from PolySciTech (West Lafayette, IN). Polyvinyl alcohol (PVA, 30,000-70,000 MW), sucrose, 2-imminothiolane hydrochloride, and ethylenediaminetetraacetic acid (EDTA) were purchased from Sigma (St. Louis, MO). Paclitaxel was purchased from Phytogen Life Science (B.C, Canada). Borate buffer stock was purchased from Alfa Aeser (Ward Hill, MA). Control Isotype IgG (Cat. No. 401114) was purchased from Calbiochem (Billerica, MA). The materials for SDS/PAGE were obtained from Bio-Rad (Hercules, CA). HPLC grade organic solvents were obtained from Fisher Scientific (Pittsburgh, PA). Deionized (DI) water was available through university resources.

3.2.2. Cell Culture

MDA-MB-231-LM2 cells were a gift from Professor Deepali Sachdev at the University of Minnesota and have been previously described as being derived from lung

metastasis developed upon intravenous injection of the parental MDA-MB-231 cells in mice. Cells between passages 2-10 were used for all the studies. Cells were cultured in minimum essential medium (MEM) with 10% v/v fetal bovine serum (FBS) and 1% v/v penicillin/streptomycin in a humidified atmosphere with 5% CO_2.

3.2.3. Preparation and Purification of Antibodies

Expi293F Expression System by Life Technologies (Carlsbad, CA) was used for the expression of human IgG antibodies. Affinity purification of antibodies was carried out using Protein A Plus (Pierce, Rockford, IL) followed by buffer exchange into tris-buffered saline containing 5mM EDTA. Zeba™ Spin Desalting Columns (87769, Pierce Biotechnology, Rockford, IL) were used for the buffer exchange step. Antibody stocks were stored at -20°C in single use aliquots until use. Once thawed, the samples were placed at 4°C for short-term storage. Quality control evaluation involved resolution via SDS/PAGE for reduced and non-reduced samples and flow cytometry for confirmation of binding affinity. For flow cytometry, the antibodies were incubated with MDA-MB-231-LM2 cells at a concentration of 100 nM for 1 hour at 4°C on a rotating platform (Barnstead International, Dubuque, IA), followed by three washes using FACS Buffer. Alexa 647 goat anti-human secondary antibody (Life Technologies, Carlsbad, CA) was added and the cells were incubated at 4°C for 30 minutes on a rotating platform, followed by 3 washes. The cells were re-suspended in flow buffer and placed on ice until analysis by flow cytometry (BD LSRFortessa).

3.2.4. Tumor growth inhibition studies

MDA-MB-231-LM2 tumors were grafted in Balb/c homozygous nude mice or Balb/c NSG mice as described above (Charles River Labs or Jackson Labs). Once tumor volumes reached 100 mm^3, three doses (5 mg/kg) of the antibodies were administered through tail vein injection once every 96 hrs. Isotype human IgG and saline were used as controls (n=7 for nude mice, and n=4-6 for NSG mice). Tumor volumes were measured every third day with digital Vernier calipers (Marathon Watch, Vaughn, Canada). Tumor volumes were calculated from the ellipsoid sphere equation $V = (L^2 * W)/2$, L being the longer measurement. Two way ANOVA, with multiple comparison post-tests, was used to determine the statistical significance of the data.

3.2.5. Cell proliferation and cell cycle analysis

For the cell cycle assay, MDA-MB-231-LM2 cells were seeded at 50,000 cells per well in a six-well plate, allowed to adhere overnight and serum starved for another 24 hours followed by addition of treatments. All antibodies were used at a final concentration of 300nM in complete media. Cells were collected by trypsinization after 48 hours and stained with PI, analyzed by flow cytometry (BD LSR II) to determine cell cycle stage.

For the cell proliferation assay, MDA-MB-231-LM2 cells were seeded at 2000 cells per well in a 96 well plate. The next day treatments were added at the indicated concentrations (antibodies and drug). After 48 hours, an MTS assay (Promega, WI) was conducted to determine relative cell survival.

3.2.6. Kinetics of antibody tumor accumulation

Mice bearing MDA-MB-231-LM2 tumors (~300 mm^3) were injected with 100 µg of labeled isotype IgG Control, Tw1S4_6 or Tw1S4_AM6 (n=3). Antibodies were labeled with Cy7 maleimide (Click Chemistry Tools, Arizona) using immunothiolation to introduce reactive thiols onto the antibody. Mice were imaged using the IVIS Spectrum In Vivo Imaging System (University of Minnesota Imaging Centre) at various time intervals over 120 hours using an excitation and emission filters of 750 nm and 775 nm, respectively. Data was acquired and analyzed using Living Image software. Data was tested for statistical significance using two way ANOVA, with multiple comparison post-tests.

3.2.7. ADCC Assays with Human PBMCs and Mouse Splenocytes

Human PBMCs (effector cells) from healthy donors were purified using Ficoll-Paque density gradient media (GE Healthcare), incubated overnight at 37˚C in RPMI (10% FBS, 1% P/S) and used for the assay the next day. Target cells (MDA-MB-231-LM2) were labeled with 8 µM CFSE (Biolegend, CA, USA) for 20 minutes at room temperature, followed by two washes. CFSE labeled target cells were then incubated with 100 nM of the relevant antibodies in suspension at 4˚C for 1 hour, washed once and then used for the assay. Effector and target cells were incubated together in 96 well plates, at the specified ratios overnight at 37˚C. The next day, plates were centrifuged at 1200 RPM for 5 minutes and 50 µL of supernatant was collected and cell cytotoxicity was measured using LDH assay kit (Thermo Fisher Scientific, CA, USA). The remaining media was aspirated,

followed by addition of 100 µL PBS. The plates were read using a plate reader at Ex/Em 485/528 nm to determine relative cell viability.

Mouse splenocytes were obtained from the spleen of healthy Balb/c homozygous nude mice [84]. The cells were stimulated for 48 hours with 500 units/mL IL2 (R&D Systems, MN, USA), after which they were washed, counted and used for ADCC assay as described above.

3.2.8. Human PBMCs Degranulation Assay

Human PBMCs ($5x10^5$/well) were seeded in a 24-well cell culture plate. To achieve sub-optimal activation of PBMCs, polyinosinic–polycytidylic acid (poly I:C) (10 µg/ml) was added to the media. After 18 hr incubation, MDA-MB-231-LM2 cells ($2.5x10^5$/well) were added to the PBMCs. Subsequently, isotype IgG control, Tw1S4_6 or Tw1S4_AM6 antibodies (200 nM) were added to the media and anti-CD107a antibody was added directly into the media. After 1 hr, brefeldin A solution (Biolegend) was added to the media. Cells were collected after 3 hr and stained with anti-CD3 and anti-CD56 antibodies. Intracellular staining of interferon gamma (IFN-ɣ) was conducted according to the manufacturer's protocol (Foxp3/Transcription Factor Staining Buffer Kit, Tonbo bioscience). Stained cells were analyzed by flow cytometry (LSRFortessa H0081, BD bioscience).

3.2.9. CDC Assays with Mouse and Human Serum

Target cells (MDA-MB-231-LM2) were incubated with varying concentrations of the relevant antibodies in suspension at 4˚C for 1 hour, washed once and then used for the assay. Target cells were incubated in serum-free media containing 10% normal mouse serum (Sigma-Aldrich, Missouri, USA) or 50% normal human serum (Sigma-Aldrich, Missouri, USA) depending on the assay, in 96 well plates overnight at 37˚C. The next day, 50 µL of supernatant was used for LDH assay (Thermo Fisher Scientific, CA, USA) and the remaining media was removed. Cell viability was determined by MTS assay (Promega, Wisconsin, USA).

3.2.10. Preparation of PEG-Maleimide Functionalized PLGA Nanoparticles

PLGA nanoparticles surface functionalized with maleimide terminated PEG and loaded with paclitaxel were synthesized as described in an earlier publication[144]. Briefly, PLGA (30 mg) and coumarin-6 (100 µg) or PLGA (25 mg) and PLGA-rhodamine (5 mg) along with paclitaxel (5 mg) were dissolved in 1 ml of chloroform. An oil-in-water emulsion was formed by emulsifying the polymer-drug solution in 8 ml of 2.5% w/v aqueous PVA solution by probe sonication (18–24 W; Sonicator XL, Misonix, Melville, NY) for 5 minutes over an ice bath. The diblock copolymer PLA-PEG-Maleimide was dissolved in chloroform (200 µl) and added drop-wise to the above emulsion with stirring. The emulsion was stirred for 16 -18 hours under ambient conditions followed by 1 hour

under vacuum to remove the residual chloroform. Nanoparticles were washed twice by ultracentrifugation (35,000 rpm for 35 min at 4°C, Optima XPN-80, Beckman Palo Alta, CA) and reconstitution in DI water. The final nanoparticle dispersion was then stored at 4°C until the conjugation reaction which was performed on the same day.

Once the thiolated antibodies were desalted, the samples were added to the nanoparticle dispersion and placed on a rotating platform at 4°C to allow the conjugation reaction to take place overnight. Nanoparticles were then washed once by ultracentrifugation (35,000 rpm for 35 min at 4°C) and dispersed in 5 ml DI water containing 30 mg sucrose (lyoprotectant). The final dispersion was probe sonicated (30 seconds, 6-9W) on an ice bath and centrifuged at 1000 RPM for 5 min to pellet any large aggregates. The supernatant was then lyophilized (Labconco, FreeZone 4.5, Kansas City, MO). The lyophilized product was stored in a desiccator at 4°C until use. An isotype human IgG was used to make control nanoparticles, termed as isotype IgG NPs.

3.2.11. *In vivo* efficacy study with nanoparticles

MDA-MB-231-LM2 tumors were grafted in Balb/c homozygous nude mice (Jackson Labs). Once tumor volumes reached 100 mm^3, a total of six doses (20 mg/kg equivalent dose of paclitaxel) of nanoparticles were administered through tail vein injection once every 96 hrs. One set of animals did not receive any treatment and served as untreated controls. Tumor volumes were measured every third day with digital Vernier calipers (Marathon Watch, Vaughn, Canada). Tumor volumes were calculated from the ellipsoid

sphere equation $V = (L^2 * W)/2$, L being the longer measurement. Two way ANOVA, with multiple comparison post-tests, was used to determine the statistical significance of the data.

3.3. Results

3.3.1. Anti-perlecan antibodies mediate their activity via components of the immune system

Human IgGs are capable of engaging with murine FcγR expressed on various immune effector cells[145]. Previously in our lab, MDA-MB-231-LM2 tumors grafted in Balb/c athymic nude mice were used as an *in vivo* model capable of facilitating ADCC when using human IgGs. Tw1S4_6 IgG produced marginal tumor growth inhibition relative to the saline treated group. Tw1S4_AM6, on the other hand, significantly inhibited tumor growth, resulting in a mean tumor volume of 500 mm^3 on day 22, relative to saline and isotype control groups, which had mean tumor volumes >1,500mm^3 ($P<0.001$, two-way ANOVA with multiple comparisons, statistical significance is based on comparison between isotype IgG and Tw1S4_AM6 on the last day of the study, Figure 3.1A).[113]

To evaluate the specific contribution of immune based effector cells in the mechanism of anti-HSPG2 antibodies, we used the severely immunocompromised NSG mouse model[146]. An identical graft model in NSG mice led to a statistically significant reduction in tumor volumes for Tw1S4_6 and Tw1S4_AM6 ($P<0.01$, two-way ANOVA with multiple comparisons, statistical significance is based on comparison between Isotype IgG and Tw1S4_AM6 on the last day of the study, Figure 3.1B). The reduction in tumor volumes, however, was severely blunted relative to that in the Balb/c nude model (mean

tumor volume >1000mm^3 on day 20), suggesting a significant contribution of immune based effector cells to the efficacy of Tw1S4_AM6.

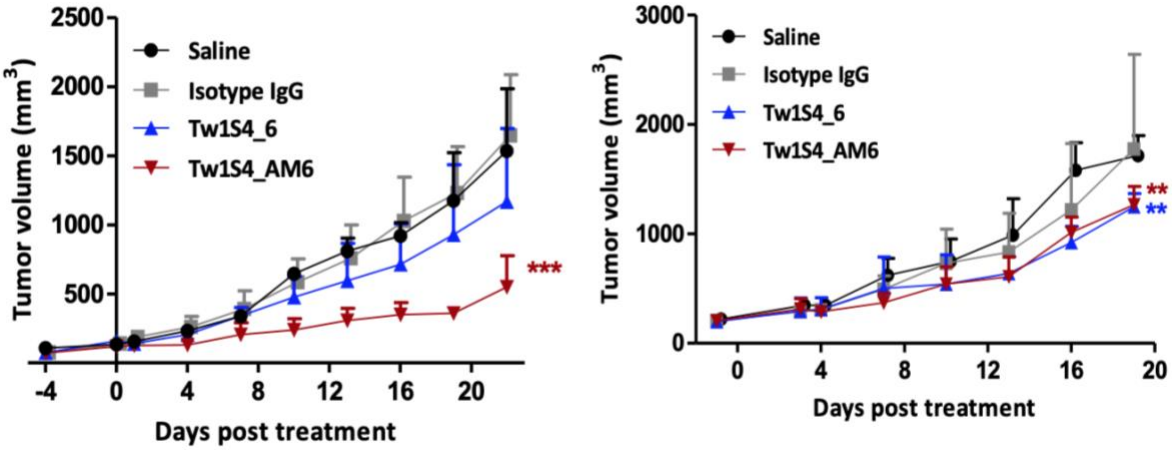

Figure 3.1: *In vivo* efficacy studies with anti-perlecan antibodies with MDA-MB-231-LM2 subcutaneous tumors grafted on variable immunocompromised models **(A)** Efficacy study in Balb/c athymic nude mice. Tw1S4_AM6 showed significant tumor inhibition (***P<0.001, two-way ANOVA with multiple comparisons, statistical significance is based on comparison between isotype IgG and Tw1S4_AM6 on the last day of the study) **(B)** Efficacy study in Balb/c NSG mice. Tw1S4_AM6 AND Tw1S4_6 showed significant tumor inhibition (**P<0.01, two-way ANOVA with multiple comparisons, statistical significance is based on comparison between Isotype IgG and the referenced groups, on the last day of the study)

3.3.2. Tw1S4_6 and Tw1S4_AM6 show no effects on cell proliferation *in vitro*

In order to further delineate the mechanism of action of Tw1S4_6 and Tw1S4_AM6, we tested the naked antibodies *in vitro* to determine their effects on the cell cycle and in turn on proliferation. Neither Tw1S4_6, nor Tw1S4_AM6 showed any statistically significant (two-way ANOVA with multiple post-comparison tests) effects on the cell cycle (Figure 3.2A) or on absolute cell proliferation (Figure 3.2B). It must be noted here that the concentrations tested were much higher than in the case of other antibodies that have shown direct activity [147,148].

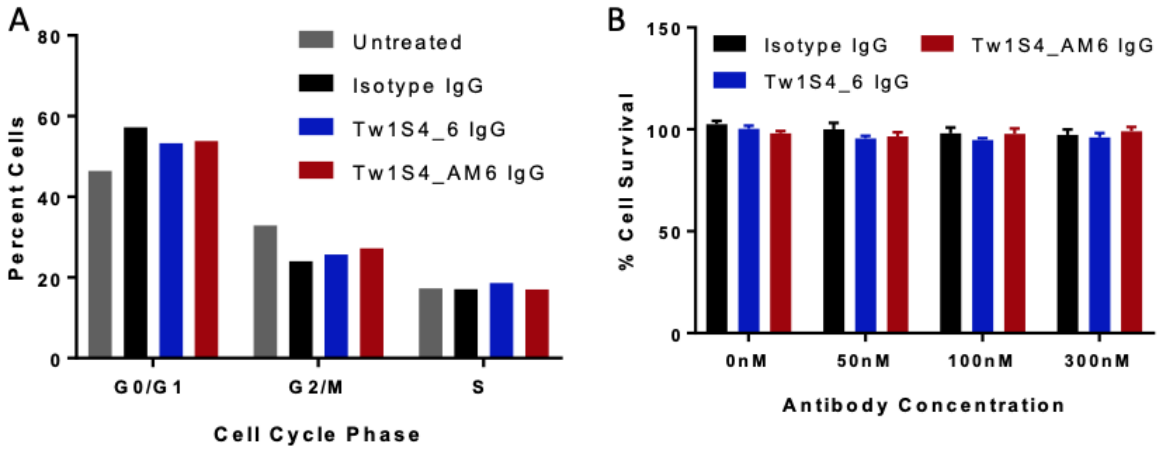

Figure 3.2*: In vitro* cell proliferation and cell cycle assays with anti-HSPG2 antibodies **(A)** Anti-HSPG2 antibodies have no effect on cell cycle at the tested concentrations i.e. 300nM **(B)** Anti-HSPG2 antibodies did not have any effect on cell survival. Statistical analysis determined via two-way ANOVA with multiple post-comparison tests.

3.3.3. Tw1S4_AM6 mediates ADCC *in vitro* with mouse splenocytes, but does not mediate CDC

The observed differences in efficacy in Balb/c nude versus Balb/c NSG mouse models suggested the possible involvement of immune based effector cells in mediating the anticancer efficacy of anti-HSPG2 antibodies, in particular antibody dependent cellular cytotoxicity (ADCC).[7] To investigate this, we carried out *in vitro* ADCC assays with mouse splenocytes.[84] Tw1S4_AM6 induced ADCC resulting in cell survival of 8%, as opposed to 33% with Tw1S4_6 and 19% with isotype IgG at an effector-to-target (E:T) ratio of 20:1 ($P<0.01$, two way ANOVA with Tukey's multiple comparison tests, statistical significance is based off comparison between Tw1S4_6 and Tw1S4_AM6 at E:T 20:1, Figure 3.3A). A similar trend was observed at lower E:T ratios of 10:1 and 5:1. The inclusion of IL-2 in the assay resulted in high non-specific cell kill. However, previous reports suggested that human antibodies do not induce cell lysis with mouse effector cells unless stimulated[84]. It was not surprising that Tw1S4_6 showed no ADCC *in vitro* considering that antibody affinity has been shown to be a critical parameter in determining ADCC outcome, as discussed in section 1.9.1[84]. Another possible mechanism exerted by antibodies is complement dependent cytotoxicity (CDC).[67] However, we did not observe any cytotoxicity *in vitro* with mouse serum (Figure 3.3B).

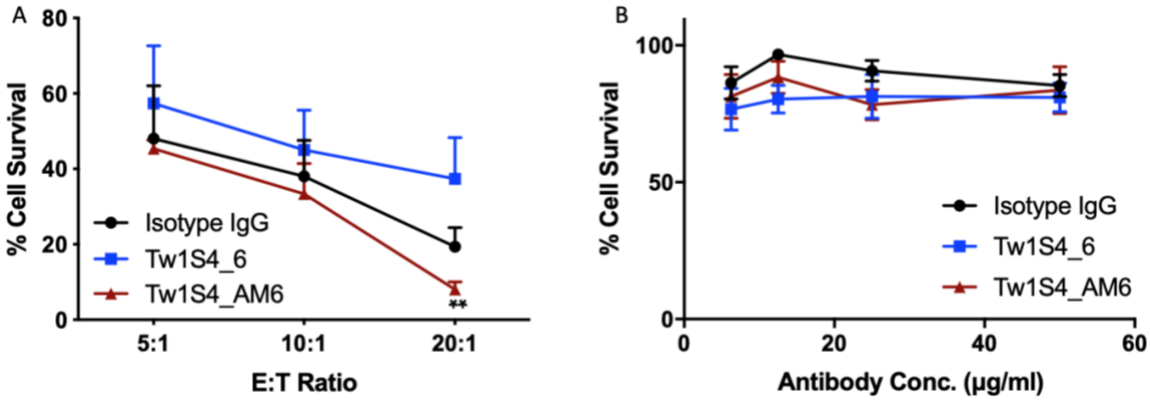

Figure 3.3*: In vitro* ADCC and CDC assays with mouse immune components **(A)** ADCC assay with mouse splenocytes. Tw1S4_AM6 treated groups showed reduced cell survival. (**P<0.01, two way ANOVA with Tukey's multiple comparison tests, statistical significance is based off comparison between Tw1S4_6 and Tw1S4_AM6 at E:T 20:1) **(B)** CDC assay with mouse serum showed no significant cytotoxicity with Tw1S4_6 or Tw1S4_AM6

3.3.4. Tw1S4_AM6 mediates NK cell degranulation *in vitro* with human PBMCs

In order to test the translational potential of the Tw1S4 antibodies, we decided first to perform an *in vitro* degranulation assay with human PBMCs. NK cells undergo degranulation (section 1.8.3) when they come in contact with the constant domain of an antibody via the Fcγ activating receptors. Degranulation involves the release of cytotoxic molecules that 'punch holes' in the cell membrane (perforin) and induce apoptosis

(granzyme B).[82] These molecules are contained in 'lytic granules' and are released when lytic granules fuse with the cell membrane. This fusion leads to the expression of CD107a (a lytic granule membrane protein) on the surface of NK cells and is commonly used as a marker for degranulation.[82]

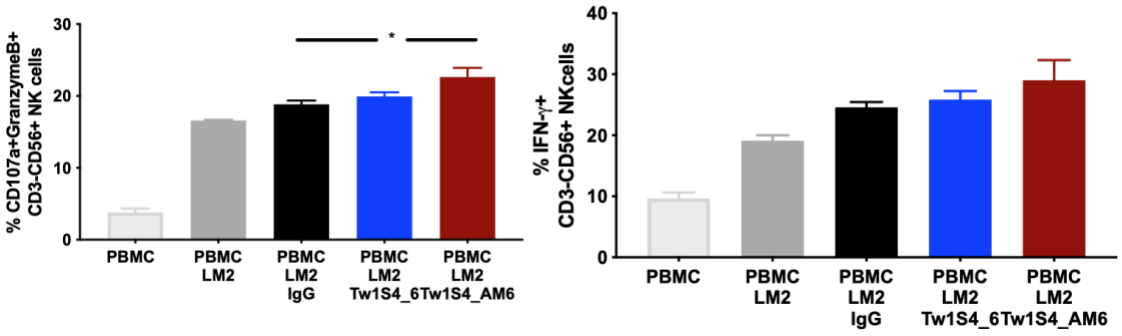

Figure 3.4: NK cell degranulation assay with human PBMCs (Donor I). Tw1S4_AM6 treated groups showed **(A)** increased fraction of NK cells undergoing degranulation (*P<0.05, one way ANOVA with multiple comparison tests) and **(B)** increased fraction of NK cells secreting IFN-G (P>0.05, one way ANOVA with multiple comparison tests)

We tested degranulation of NK cells in response to treatment with different antibodies using PBMCs from two donors. We observed an increase in the fraction of CD3/CD56^{+} NK cells positive for CD107a (P<0.01, one way ANOVA with multiple comparison tests, Figure 3.5A), a degranulation marker (11% for Isotype IgG v/s 20% for Tw1S4_AM6). In addition, we also observed an increase in the fraction of CD3^{-}/CD56^{+}

secreting IFN-γ (P<0.01, one way ANOVA with multiple comparison tests, Figure 3.5B), a cytokine responsible for T cell activation (11% for Isotype IgG v/s 19% for Tw1S4_AM6). A similar trend was observed in studies with PBMCs from a second donor (Figure 3.4).

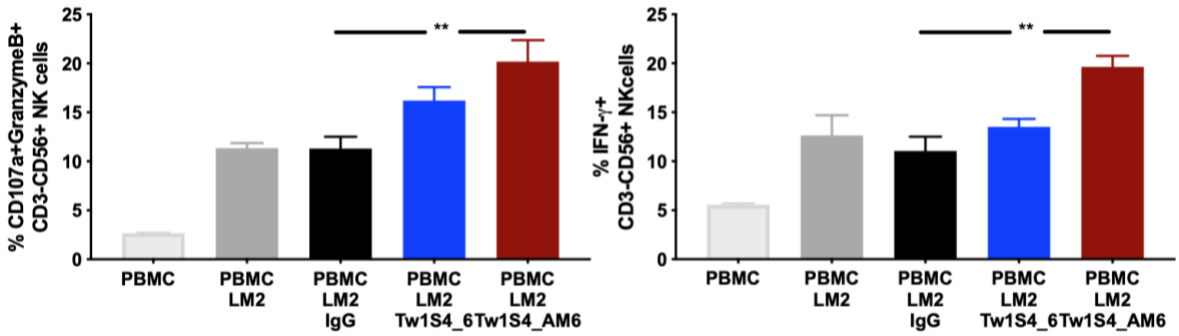

Figure 3.5: NK cell degranulation assay with human PBMCs (Donor II). Tw1S4_AM6 treated groups showed **(A)** increased fraction of NK cells undergoing degranulation (**P<0.01, one way ANOVA with multiple comparison tests) and **(B)** increased fraction of NK cells secreting IFN-G (**P<0.01, one way ANOVA with multiple comparison tests)

3.3.5. Tw1S4_AM6 mediates ADCC *in vitro* with human PBMCs, but does not mediate CDC

Next, we tested *in vitro* ADCC with healthy human PBMCs from two donors. At an E:T ratio of 20:1, we observed that treatment with Tw1S4_AM6 resulted in a significantly higher tumor cell kill (35% viability as opposed to 99% and 94% in case of

Isotype IgG and Tw1S4_6 antibodies, respectively) (P<0.05, two way ANOVA with Tukey's multiple comparison tests, Figure 3.6B), with similar trends at lower ratios. A similar trend was observed in studies with PBMCs from a second donor (Figure 3.7), however the overall cytotoxicity observed was lower in the case of donor II. We did not observe any cytotoxicity with human serum (Figure 3.8).

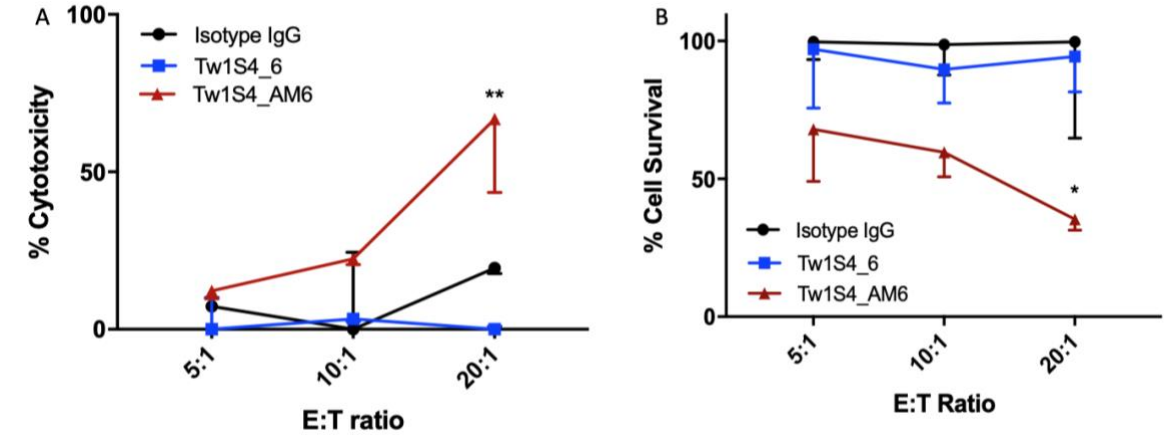

Figure 3.6: ADCC assay with human PBMCs (Donor I). Tw1S4_AM6 treated groups showed **(A)** higher cytotoxicity (**P<0.01, two way ANOVA with Tukey's multiple comparison tests, statistical significance is based off comparison between Isotype IgG and Tw1S4_AM6 at E:T 20:1) and **(B)** reduced cell survival (*P<0.05, two way ANOVA with Tukey's multiple comparison tests, statistical significance is based off comparison between Isotype IgG and Tw1S4_AM6 at E:T 20:1)

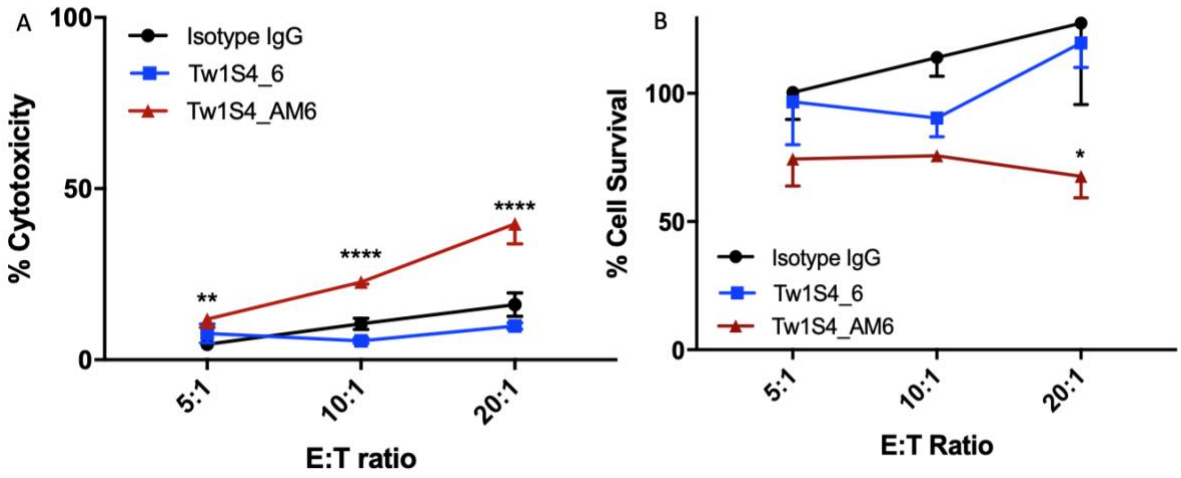

Figure 3.7: ADCC assay with human PBMCs (Donor II). Tw1S4_AM6 treated groups showed **(A)** higher cytotoxicity (**P<0.01, ****P<0.0001, two way ANOVA with Tukey's multiple comparison tests, statistical significance is based off comparison between Isotype IgG and Tw1S4_AM6 at the referenced E:T ratios) and **(B)** reduced cell survival (*P<0.05, two way ANOVA with Tukey's multiple comparison tests, statistical significance is based off comparison between Isotype IgG and Tw1S4_AM6 at E:T 20:1)

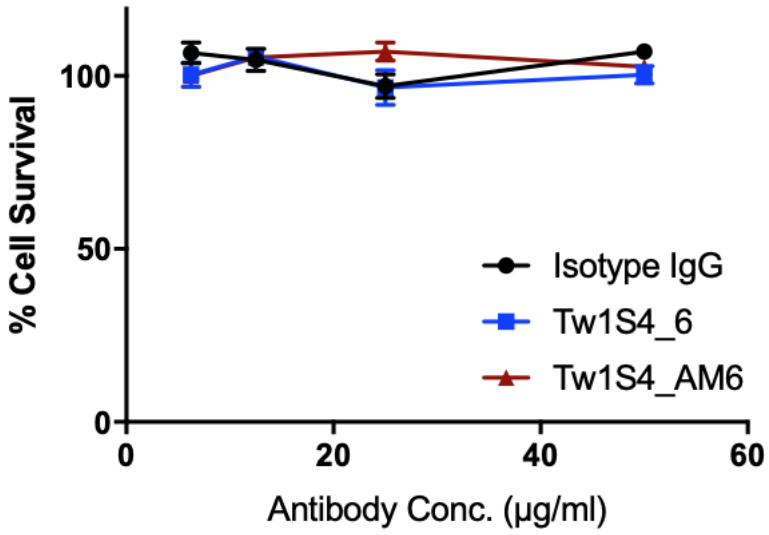

Figure 3.8: CDC assay with human serum showed no significant cytotoxicity with Tw1S4_6 or Tw1S4_AM6.

3.3.6. Tw1S4_AM6 accumulates in the tumor

To investigate the tumor distribution of the two antibodies, an imaging study was carried out in tumor-bearing mice with fluorescently labeled antibodies. Following IV administration, fluorescence was visible in the liver at one hour. Starting at 12 hours, significant accumulation of the antibodies could be observed in the tumor. Quantitative analysis of fluorescence in the tumors revealed a 2-4 fold higher accumulation of Tw1S4_AM6 versus the isotype IgG control ($P<0.05$ at 6 and 72-120 hours, $p<0.001$ at 12-48 hour, two-way ANOVA with multiple comparisons) (Figure 3.9A), similar to reports testing other tumor-targeting antibodies[149,150]. Tw1S4_6 on the other hand showed

a modest, statistically not significant, improvement in accumulation (1.5- to 2-fold, P>0.05). The T_{max} (in tumor) for both Tw1S4_6 and Tw1S4_AM6 was 24 hours. On the contrary, T_{max} in the liver was the first measured time-point i.e. 1 hour (Figure 3.95B) and there were no statistically significant differences in the liver distribution of the three antibodies (P>0.05, two-way ANOVA with multiple comparisons).

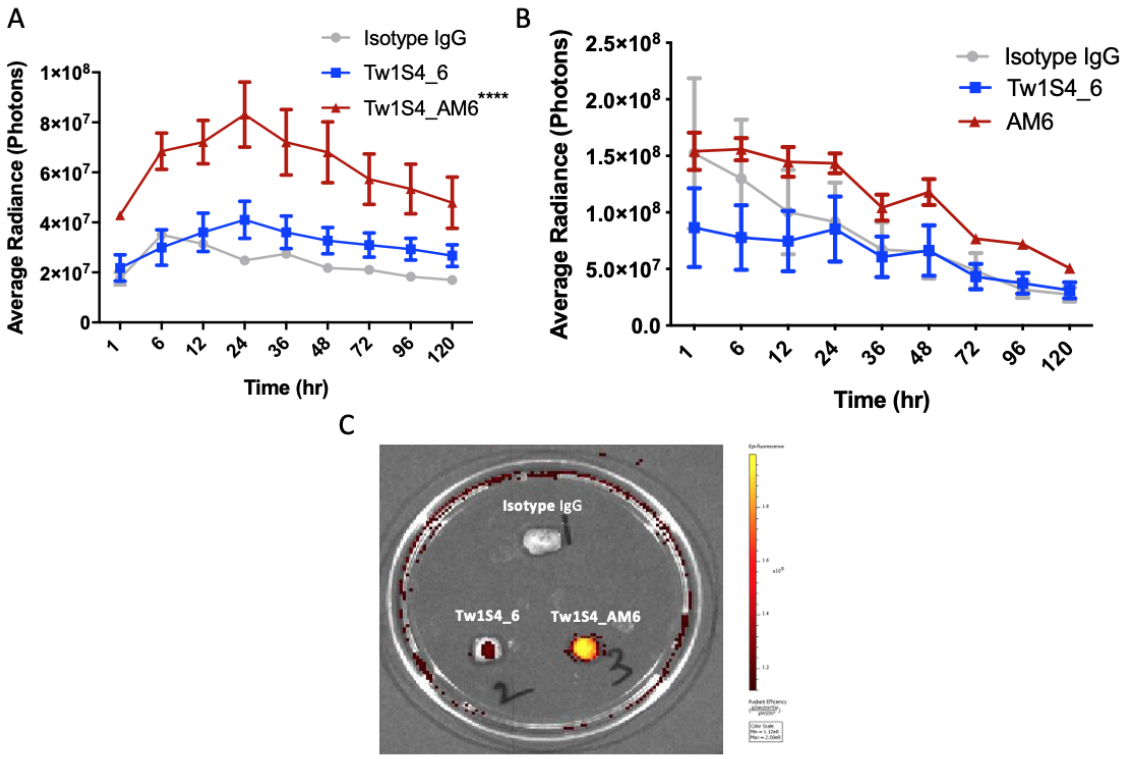

Figure 3.9: Antibody targeting *in vivo* by fluorescence based imaging **(A)** Quantified fluorescence values in tumor post antibody administration. Tw1S4_AM6 accumulated between 2-4-fold higher concentrations in the tumor (***P<0.001, two-way ANOVA with multiple comparisons, statistical significance is based on comparison between isotype IgG

and Tw1S4_AM6 at 24 hours). **(B)** Quantified fluorescence values in liver post antibody administration. No statistical significance was observed between different treatment groups at all the time points analyzed (two-way ANOVA with multiple comparisons) **(C)** Tumors imaged *ex vivo* at 120 hours. One representative tumor from each group is shown in the image.

3.3.7. HSPG2 targeted nanoparticles show improved drug delivery to the tumor

We have previously shown that conjugation of Tw1S4_AM6 to a nanoparticle surface improved their cellular uptake in MDA-MB-231-LM2 cells, resulting in enhanced cytotoxicity of nanoparticle-encapsulated paclitaxel.[143] In order to determine the ability of Tw1S4_AM6 NPs to improve drug delivery *in vivo*, we tested the efficacy of paclitaxel loaded nanoparticles in the MDA-MB-231-LM2 orthotopic mouse tumor model (Figure 3.10). Nanoparticles are known to have improved accumulation in the tumor due to the enhanced permeability and retention (EPR) effect[151]. Targeted nanoparticles on the other hand have improved internalization into the tumor cells in addition to the EPR effect[152,153]. Based on improved cellular uptake, retention and cytotoxicity of Tw1S4_AM6 NPs relative to that of Tw1S4_6 NPs, we tested Tw1S4_AM6 NPs *in vivo*. We observed improved tumor growth inhibition with Tw1S4_AM6 NPs relative to isotype IgG NPs ($P<0.001$, two-way ANOVA with multiple comparisons, statistical significance is based

on comparison between Isotype IgG NPs and Tw1S4_AM6 NPs on the last day of the study). On day 30, the untreated animals reached an average tumor volume of ~950 mm^3. Isotype IgG NPs showed 18% tumor inhibition. On the other hand, AM6 NPs showed 37% tumor inhibition at the end of the study.

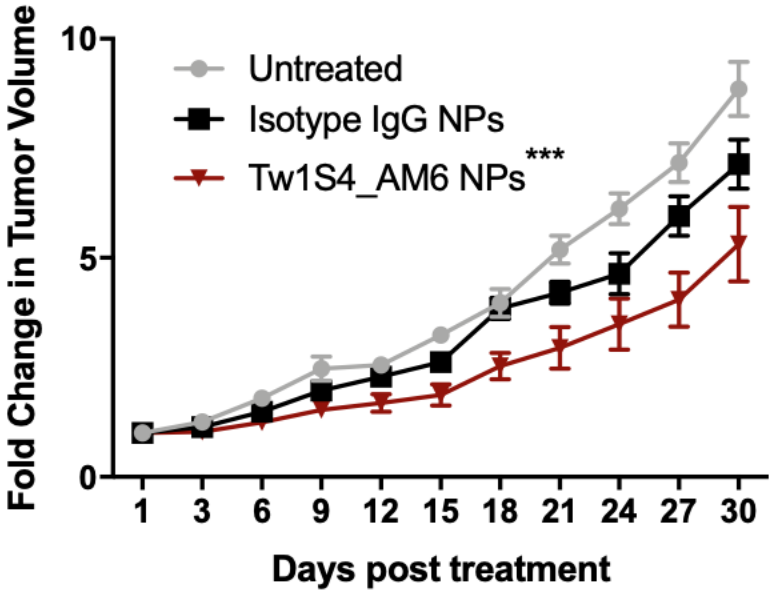

Figure 3.10: Efficacy study in Balb/c athymic nude mice. Tw1S4_AM6 NPs showed significantly enhanced tumor inhibition over Isotype IgG nanoparticles (***P<0.001, two-way ANOVA with multiple comparisons, statistical significance is based on comparison between Isotype IgG NPs and Tw1S4_AM6 NPs on the last day of the study)

3.4. Discussion

Tw1S4_6 and Tw1S4_AM6 are both fully human IgG1s that showed specific binding to the metastatic cell line MDA-MB-231-LM2.[113] Since IgG1 antibodies are the most commonly used format for therapeutic antibodies, we previously tested them for *in vivo* efficacy in a breast cancer model.[113] The *in vivo* efficacy observed with Tw1S4_AM6 in that study prompted us to further examine its mechanism of action.

Antibodies used for cancer therapies can have one of three mechanisms of action[5], as discussed in section 1.7. The first involves direct receptor mediated activity, where binding of the antibody to its antigen leads to downstream signaling or prevents downstream signaling (e.g. trastuzumab). The second mechanism involves binding to the target and recruitment of immune components such as NK cells, macrophages or the complement system to cause cytotoxicity (e.g. cetuximab). The third mechanism of action is checkpoint inhibition (e.g. nivolumab). Checkpoint inhibitors bind to inhibitory receptors on T-cells, thus preventing the inactivation of the immune system.

In the case of our anti-HSPG2 antibodies, checkpoint inhibition could be eliminated since the target (HPSG2) is not known to play a role in the immune system. Thus, the anti-HSPG2 antibodies were likely exhibiting activity via a target mediated mechanism or through the recruitment of immune cells. NSG mice are severely immune-compromised and lack T cells, NK cells and B cells. Balb/c nude mice (utilized in the previous efficacy study) on the other hand retain NK cell activity. Thus, any differences in efficacy observed

between the two models would provide a basic understanding of the involvement of NK cells. We found that the efficacy of Tw1S4_AM6 was significantly diminished in the NSG mouse model compared to that observed in the Balb/c nude mouse model, indicating that NK cells were likely involved in mediating the efficacy of anti-HSPG2 antibodies. Using *in vitro* assays with mouse splenocytes and human PBMCs, we were able to confirm that Tw1S4_AM6 indeed was acting through NK cell mediated ADCC. Tw1S4_6 on the other hand did not show robust ADCC in the *in vitro* assays, thus explaining its weak *in vivo* efficacy. These studies also confirmed that antibody affinity plays a critical role in ADCC. Interestingly, the degranulation assays did not show a significant difference between Tw1S4_6 and Tw1S4_AM6, likely because the Fc domain (that interacts with NK cells) of both antibodies are identical. We also carried out *in vitro* assays to examine the involvement of CDC and direct receptor mediated activity, however, we did not observe any such activity with either Tw1S4_6 or Tw1S4_AM6. Additionally, the lack of efficacy observed with Tw1S4_6 could also be explained by its poor accumulation in the tumor *in vivo*. It is important to note that the efficacy observed with Tw1S4_AM6 was not completely abolished in the NSG model. It is possible that even though the major mechanism of action for Tw1S4_AM6 is ADCC, mechanisms that are not comprehensively covered by the *in vitro* assays carried out here may be involved.

Biodistribution studies demonstrating significant tumor accumulation of Tw1S4_AM6 suggested that this antibody could also be used as a targeting ligand. Thus, we developed HSPG2 targeted, paclitaxel loaded polymeric nanoparticles by conjugating

Tw1S4_6 or Tw1S4_AM6 to their surface using thiol-maleimide chemistry. The presence of Tw1S4_6 or Tw1S4_AM6 on the surface of these nanoparticles improved cellular uptake by five-fold, improved the retention of nanoparticles within cells and subsequently enhanced the cytotoxicity of paclitaxel *in vitro*.[143] Current studies show that Tw1S4_AM6 conjugated nanoparticles also result in enhanced tumor growth inhibition *in vivo*. Thus, not only is HSPG2 a relevant marker for drug discovery but it could also be leveraged the development of targeted drug delivery systems. Additional optimization of the nanoparticle formulation and the antibody conjugation strategy may help improve the efficacy of this approach further. Also, HSPG2 targeting could be extended to other formats of targeted drug delivery, such as ADCs, radio-immunoconjugates and liposomal formulations.

3.5. Conclusion

Despite significant progress in the treatment of breast cancer, options for patients diagnosed with the triple negative breast cancer (TNBC) subtype are limited to traditional chemotherapy, surgery and radiation[154]. The lack of targetable markers that can be leveraged for therapy remain an important limitation. The data presented here suggests that anti-HSPG2 antibodies could be a promising new class of therapeutics for TNBC patients. Specifically, Tw1S4_AM6 antibody, which mediates ADCC, could be particularly beneficial when combined with agents that enhance ADCC. Further, we were also able to show that drug delivery could be significantly improved when anti-HSPG2 antibodies are utilized as targeting ligands. In conclusion, HSPG2 is a promising target for designing therapeutics that could help improve the treatment outcomes for TNBC patients.

Chapter 4: TLR 7/8 agonists for improving NK cell mediated antibody - dependent cellular cytotoxicity (ADCC)

4.1. Introduction

It is now well established that the immune system has the ability to recognize and fight cancer. The two major players that mediate anti-cancer immunity are T cells and NK cells.[1] However, despite the meticulous design of our immune system, sometimes it is unable to recognize tumor cells. More often than not, this is because tumor cells develop from normal cells and thus it can be difficult to distinguish them from normal cells.[111] Importantly, tumor cells can actively suppress T cell mediated immune response through downregulation of MHC class I[1], antigen shedding[62], secretion of immunosuppressive cytokines[7] and upregulation of checkpoints such as PD-L1.[31] Monoclonal antibody therapy aims to overcome some of these resistance mechanisms by engaging and activating NK cells.

Antibodies have the ability to recognize tumor antigens and direct various components of the immune system against the tumor. The most well-studied mechanism is ADCC, involving NK cells.[5] Several FDA approved monoclonal antibodies have been shown to mediate ADCC, including cetuximab[28], rituximab[16] and trastuzumab[27]. However, patients do not show a uniform ADCC response. A large percentage (as high as 75-93%) of the population express NK cells with an isoform of the Fcγ receptor that mediates lower levels of ADCC (section 1.10.1).[88,89,90] Compounding the issue is the lack of NK cell infiltration into the tumor (section 1.10.2) and the inherently low efficacy observed with

ADCC (section 1.10.3). Thus, rational combination therapies that leverage ADCC should improve the outcome of antibody-based therapeutics.

Several groups have reported the application of TLR agonists, specifically TLR 7/8 agonists, to enhance ADCC.[106–108] These agonists directly activate dendritic cells, which in turn release a number of NK cell activating cytokines, IL-12, IL-18 and IL-15.[75] NK cell activation is dictated by the delicate balance between activating and inhibitory receptors. The presence of TLR7/8 agonists engages an additional set of activating receptors on NK cells which results in , activation in a larger fraction of cells and thereby improved ADCC. In a previous study, we observed about a two-fold higher NK cell degranulation in human PBMCs when cetuximab was combined with a novel TLR7/8 agonist, 522, encapsulated in gas generating nanoparticles (522GGNPs). .[155]. Consequently, cytotoxicity mediated by cetuximab increased from ~20% to ~60% when combined with 522GGNPs.

Here, this combination therapy was applied to an *in vivo* model of human lung cancer. Additionally, we evaluated the efficacy of six, second generation TLR7/8 agonists in an immunocompetent mouse model.

4.2. Methods

4.2.1. Materials

All cell culture supplies were obtained from Invitrogen (ThermoFisher Scientific, Waltham, MA) unless otherwise specified. Fetal bovine serum (FBS) was purchased from

Atlanta Biologicals (Flowery Branch, GA). All TLR7/8 compounds were provided by Dr. David Ferguson, University of Minnesota.[156]

4.2.2. Cell culture

A549 lung cancer cells were purchased from the American Type Culture Collection (ATCC, Manassas, Virginia) and were cultured in RMPI supplemented with 10% FBS and 1% Penicillin/Streptomycin. TuBo cells were a gift from Dr. Wei-Zen Wei (Wayne State University) and were cultured in RMPI supplemented with 10% FBS and 1% Penicillin/Streptomycin.

4.2.3. PBMCs Cytokine Secretion Assay

PBMCs were purified from human blood using Ficoll density gradient medium (GE Healthcare) and seeded at 1.5 million cells per well in a 6-well plate. The TLR agonists were added to the wells at specified concentrations and incubated overnight at 37 ˚C. The next day, cells were collected and centrifuged at 1200 RPM for 5 minutes. The supernatant was collected and frozen at -80˚C until analyzed using the Luminex Human XL Cytokine Discovery Panel (R&D Systems). The cells were used for analysis of NK cell degranulation and T cell activation, as described in section 4.2.5. The experimental analysis was performed by the Cytokine Reference Laboratory (University of Minnesota).

4.2.4. NK Cell ADCC

ADCC assay was performed using a modified version of an assay reported previously[107,108]. PBMCs were isolated from human blood (healthy donor) using Ficoll density gradient medium (GE Healthcare) and seeded at 0.5 million/ml in RPMI (10% FBS, 1% Pen/Strep) in 6 well plates. Agonists were added to the cells at the specified concentrations and incubated overnight. Target cells were pre-labeled with 8 µM CFSE (Biolegend, San Diego, CA) and plated in 96-well plates on the day of PBMC isolation. The next day, treated PBMCs were counted and added to target cells at the specified ratios. The plates were incubated overnight at 37 ˚C. The supernatant was then analyzed using the Pierce LDH Cytotoxicity Assay (Thermofisher, Waltham, MA), and the plate was analyzed for tumor-cell associated fluorescence intensity at excitation and emission wavelengths of 492 nm and 517 nm, respectively, using Spectramax i3x (Molecular Devices, San Jose, CA).

4.2.5. NK Cell degranulation and T cell activation

Healthy human PBMCs were seeded at 0.5 million/ml in RPMI (10% FBS, 1% Pen/Strep) in a 24 well plate. Agonists were incubated with the PBMCs at the specified concentrations overnight. The next day, the supernatant was utilized for cytokine analysis as described in section 4.2.3. Target cells were trypsinized and added to the wells at an effector to target ratio of 2:1. Cetuximab was added at a final concentration of 200 nM. Anti-CD107a APC Cy7 (Biolegend, San Diego, CA) was added to all samples. One hour

later, Brefeldin A (Biolegend, San Diego, CA) was added. Four hours later, cells were collected and stained for extracellular markers with anti-CD3 FITC, anti-CD56 Brilliant Violet 650, anti-CD4 PE-Cy7, and anti-CD69 PerCP-Cy 5.5 (Biolegend, San Diego, CA) antibodies. Intracellular staining was performed with anti-IFN-γ APC antibody (Biolegend, San Diego, CA) using eBioscience Foxp3 Transcription Factor Staining Buffer Set (Thermofisher, Waltham, MA). Samples were analyzed using a BD Fortessa H0081 flow cytometer at the University of Minnesota Flow Cytometry Core Facility.

4.2.6. *In vivo* efficacy studies

Balb/c athymic nude mice (Strain 002019, The Jackson Laboratory) were used to graft heterotopic A549 tumors. A549 cells were counted, re-suspended in saline and diluted 1:1 with Matrigel (Corning, Tewksbury, MA). Two million cells in 100 µL were grafted subcutaneously. Tumor volumes were measured three times a week, using a digital Vernier calipers (Marathon Watch, Vaughn, Canada). Treatment begun when tumors reached 100 mm^3 (n=5-6 per treatment group). Cetuximab (ImClone, NY) was dosed at 10 mg/kg every fourth day, starting day 0, for five doses (Days 0, 4, 8, 12, 16) by IV tail vein injections. 522GGNPs were dosed at 2 mg/kg (522 dose equivalent) peritumorally every fourth day, starting day 1 for five doses (days 1, 5, 9, 13, 17) through SC injections. TLR7/8 agonists were dosed at 2 mg/kg (free drug in DMSO diluted with saline) every fourth day, starting day 1 for five doses (days 1, 5, 9, 13, 17) through IP injections. On day 30, mice were sacrificed, tumors were resected and frozen in Tissue-Tek O.C.T. Compound (Sakura Finetek, Torrance, CA) for immunohistochemistry.

Wild type Balb/c mice (Strain 000651, The Jackson Laboratory) were used to graft orthotopic TuBo tumors.[99] TuBo cells were counted, re-suspended in saline and diluted 1:1 with Matrigel (Corning, Tewksbury, MA). Two hundred thousand cells in 100 µL were grafted subcutaneously into the fourth mammillary fat pad. Tumor volumes were measured three times a week using digital Vernier calipers (Marathon Watch, Vaughn, Canada). Treatment began when tumors reached 100 mm^3 (n=7-8 per treatment group). Anti-HER2/neu antibody (Clone 7.16.14, BioXcell, West Lebanon, NH) was dosed at 5 mg/kg, on day 0, through IV tail vein injection. 522GGNPs were dosed at 2 mg/kg (522 dose equivalent) peritumorally, every day, for five doses, starting day 1 (days 1, 2, 3, 4, 5) through SC injections. TLR7/8 agonists were dosed at 2 mg/kg (free drug dissolved in DMSO and diluted with saline) every day, for five doses, starting day 1 (days 1, 2, 3, 4, 5) through IP injections. Mice were sacrificed when the group average tumor volume exceeded 1000 mm^3 or on day 30 of the study, whichever was earlier.

4.2.7. *Ex vivo* analysis of NK cells

Wild type Balb/c mice were grafted with orthotopic TuBo tumors as described above. Treatment began when tumors reached 100 mm^3. The dosing scheme was identical to that described above. On day 8, mice were sacrificed, the tumor and spleen were excised and collected into HBSS (Genesee Scientific, San Diego, CA). One half of the tumor was stored in RNAlater (Thermofisher, Waltham, MA) at 4˚C until processed. Tissues were processed to single cells using a previously described protocol[157]. Tissues were homogenized using GentleMACS (Miltenyi Biotec, Germany) in MACS C Tubes

(Miltenyi Biotec, Germany), as per manufacturer's protocol. Liberase TH Research Grade (0.026 Wunsch units/mL, Sigma-Aldrich, St. Louis, MO) and DNAase I (0.015 mg/ml, Sigma-Aldrich, St. Louis, MO) were added to the samples and incubated for 15-30 minutes to allow for dissociation at 37 ˚C. Enzymes were neutralized using IMDM (Life Technologies, Grand Island, NY), cells were washed once and re-suspended in PBS (0.5% BSA, 2 mM EDTA) and filtered through a 100 µm mesh (Fisher Scientific, Hampton, NH). ACK Lysis Buffer (Life Technologies, Grand Island, NY) was used for RBC lysis. Samples were re-suspended in FACs buffer and 5-10% of the sample was stained with anti-CD3 APC-Cy7, anti-CD49b PE-Cy7, anti-CD8 FITC, anti-CD69 Brilliant Violet 605, anti-NKG2D APC, anti-CD45 PerCP-C5.5 (tumor samples only) antibodies (Biolegend, San Diego, CA) for flow cytometry. Samples were analyzed using a BD Fortessa H0081 flow cytometer at the University of Minnesota Flow Cytometry Core Facility.

4.2.8. *Ex vivo* mRNA analysis

Wild type Balb/c mice were grafted with orthotopic TuBo tumors as described above. Treatment began when tumors reached 100 mm^3. The dosing scheme was identical to that described above. On day 8, mice were sacrificed, the tumor and spleen were excised and collected into HBSS (Genesee Scientific, San Diego, CA) until processing. One half of the tumor was stored in RNAlater (Thermofisher, Waltham, MA) at 4 ˚C until processed. This method was partially adapted from Wendel et al.[158] On the day of processing, the tissues were carefully removed from RNAlater (ThermoFisher Scientific, MA, USA) and homogenized using GentleMACS (Miltenyi Biotec, Germany) in MACS M Tubes

(Miltenyi Biotec, Germany), as per manufacturer's protocol. The tissue homogenate was then processed using the Qiagen RNeasy Mini Kit (Qiagen, Germany) as per the manufacturer's protocol. The final extracted RNA sample was submitted to the University of Minnesota Genomics Centre for analysis of CXCL9, CXCL10 and CXCL11. Data was analyzed using the $2^{-\Delta\Delta C_T}$ [159] method.

4.2.9. *Ex vivo* immunohistochemistry (IHC)

Wild type Balb/c mice were grafted with orthotopic TuBo tumors as described above. Treatment began when tumors reached 100 mm^3. The dosing scheme was identical to that described above. Mice were sacrificed when the group average tumor volume exceeded 1000 mm^3 or on day 30 of the study. For CD8 T cells, tumors were excised and formalin fixed for 48 hours. The tissues were then transferred to 70% ethanol until processed. The samples were submitted to the University of Minnesota Comparative Pathology Shared Resource for IHC processing. The sections were stained for CD8 T cells using an anti-mouse CD8α antibody (Catalog #MA5-17594, Thermofisher Scientific, MA). The IHC slides were submitted to the University of Minnesota Imaging Centre for slide scanning. Three snippets of approximately 1700 μm x 800 μm size were selected at random in the slide field, at 10X magnification and quantified for positive staining using the software ImageJ (NIH).

4.3. Results

4.3.1. 522GGNPs significantly enhance NK cell mediated ADCC in combination with Cetuximab

A549 is a human lung cancer cell line that overexpresses EGFR.[160] Cetuximab is an anti-EGFR antibody that has shown efficacy in A549 tumor models.[161] 522GGNPs is an optimized formulation of 522 encapsulated in pH sensitive PLGA nanoparticles.[162] Balb/c nude mice, although immunocompromised and lacking functional T cells, retain NK cell activity and can be used to test ADCC mediated mechanisms. Cetuximab showed only modest tumor growth inhibition in this model, despite a relatively high dose of 10 mg/kg x5d. (Figure 4.1A). On day 32, relative tumor volume for the cetuximab treated group was 5.5 ± 2-fold, as opposed to the untreated group, which had an average tumor volume of 7.3 ± 3.4-fold ($P<0.05$, two-way ANOVA with multiple comparisons). 522GGNPs in combination with cetuximab were able to significantly inhibit tumor growth, resulting in an average tumor volume of 3.7 ± 1.3-fold on day 32 (Figure 4.1A, $P<0.05$ compared with cetuximab treated group, two-way ANOVA with multiple comparisons). 522GGNPs alone were not significantly different than the untreated group.

An additional group that was included in the study was the cetuximab+522GGNPs+anti-asialo antibody treatment group**.** Mice treated with the anti-asialo antibody show near complete NK cell depletion.[163] Thus, the anti-asialo treated group served as a negative control to determine the involvement of NK cells. Inclusion of

the anti-asialo antibody almost completely abolished the efficacy observed with the combination of cetuximab+522GGNPs, thus supporting the involvement of NK cells in the observed activity.

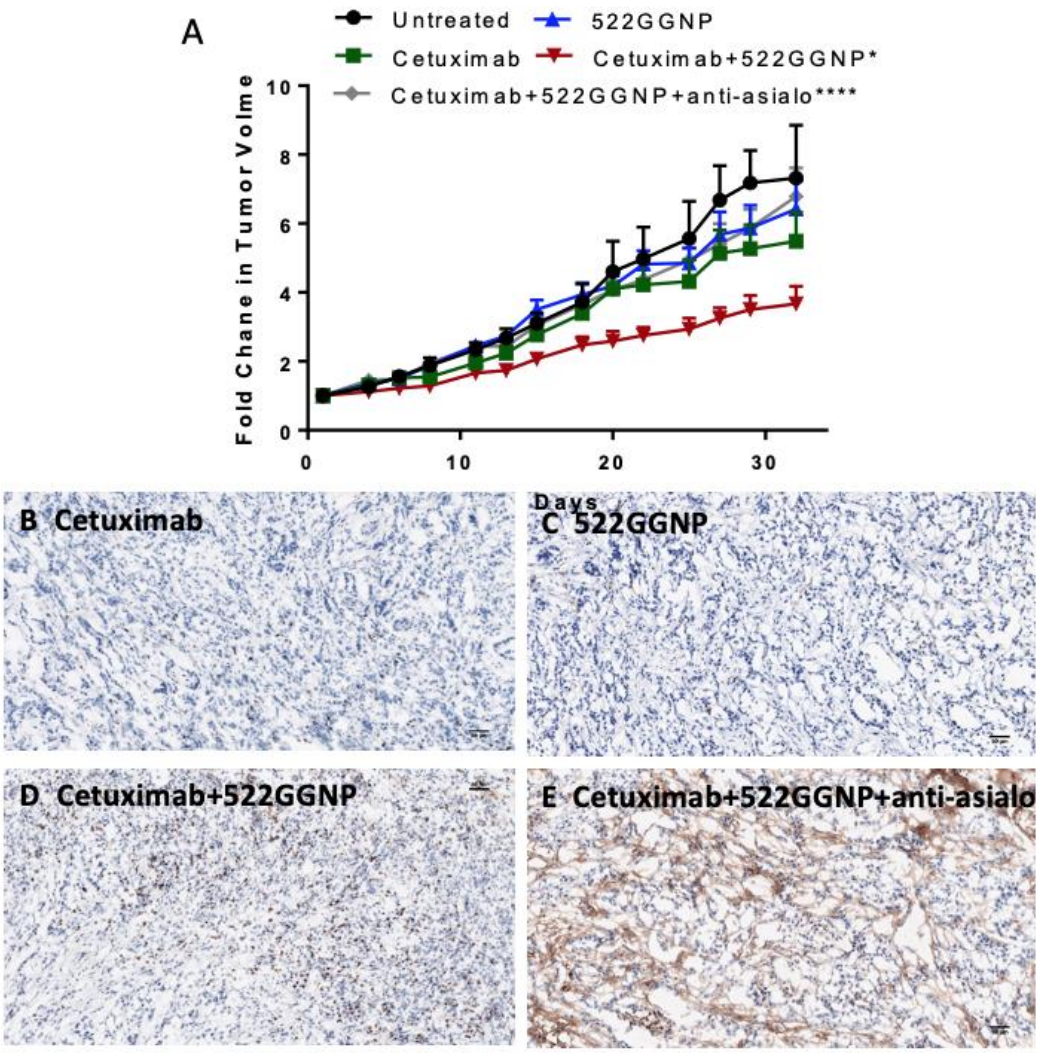

Figure 4.1: Cetuxmimab+522GGNPs efficacy study in an A549 subcutaneous model, grafted in Balb/c athymic nude mice **(A)** Cetuximab+522GGNPs showed significantly improved tumor growth inhibition over Cetuximab alone (*P<0.05 for Cetuximab v/s

Cetuximab+522GGNPs, P<0.001 for 522GGNPs v/s Cetuximab+522GGNPs, ****P<0.0001 for Cetuximab+522GGNPs v/s Cetuximab+522GGNPs+anti-asialo, two-way ANOVA with multiple comparisons, statistical significance is based on comparisons from the last day of the study) **(B-E)** Representative IHC images from excised tumors at the end of the study. Sections were stained for CD49b (NK cell marker). Brown is indicative of positive staining.

4.3.2. 522GGNPs significantly enhance NK cell infiltration into tumors in combination with Cetuximab

Both cetuximab and 522GGNPs as single agents resulted in very little NK cell infiltration in the tumor, with occasional NK cells being observed in the tumor periphery (Figures 4.1B and 4.1C, respectively). However, when the two treatments were combined, there was a clear increase in the number of NK cells infiltrating the tumor (Figure 4.1D), albeit limited to the periphery of the tumor. The anti-asialo treated group showed dispersed background staining (Figure 4.1E), likely a non-specific reaction, unlike the pin-point cellular staining observed in the other groups.

4.3.3. Second generation TLR7/8 agonists result in improved cytokine induction in human PBMCs

In order to screen the panel of second generation TLR7/8 agonists for their activity *in vitro,* we tested 45 cytokines secreted by human PBMCs in response to the compounds.

We tested PBMCs from two healthy donors (Figures 4.2 and 4.3). 522 was included in the compounds as a benchmark control. Several of the second-generation compounds, 558 in particular, showed improved cytokine secretion over 522. Cytokines traditionally thought to be critical for activation of NK cells include IFN-α, IFNβ, IL-2, IL-12, IL-15 and IL-18.[75] Of these, we tested IFN-α, IFN-β, IL-2, IL-12, and IL-15 and observed that each was significantly higher in the 558 treated group as compared to that in the 522 treated group. Similarly, IFN-γ, a cytokine that stimulates T cell activation, was significantly upregulated in both donors when treated with 558 as compared to 522. IL-10, a cytokine considered to inhibit T cell activation, was also upregulated.

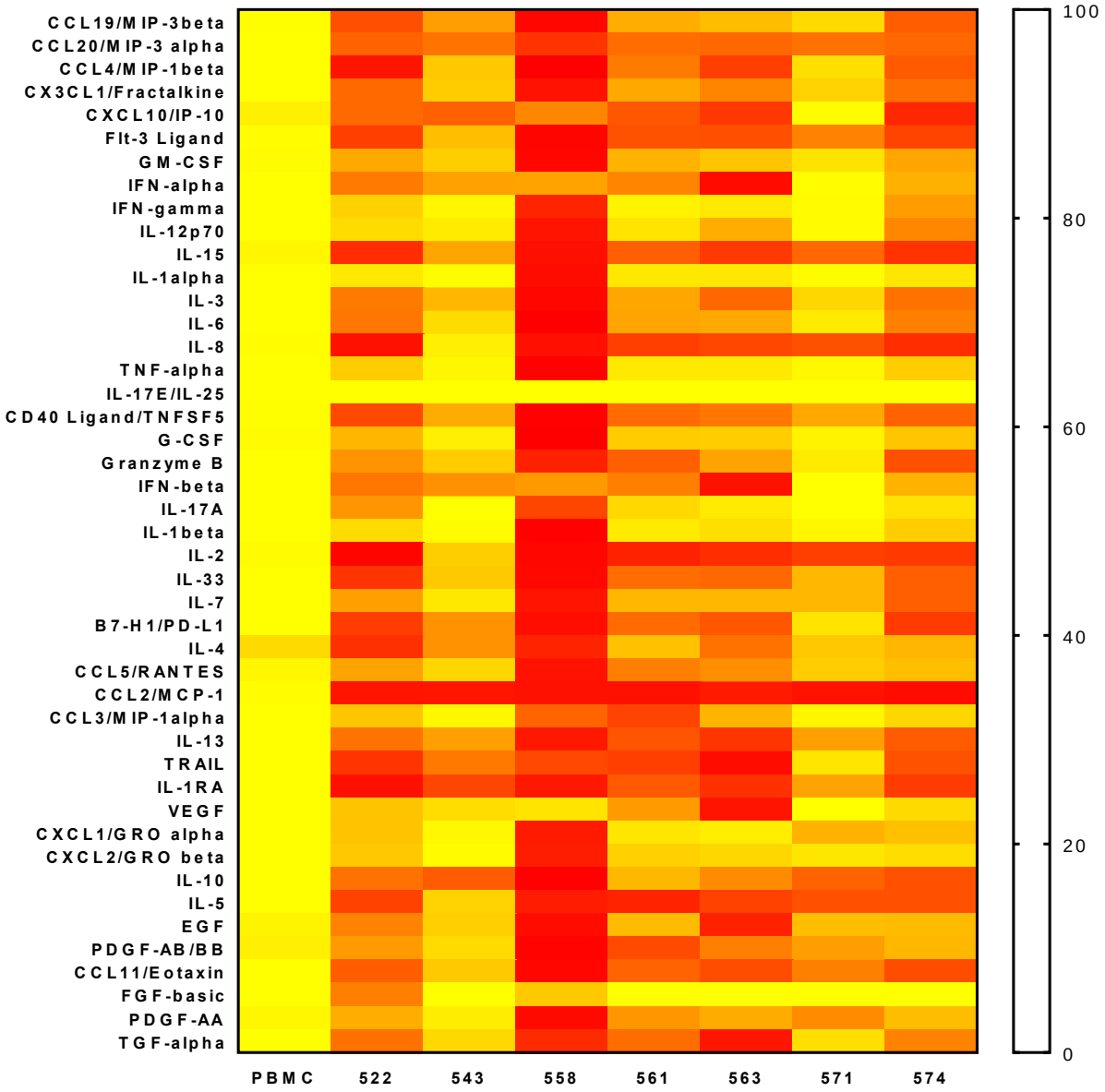

Figure 4.2: Cytokines secreted by PBMCs (Donor I) upon treatment with the different TLR7/8 agonist compounds (1μM). Data is scaled from 0-100 for each group (0 was assigned to the lowest value in the group and 100 was assigned to the highest value in the group)

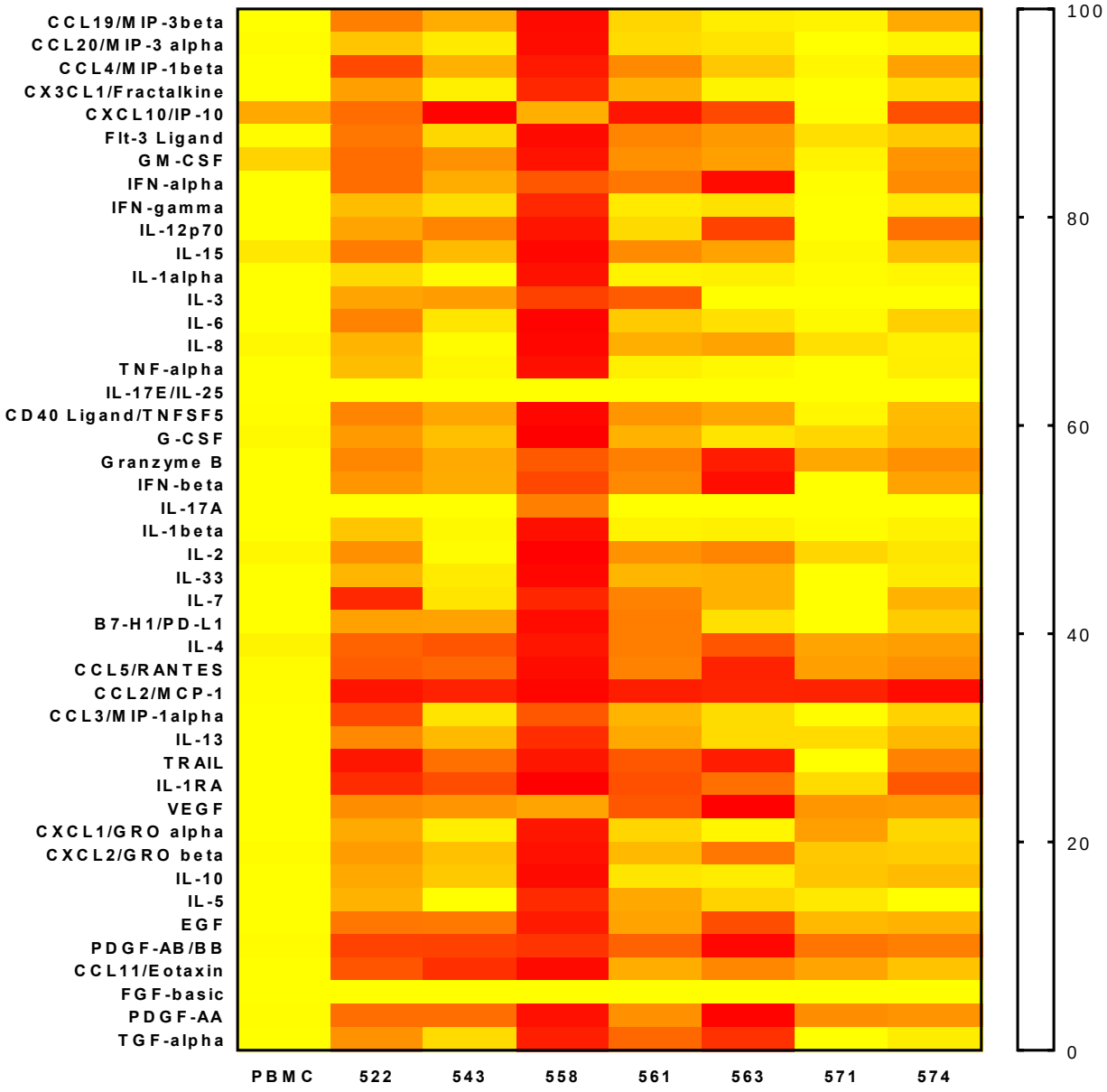

Figure 4.3: Cytokines secreted by PBMCs (Donor II) upon treatment with the different TLR7/8 agonist compounds (1μM). Data is scaled from 0-100 for each group (0 was assigned to the lowest value in the group and 100 was assigned to the highest value in the group)

4.3.4. Second generation agonists improve cetuximab mediated NK cell degranulation

We examined CD107a, a degranulation marker and IFNγ, a cytokine indicative of NK cell activation, which also activates T cells, and CD69,an early activation marker for NK cells. CD69 was upregulated in almost the entire population of NK cells tested, for all the compounds tested, and in both donors (Figures 4.4C and 4.5C). This was significantly higher than the baseline levels of CD69 observed in PBMCs, as well as the CD69 levels observed when treated with cetuximab alone.

CD107a and IFN-γ, on the other hand, showed varied responses to the compounds and was also dependent on the donor. Several compounds were significantly better at degranulation and activation of NK cells than 522, as observed by the expression of CD107a and IFN-γ respectively (Figure 4.4A,B and 4.5A,B). Specifically, compounds 558, 543, and 574 were significantly better than the other compounds tested. It is interesting to note that different donors responded differently to the various compounds tested. In case of donor I, compounds 543, 558, 571 and 574 showed improved activity over 522. However, for donor II, only compounds 543, 558 and 574 showed improved activity.

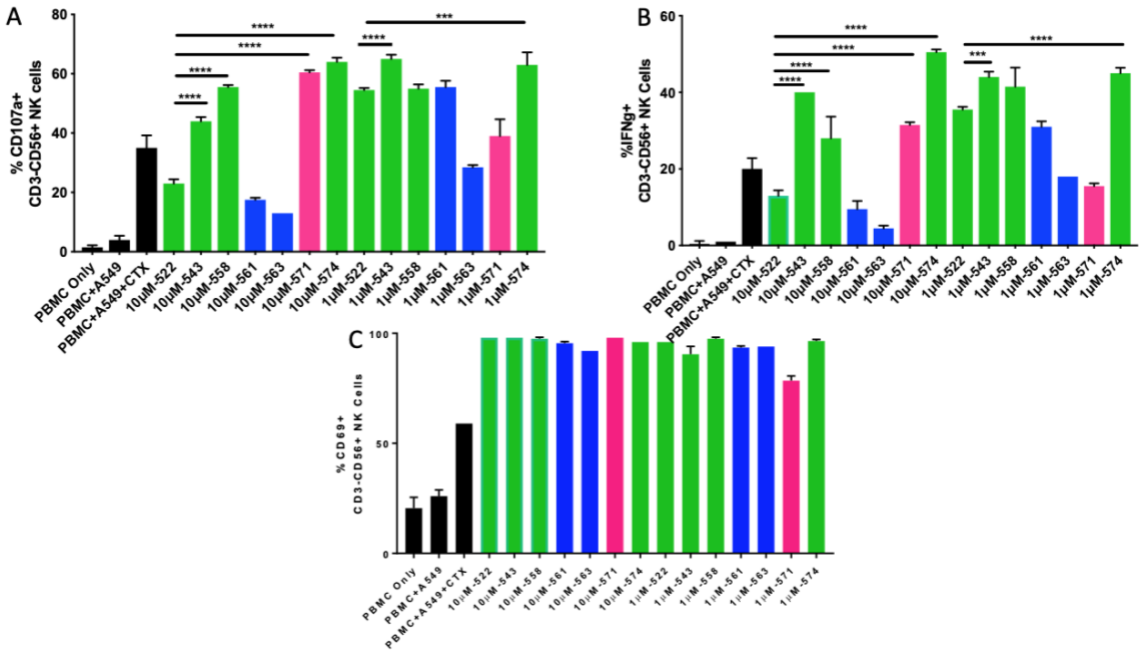

Figure 4.4: NK cell degranulation assay with human PBMCs (Donor I) using flow cytometry. CD3-/CD56+ cells were gated as NK cells. NK cells were then gated for **(A)** the degranulation marker CD107a, **(B)** the cytokine IFN-G and **(C**) the activation marker CD69. Percentage of NK cells positive for the different markers are plotted on bar graphs. Different concentrations of the compounds were tested, as have been indicated on the x-axis. All samples other than 'PBMC Only' contained A549 (target) cells. All samples other than 'PBMC Only' and 'PBMC+A549' contained cetuximab (200nM). Statistical significance was measured by two-way ANOVA with multiple comparisons. ***P<0.001, ****P<0.0001. Statistical significance is shown only for compounds that performed better than 522.

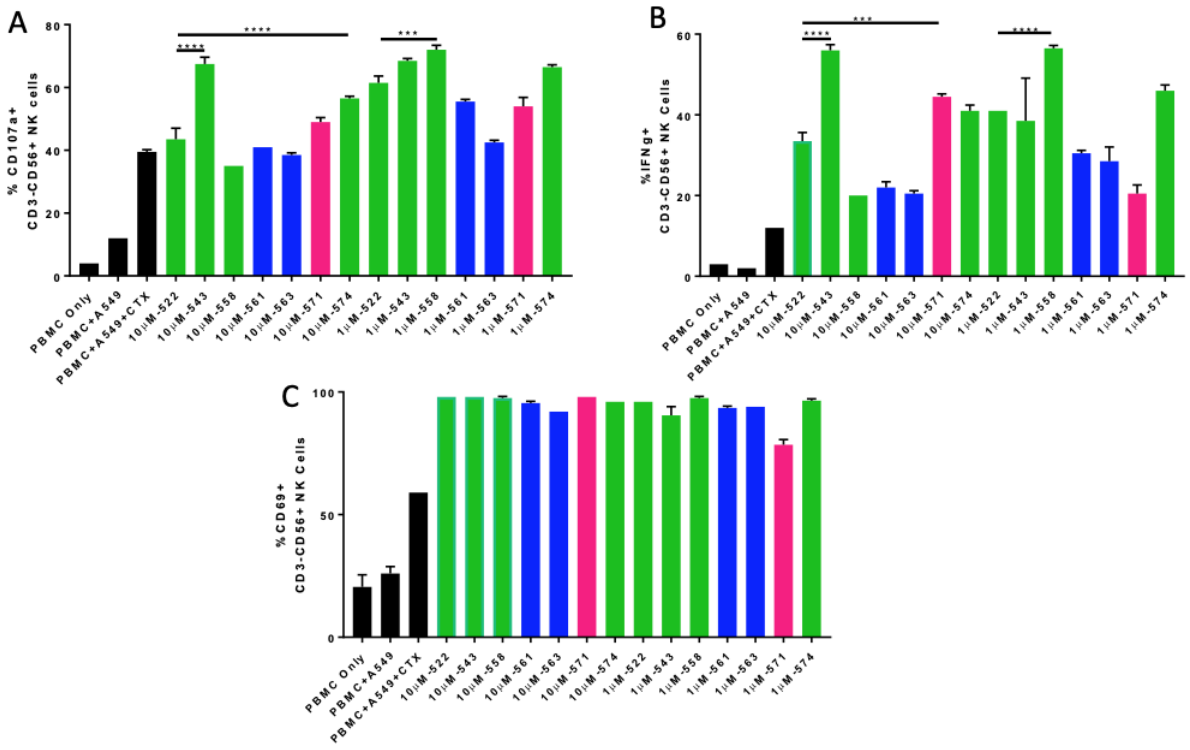

Figure 4.5: NK cell degranulation assay with human PBMCs (Donor II) using flow cytometry. $CD3^{-}/CD56^{+}$ cells were gated as NK cells. NK cells were then gated for **(A)** the degranulation marker CD107a, **(B)** the cytokine IFN-G and **(C)** the activation marker CD69. Percentage of NK cells positive for the different markers are plotted on bar graphs. Different concentrations of the compounds were tested, as have been indicated on the x-axis. All samples other than 'PBMC Only' contained A549 (target) cells. All samples other than 'PBMC Only' and 'PBMC+A549' contained Cetuximab (200nM). Statistical significance was measured by two-way ANOVA with multiple comparisons. ***P<0.001, ****P<0.0001. Statistical significance is shown only for compounds that performed better than 522.

4.3.5. Second generation agonists improve T cell activation

In addition to NK cells, the other two major cell types found in PBMCs are T cells and B cells. T cells are key players of the adaptive immune system. We also analyzed the T cell component of PBMCs in response to stimulation with cetuximab and the relevant TLR7/8 compounds. We analyzed two markers on CD8 T cells ($CD3^+/CD8^+$) and CD4 T cells ($CD3^+/CD4^+$) – CD69, an early activation marker, and IFN-γ, a cytokine secreted by activated T cells.

There was an increase in the percentage of T cells activated ($CD69^+$) with the addition of TLR7/8 compounds, as compared to A549+cetuximab alone (Figures 4.6A and 4.7A). This was true for both CD8 and CD4 T cells. However, for donor I, only 558 significantly outperformed 522, but this was only true for CD4 T cells (Figure 4.7A). IFN-γ secretion was less than 2% of CD8 and CD4 T cells in case of donor 1, despite the presence of the various TLR7/8 agonists (Figures 4.6B and 4.7B).

This was in contrast for donor II, where 558 as well as 574 significantly outperformed 522 in CD8/CD4 T cell activation (i.e. $CD69^+$) (Figures 4.8A and 4.9A). IFN-γ secretion was better than that observed in the case of donor I (up to 10% CD4/CD8 T cells were IFN-γ positive). Although not statistically significant, several of the compounds (558, 574, and 571) showed improved IFN-γ secretion as compared to 522 (Figures 4.8B and 4.9B).

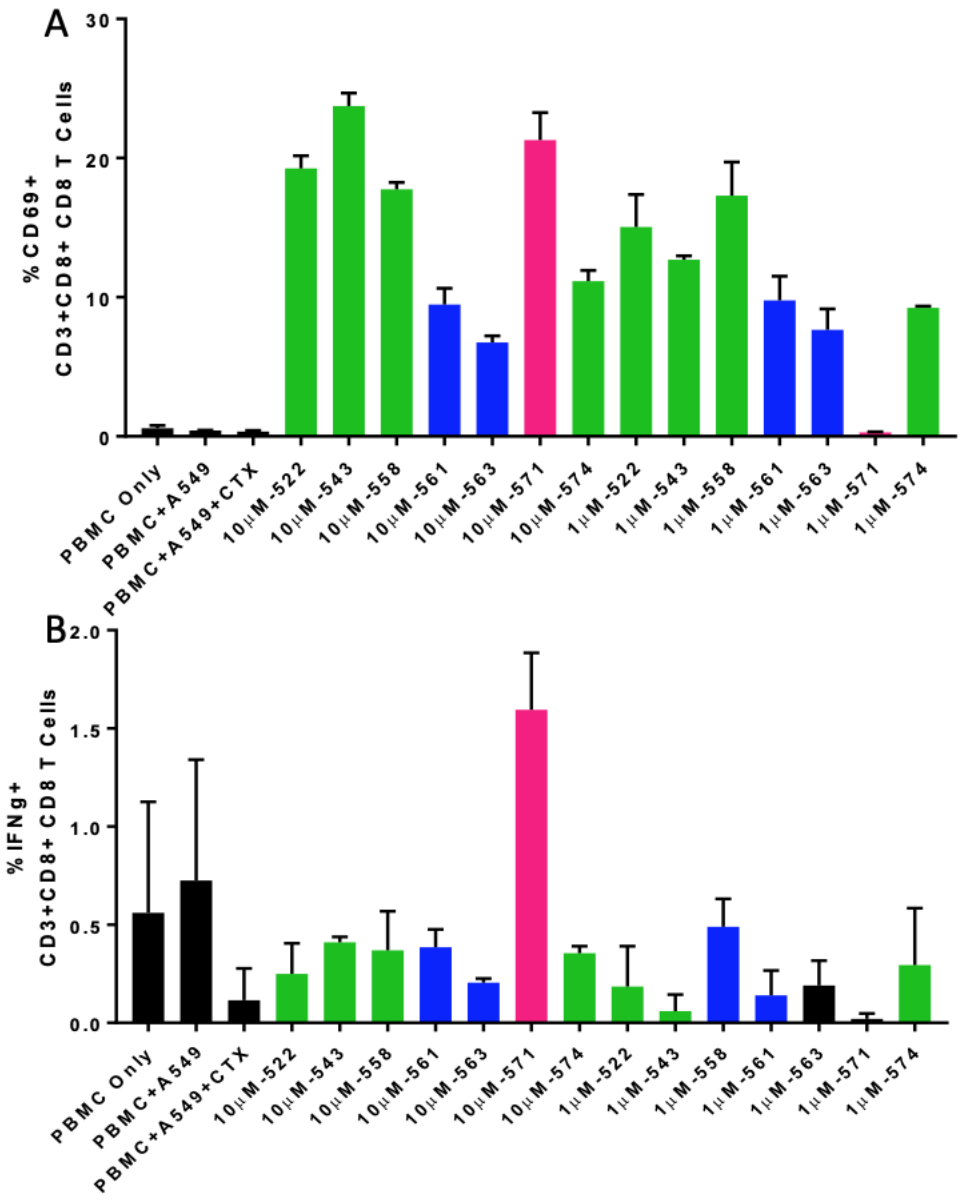

Figure 4.6: CD8 T cell activation assayed with human PBMCs (Donor I) using flow cytometry. $CD3^+/CD8^+$ cells were gated as CD8 T cells. CD8 T cells cells were then gated for **(A)** the activation marker CD69 and **(B)** the cytokine IFN-G. Percentage of CD8 T cells positive for the different markers are plotted on bar graphs. Different concentrations of the

compounds were tested, as have been indicated on the x-axis. All samples other than ‘PBMC Only’ contained A549 (target) cells. All samples other than ‘PBMC Only’ and ‘PBMC+A549’ contained Cetuximab (200nM). Statistical significance was measured by two-way ANOVA with multiple comparisons. Statistical significance is shown only for compounds that performed better than 522.

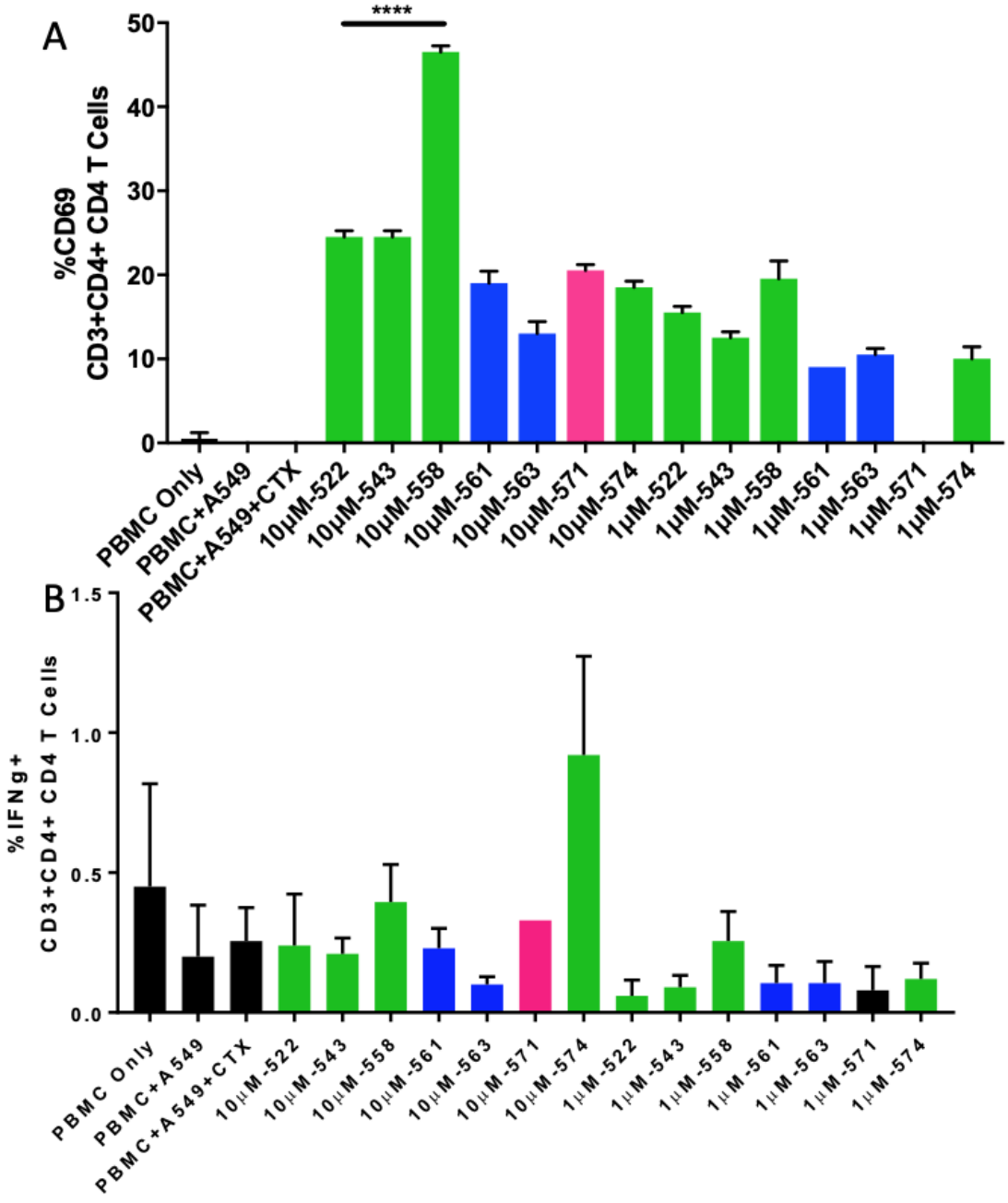

Figure 4.7: CD4 T cell activation assayed with human PBMCs (Donor I) using flow cytometry. $CD3^{+}/CD4^{+}$ cells were gated as CD4 T cells. CD4 T cells cells were then gated for **(A)** the activation marker CD69 and **(B)** the cytokine IFN-G. Percentage of CD4 T cells

positive for the different markers are plotted on bar graphs. Different concentrations of the compounds were tested, as have been indicated on the x-axis. All samples other than 'PBMC Only' contained A549 (target) cells. All samples other than 'PBMC Only' and 'PBMC+A549' contained Cetuximab (200nM). Statistical significance was measured by two-way ANOVA with multiple comparisons. ****P<0.0001. Statistical significance is shown only for compounds that performed better than 522.

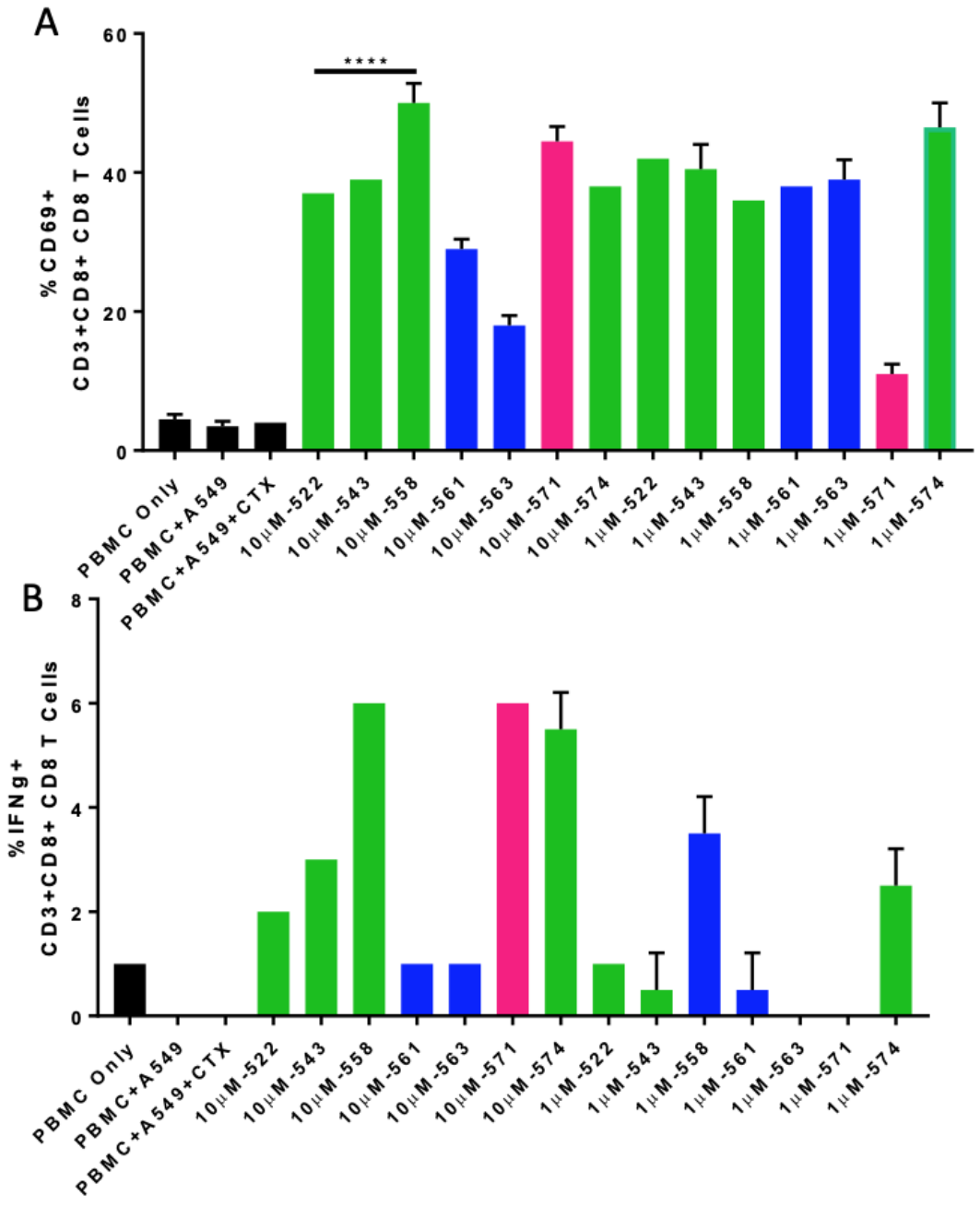

Figure 4.8: CD8 T cell activation assayed with human PBMCs (Donor II) using flow cytometry. $CD3^{+}/CD8^{+}$ cells were gated as CD8 T cells. CD8 T cells cells were then gated for **(A)** the activation marker CD69 and **(B)** the cytokine IFN-G. Percentage of CD8 T cells

positive for the different markers are plotted on bar graphs. Different concentrations of the compounds were tested, as have been indicated on the x-axis. All samples other than 'PBMC Only' contained A549 (target) cells. All samples other than 'PBMC Only' and 'PBMC+A549' contained Cetuximab (200nM). Statistical significance was measured by two-way ANOVA with multiple comparisons. ***P<0.001, ****P<0.0001. Statistical significance is shown only for compounds that performed better than 522.

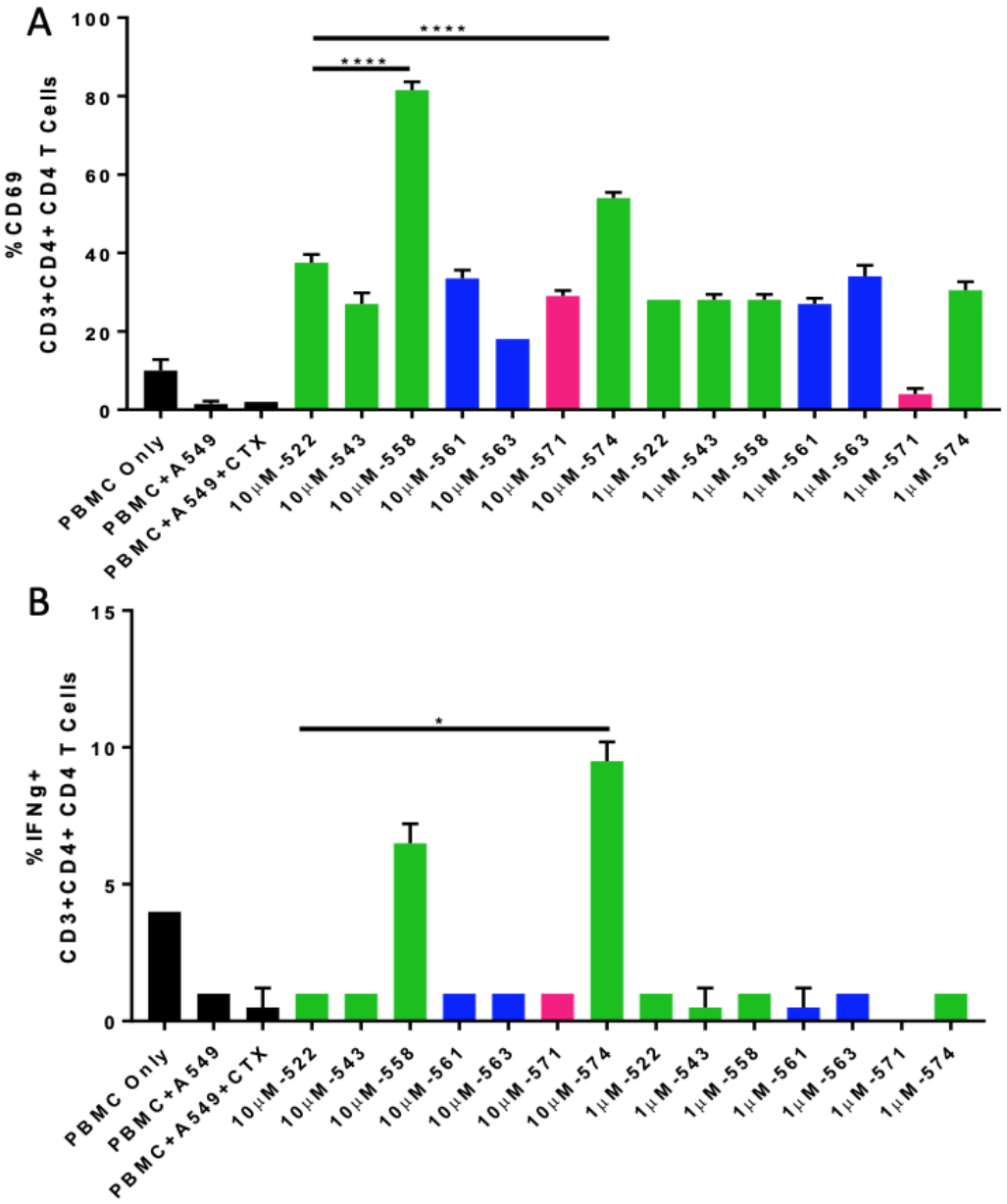

Figure 4.9: CD4 T cell activation assayed with human PBMCs (Donor II) using flow cytometry. $CD3^{+}/CD4^{+}$ cells were gated as CD4 T cells. CD4 T cells cells were then gated for **(A)** the activation marker CD69 and **(B)** the cytokine IFN-G. Percentage of CD4 T cells positive for the different markers are plotted on bar graphs. Different concentrations of the

compounds were tested, as have been indicated on the x-axis. All samples other than 'PBMC Only' contained A549 (target) cells. All samples other than 'PBMC Only' and 'PBMC+A549' contained Cetuximab (200nM). Statistical significance was measured by two-way ANOVA with multiple comparisons. *P<0.05, ****P<0.0001. Statistical significance is shown only for compounds that performed better than 522.

4.3.6. Compounds 543, 558 and 574 improve cetuximab mediated ADCC *in vitro*

Only compounds 543, 558 and 574, which showed significant improvement over 522 in the degranulation assay, were tested for ADCC. We tested the compounds at two effector cell to target cell (E:T) ratios of 10:1 and 20:1. All showed significantly better cytotoxicity (and correspondingly reduced cell survival) as compared to the samples treated with 522+cetuximab or cetuximab alone (P<0.0001 for cetuximab+522 v/s cetuximab+558/543/574 at both effector to target ratios, Figure 4.10A).

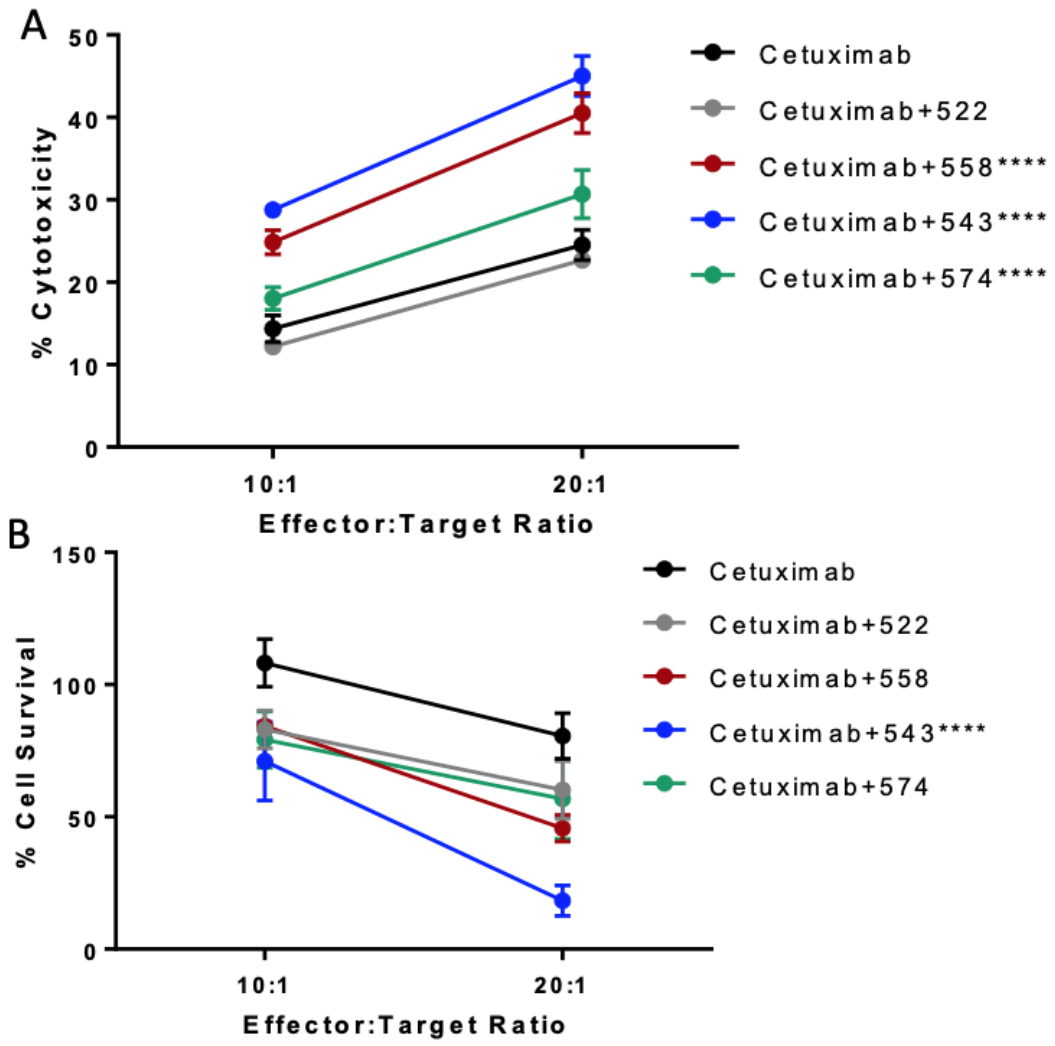

Figure 4.10: ADCC assay with human PBMCs. 558, 543, 574 (1μM) improved Cetuximab mediated ADCC. **(A)** Percentage cytotoxicity. (****P<0.0001 for Cetuximab+522 v/s Cetuximab+558/543/574 at both Effector:Target ratios, two-way ANOVA with multiple comparisons) **(B)** Percentage cell survival. ****P<0.0001 for Cetuximab+522 v/s

Cetuximab+543 at Effector:Target ratio of 20:1, two-way ANOVA with multiple comparisons)

4.3.7. Compounds 543, 558 and 574 show enhanced tumor growth inhibition in immunocompromised mouse model

For *in vivo* efficacy in the A549 Balb/c nude mouse model, compounds 574, 558 and 543 showed significantly improved tumor growth inhibition relative to 522, when combined with cetuximab ($P<0.0001$ for cetuximab+558/574/543 v/s cetuximab+522) (Figure 4.11). However, in this study the only compound that outperformed cetuximab alone was 558 (cetuximab+558 v/s cetuximab alone). 543 on the other hand was only marginally better than cetuximab alone (not statistically significant). This is particularly interesting because 543 demonstrated the most promising *in vitro* ADCC activity. This suggests that factors other than NK cell activation also play a role in mediating the activity of these agonists and require further investigation.

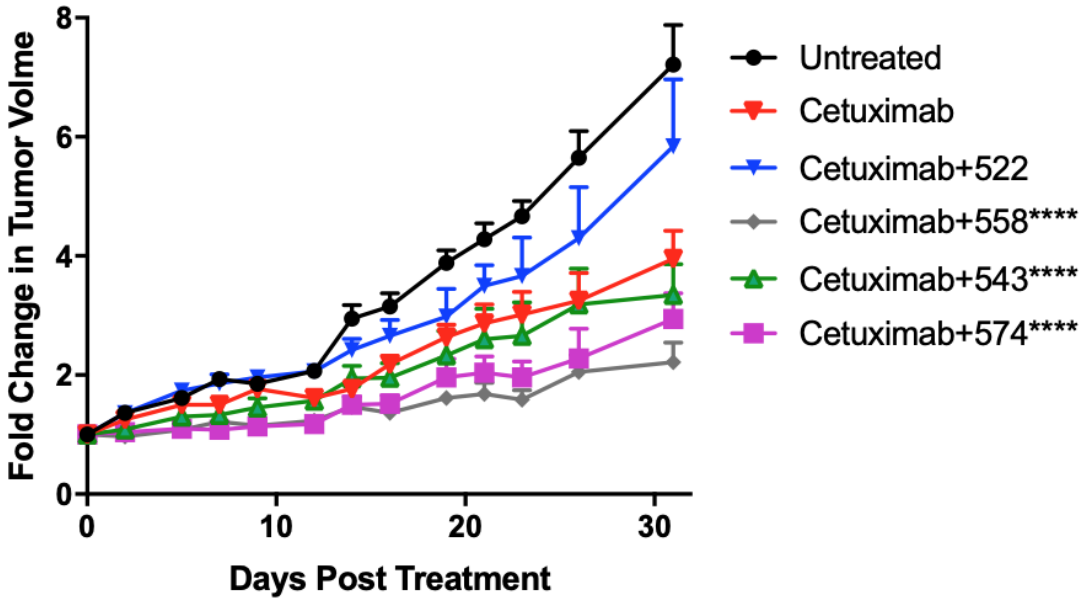

Figure 4.11: Efficacy study in Balb/c nude mice, grafted with A549 subcutaneous tumors. Cetuximab+558/574/543 showed significantly improved tumor growth inhibition over cetuximab+222 (****P<0.0001 for cetuximab+558/574/543 v/s Cetuximab+522, two-way ANOVA with multiple comparisons) Cetuximab+558 showed significantly improved tumor growth inhibition over Cetuximab alone (P<0.001 for Cetuximab+558 v/s Cetuximab alone, two-way ANOVA with multiple comparisons). Statistical significance is based on comparisons from the last day of the study.

4.3.8. Compounds 543, 558 and 574 show enhanced tumor growth inhibition in a TuBo Balb/c wild type mouse model

Our *in vitro* studies using human PBMCs suggested that in addition to NK cell degranulation and ADCC, TLR7/8 agonists also activated T cells. Activation of T cells can lead to memory response and facilitate long-term immunity. To test for the role of T cells, we used orthotopic TuBo tumors grafted in wild type Balb/c mice. TuBo cells expresses the HER2/neu antigen and are syngeneic to Balb/c mice. The monoclonal antibody 7.16.4 is an anti-HER2/neu antibody that has shown efficacy in the TuBo model in a previous study.[99]

The anti-HER2/neu antibody was only marginally better at tumor growth inhibition than the untreated group ($P<0.0001$ for untreated v/s anti-neu on day 10, Figure 4.12A). Compounds 522, 558 and 574 were all significantly better in combination with anti-HER2/neu as opposed to anti-HER2/neu treatment alone ($P<0.0001$ for anti-neu v/s anti-neu+522/558/574 on day 14). Interestingly, 543 (in combination with the antibody) did not perform significantly better than the antibody treatment alone. In contrast, 558 in combination with anti-HER2/neu, resulted in significantly greater tumor growth inhibition than 522. In 1 out of 8 mice in the anti-HER2/neu+574 group, the tumor was completely eradicated. In 2 out of the 7 mice in the anti-HER2/neu+558 group, the tumors were completely eradicated. Survival data from this study is presented in Figure 4.12B.

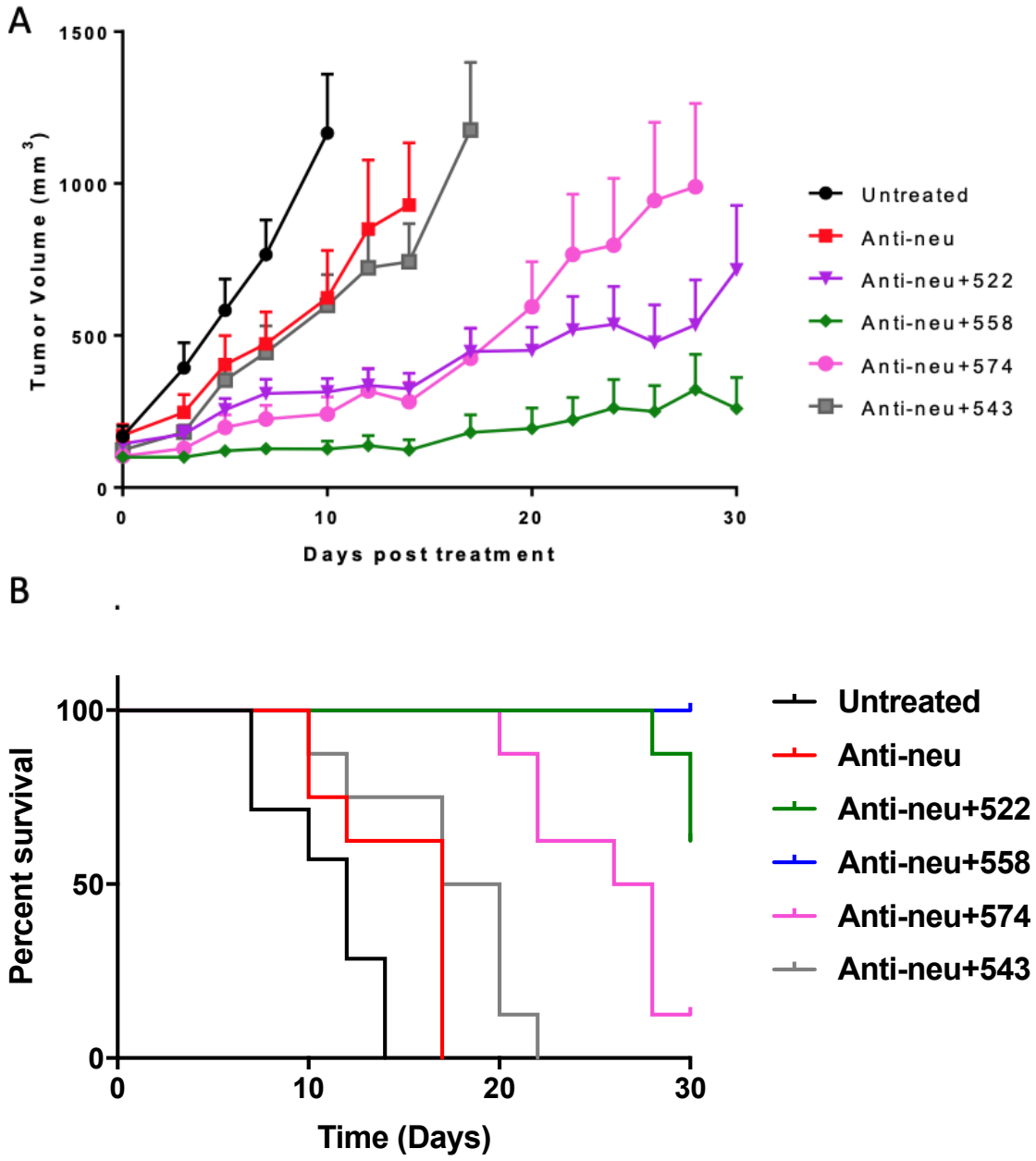

Figure 4.12: Efficacy study in wild-type Balb/c mice. **(A)** Absolute tumor volumes plotted against time. The anti-neu antibody showed significantly improved tumor growth inhibition in comparison to the untreated group. P<0.0001 for Untreated v/s anti-neu on

Day 10. Compounds 522, 558 and 574 performed significantly better in combination with the anti-neu antibody as opposed to the anti-neu antibody alone. $P<0.0001$ for anti-neu v/s anti-neu+522/558/574 on Day 14. $P>0.05$ for anti-neu v/s anti-neu+543 on Day 14. 558 was significantly better than 522, at inhibiting tumor growth when combined with anti-neu antibody. $P<0.05$ for anti-neu+522 v/s anti-neu+558 on Day 30. All statistical significance were calculated using two way ANOVA with multiple comparisons. **(B)** Survival curves of mice from the efficacy study.

4.3.9. Compound 558 increases NK cell activation in the tumor and spleen of wild type Balb/c mice grafted with TuBo tumors

For the effect of selected agonists on NK cells, tumors from mice sacrificed three days after the final dose that underwent treatment with anti-HER2/neu antibody and 558 had a significantly higher percent of NK cells ($P<0.05$, Figure 4.13A), as well as activated NK cells (analyzed as $NKG2D^+$ NK cells) ($P<0.05$, Figure 4.13C). The percent $CD69^+$ NK cells in the tumor also increased overall (Figure 4.13B), a trend similar to that observed *in vitro*. Interestingly, the percentage of 'non-tumor' cells, as determined by CD45 expression, was also significantly higher in case of anti-HER2/neu+558 treatment ($P<0.05$, ordinary one-way ANOVA with multiple comparisons Figure 4.13D). It is plausible that these 'non-tumor' cells are actually immune cells other than NK cells, such as T cells, dendritic cells and macrophages that infiltrate into the tumor and promote an improved immune response.

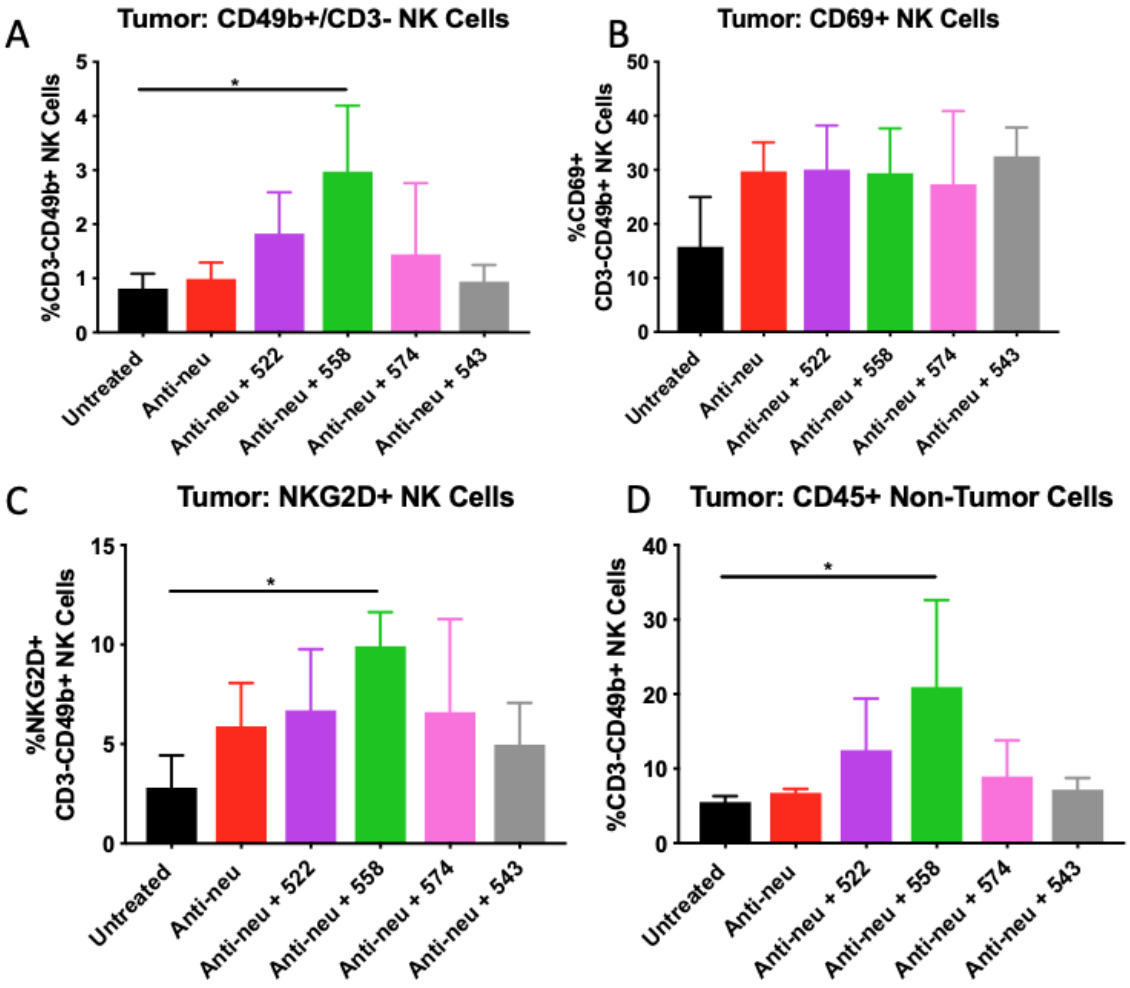

Figure 4.13: *Ex vivo* analysis of tumor post treatment with anti-HER2/neu antibody and TLR7/8 agonists **(A)** Percentage of $CD49b^{+}/CD3^{-}$ NK cells in tumor, *P<0.05 **(B)** Percentage of $CD69^{+}$ NK cells in tumor **(C)** Percentage of $NKG2D^{+}$ NK cells in tumor, *P<0.05 **(D)** Percentage of $CD45^{+}$ 'non-tumor' cells in tumor, *P<0.05. All statistical analysis is based on ordinary one-way ANOVA with multiple comparisons.

In the case of spleen, the absolute percent of NK cells in the anti-HER2/neu+558 treated group was similar to that observed in the untreated group (Figure 4.14A). This may be a reflection of a change in the composition of splenocytes in terms of other immune cells, such as T cells. However, the percentage of $CD69^{+}$ NK cells was higher in case of anti-HER2/neu+558 as compared to that observed in untreated animals ($P<0.05$, Figure 4.14B). There was no change in the percent activated NK cells in the spleen as reflected by NKG2D expression (Figure 4.14C)

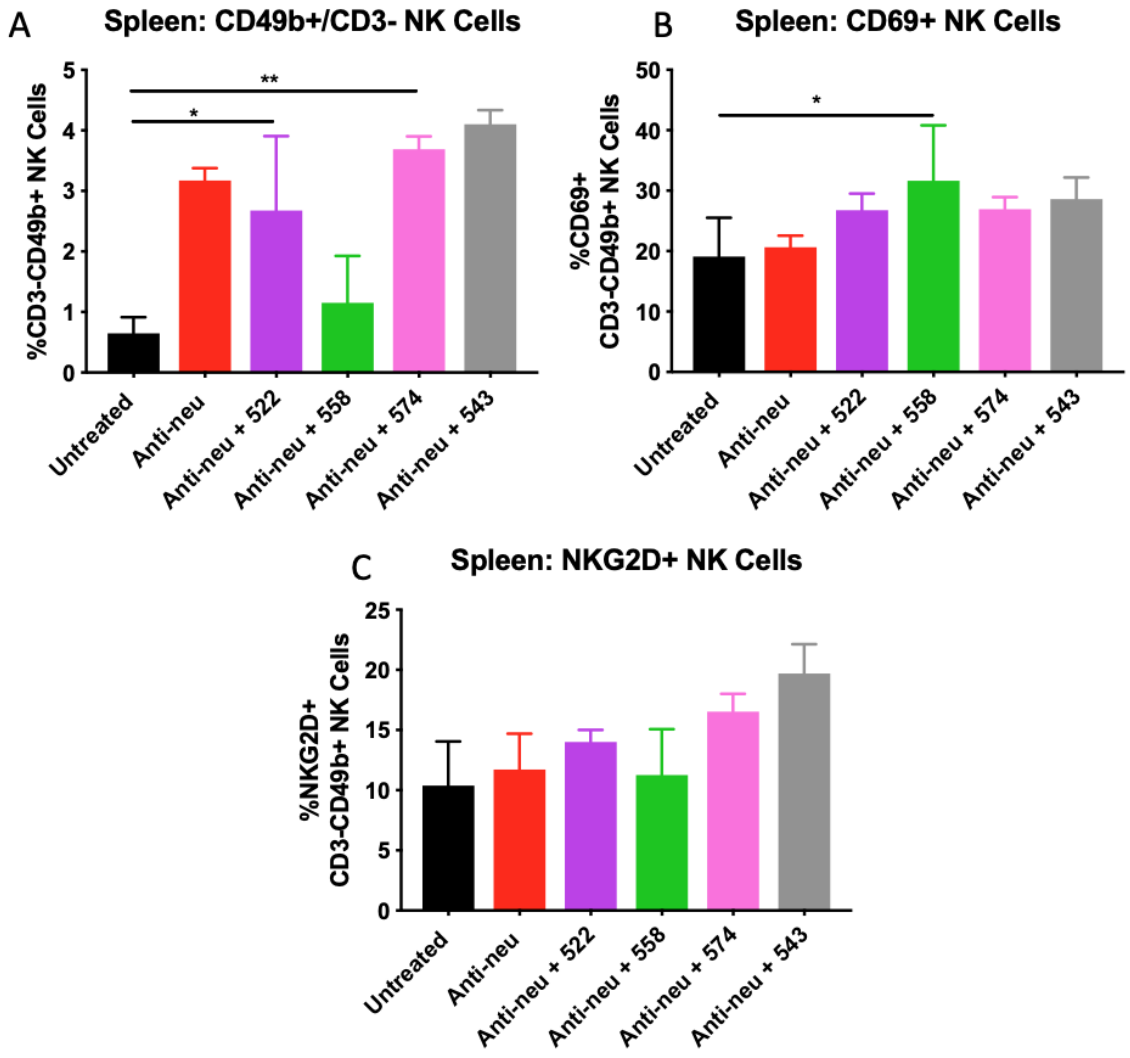

Figure 4.14: *Ex vivo* analysis of spleen post treatment with anti-HER2/neu antibody and TLR7/8 agonists **(A)** Percentage of $CD49b^{+}/CD3^{-}$ NK cells in spleen, *P<0.05, **P<0.01 **(B)** Percentage of $CD69^{+}$ NK cells in spleen *P<0.05 **(C)** Percentage of $NKG2D^{+}$ NK cells in spleen. All statistical analysis is based on ordinary one-way ANOVA with multiple comparisons.

4.3.10. Compound 558 increases the expression of chemokines CXCL9 and CXCL10 in tumor

CXCL9, CXCL10 and CXCL11 are chemokines overexpressed in tumors that lead to the recruitment of NK cells and T cells to the tumor[164]. It has been previously reported that the ligand on T cells and NK cells involved in this interaction is CXCR3. However, upon recruitment to the tumor, CXCR3 is depleted and thus the chemokines CXCL9, CXCL10 and CXCL11 can be measured as indirect markers for NK cell and T cell recruitment. We observed an increase in CXCL9 (data not significant, Figure 4.15A) and CXCL10 (data not significant, Figure 4.15B) mRNA expression when the mice were treated with anti-HER2/neu+558. However, there was significant variability in this data, which is similar to that observed for T cell infiltration studied using IHC. CXCL11 expression did not vary among the different treatment groups.

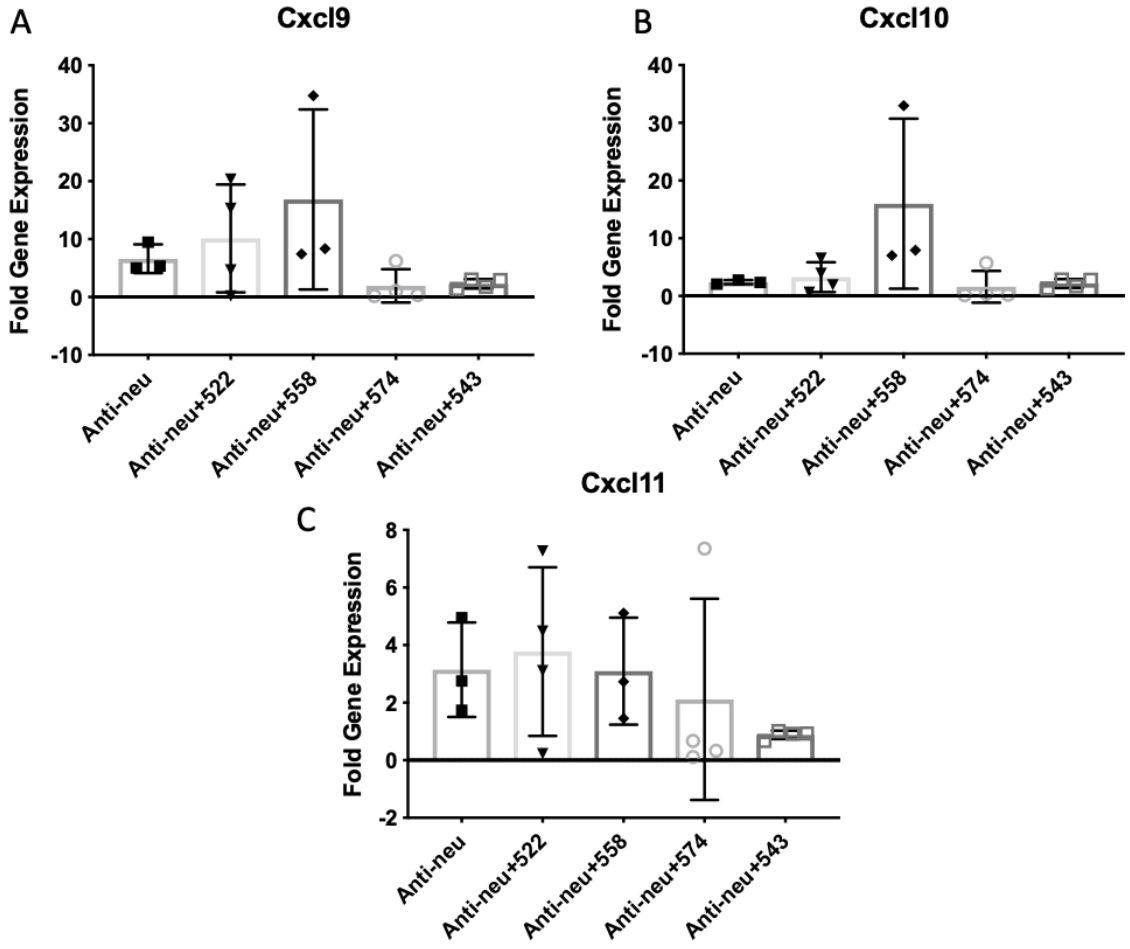

Figure 4.15: *Ex vivo* analysis of **(A)** CXCL9, **(B)** CXCL10 and **(C)** CXCL11 chemokines (mRNA) in tumor. Data not statistically significant, ordinary one-way ANOVA with multiple comparisons.

4.3.11. 522 and 558 increase CD8 T cell infiltration into the tumor

There was significant T cell infiltration in almost all the sections analyzed (Figure 4.16). The addition of 558 or 522 to the anti-HER2/neu antibody treatment resulted in significantly higher CD8 T cell infiltration ($P<0.05$, Figures 4.16B, C, E). It is important to note that in the anti-neu/HER2+558 treated group 2 out of 8 mice did not have tumors at the end of the study, and thus we were unable to evaluate T cell infiltration in those animals. The addition of 574 also trended towards an increase in CD8 T cell infiltration; however, the data was not statistically significant.

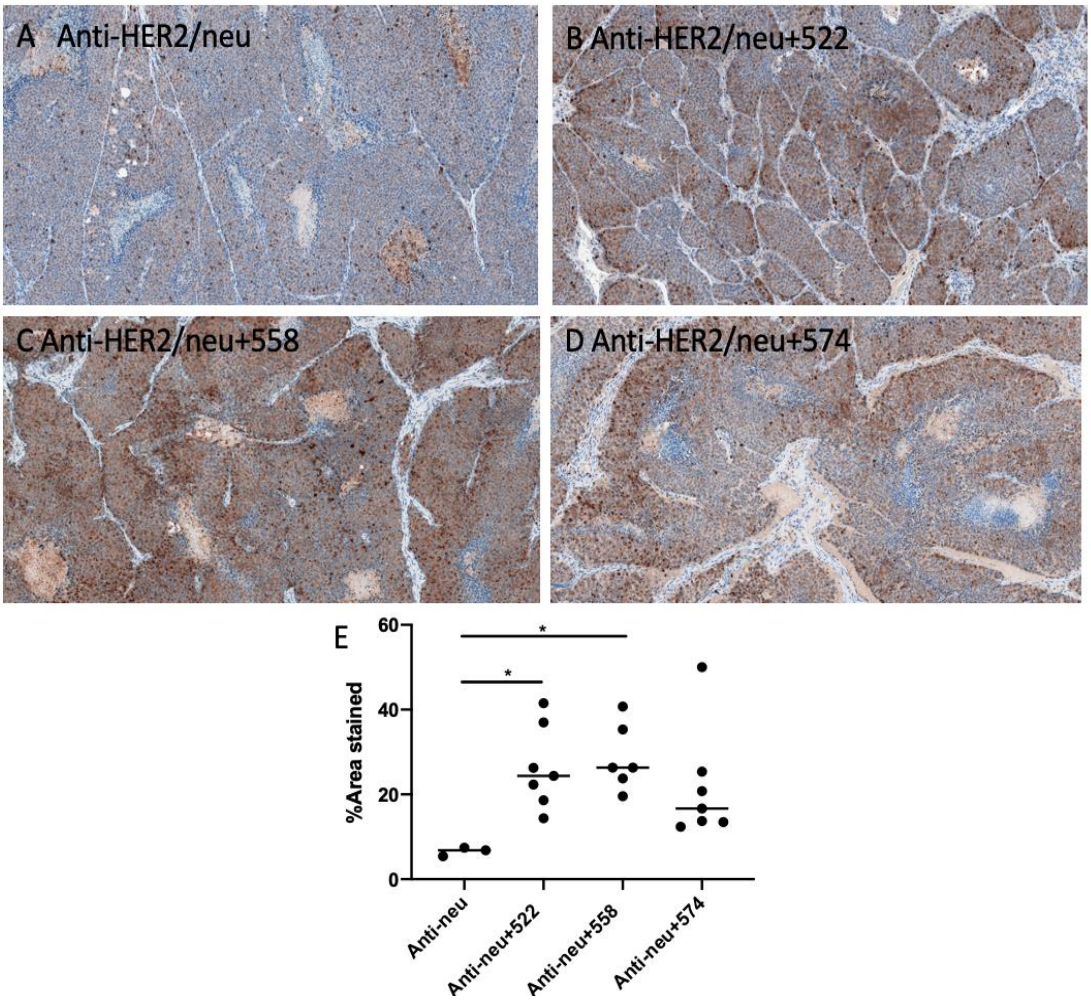

Figure 4.16: *Ex vivo* IHC analysis of CD8 T cell infiltration. Representative images presented from each group. Brown is indicative of positive staining. **(A)** Anti-HER2/neu **(B)** Anti-HER2/neu **(C)** Anti-HER2/neu+558 **(D)** Anti-HER2/neu+574 **(E)** Quantified data for percentage area stained. *P<0.05, ordinary one-way ANOVA with multiple comparisons.

4.4. Discussion

Monoclonal antibody therapy has improved the treatment outcomes in different cancers. Yet, many limitations exist. As such, combination therapies are being explored that can further improve the therapeutic efficacy of antibodies, such as cetuximab, rituximab and trastuzumab, that work primarily through NK cell mediated ADCC.

Previous reports have described the successful use of TLR7 and TLR 8 agonists for augmenting ADCC *in vitro*[107]. A recent publication from our lab explored the use of a novel TLR7/8 agonist (522) for improving ADCC.[155] 522 was encapsulated in gas generating nanoparticles (522GGNPs) to enhance delivery to dendritic cells.[162] The combination of 522GGNPs with cetuximab was able to significantly enhance ADCC *in vitro*.[155] Here, we tested 522GGNPs *in vivo*, in combination with cetuximab, for the treatment of subcutaneously grafted $EGFR^+$ A549 tumors in Balb/c nude mice. Despite the improved tumor growth inhibition efficacy observed with 522GGNPs, we were able to prolong survival of the tumor-bearing mice by only an estimated ~10 days. Further, NK cell infiltration, although better than that observed with cetuximab monotherapy, was still limited to the periphery of the tumor.

In order to further improve cetuximab monotherapy, we evaluated several second generation compounds.[156] These compounds not only showed significantly higher cytokine production as compared to 522 but also induced higher NK cell degranulation *in vitro*. Interestingly, several of these compounds also showed potent T cell activation *in vitro*.

Through multiple *in vitro* assays, we determined that the most promising compounds from this panel were 543, 574 and 558.

The Balb/c nude mouse model lacks T cells but retains NK cell activity. Our primary goal was to evaluate these compounds for their ability to enhance NK cell mediated ADCC. Thus, the Balb/c nude mouse model was well-suited for this purpose. For this model, the dosing was evenly spaced over a span of sixteen days. This is because NK cells have long been understood to undergo short-term activation in response to stimuli, although there has been some debate in the field over this.[165,166] Thus, each cetuximab dose was proceeded with an agonist dose. We found that all three compounds performed significantly better than 522 *in vivo*. In particular, the compound 558 was quite effective in inhibiting tumor growth. Interestingly though, 522 (in combination with cetuximab) did not show improved activity over cetuximab alone. This can likely be explained either due to the pharmacokinetics of 522 (all previous studies have evaluated 522 in a nanoparticle formulation that provided controlled release of the drug) or due to the lack of T cells in this model (T cells have been understood to have sustained activation, unlike NK cells). However, further studies are needed to confirm these suppositions.

TLR7/8 agonists have been commonly used as vaccine adjuvants, because these compounds activate DCs to secrete a number of cytokines that are then thought to activate NK cells. However, their main mechanism of action as anti-cancer vaccine adjuvants has been their indirect activation of T cells. We observed substantial T cell activation *in vitro*. For T cells to mount a specific anti-cancer immune response, not only must they be

activated but they must also be presented with the target antigen.[7] Park et al[99] identified a link between therapeutic antibodies and adaptive immunity mediated T cells. They found that an anti-HER2/neu antibody promoted ADCC as its major mechanism but also enhanced cross-priming of T cells, essentially providing T cells with the antigen '*in situ*'. Of note, the paper also reported a memory immune response at high doses of the antibody, very similar to that observed following anti-cancer vaccination. Such effects have also been reported with radiation therapy.[167] Thus we extended our studies to include a fully immunocompetent model to evaluate T cell responses to combination therapy with a monoclonal antibody and TLR7/8 agonists.

For this model, the dosing was completed within five days, based on our previous experience with immunocompetent models. Compounds 522, 574 and 558 but not 543 showed effective tumor growth inhibition in combination with the anti-HER2/neu antibody, relative to that with antibody alone. In a fully immunocompetent model, there are at least three parameters that would determine the treatment outcome (1) pharmacokinetics of the agonist, (2) NK cell activation, and (3) T cell activation. It is possible that 543, although a potent inducer of ADCC, is not a good compound for T cell activation. Similarly, 522, is possibly better at T cell activation than it is at NK cell activation and thus we see a difference in the outcome between the two tumor models. Further experiments are needed to test these theories.

Ex vivo analysis of the tumors from the TuBo model showed significant NK cell infiltration, especially NK cells with an activated phenotype. We also observed an increase

in the activated NK cells in the spleen of mice treated with the agonists. There was an increase in the expression of CXCL9 and CXCL10, both chemokines that are known to recruit NK cells and T cells to the tumor.[158] Finally, upon examination of the tumor sections at the end of the study we saw significantly higher T cell infiltration in the tumors of mice that were treated with 522 and 558, thus suggesting the involvement of the adaptive immune system.

Although Park et al[99] were successful at eradicating tumors in a large number of mice by using high dose antibody treatment, this is often not replicated in the clinic. Currently, despite the success of monoclonal antibody therapy, some patients relapse.[168] Our rationale behind combining the novel TLR7/8 agonists with an antibody therapeutic was to stimulate an intense adaptive immune response.[169] In our studies, although there were several indications that a strong T cell response with the TLR7/8 agonists, tumors were eradicated in only a small fraction of treated mice. This is likely because the antibody dose used in our studies was lower than that used by Park et al.[99] Thus, further dose refinement may be needed to realize the full potential of the agonists.

4.5. Conclusion

The TLR7/8 agonist 522, when encapsulated in nanoparticles was able to effectively retard tumor growth in combination with cetuximab. Second generation TLR7/8 agonists 543, 574 and 558 were more effective than 522 in activating cytokine secretion as well as in inducing ADCC. *In vivo* studies in immunocompromised and immunecompetent mouse models showed that compound 558 can significantly improve the anticancer efficacy of monoclonal antibodies.

Chapter 5: Summary

One of the first considerations in the development of therapeutic antibodies is finding the right target. Often, targets explored through gene expression analysis are intracellular, and thus not suitable for antibody development. Alternatively, some targets undergo post-translational modifications that might mislead development efforts that are simply based on protein sequences. Phage display is a versatile technique, developed by George P. Smith and Sir Gregory Winter, that allows development of antibodies *in vitro*.[22,170,171] Phage display also allows for the discovery of novel tumor antigens.

In chapter 2, we described the discovery of a novel tumor antigen, HSPG2/perlecan, in metastatic triple negative breast cancer using phage display. HSPG2 overexpression correlated with poor patient survival in triple negative breast cancer, bladder cancer, melanoma and ovarian cancer. Thus, we utsed an *in vitro* phage display based bio-panning procedure to identify a novel antigen that was further applied towards the development of antibody-based therapeutics.

The mechanism of action for monoclonal antibodies, unlike most chemotherapeutics, can be quite complex. Often, more than one mechanism contributes to the efficacy observed with antibodies. In chapter 3, we described the development and evaluation of the two anti-HSPG2 antibodies – Tw1S4_6 and Tw1S4_AM6. We found that Tw1S4_AM6 resulted in significant tumor growth inhibition in an *in vivo* mouse model of metastatic triple negative breast cancer. Additional studies showed that Tw1S4_AM6 mediated its activity primarily through ADCC. Although extensive studies are required to conclusively rule out the involvement of HSPG2 related mechanisms, the current studies

enable the rational selection of combination therapeutics that leverage ADCC in order to potentiate the efficacy of Tw1S4_AM6.

Monoclonal antibodies are often combined with various chemotherapeutic agents for the treatment of cancer. However, the main advantage of antibodies is their high specificity and lower off-target toxicity concerns. Combining monoclonal antibodies with chemotherapeutics, although beneficial in terms of treatment outcomes, mitigates the advantages of lower off-target effects. It follows that combining antibody therapy with molecules that potentiate their on-target effects would be a better option. Recently, several monoclonal antibody therapeutics have been combined in the clinic with drugs that are immune-stimulants and/or with radiation. For example, trastuzumab and cetuximab are both being tested in combination with a PD-1 inhibitor (pembrolizumab), to enhance patient outcomes.[172,173]

In chapter 4, we tested seven novel small molecule TLR7/8 agonists in combination with monoclonal antibody therapy, with the main goal of enhancing ADCC. We found that the agonists 522, 574 and 558 significantly enhanced NK cell mediated ADCC *in vitro* as well as enhanced the efficacy of monoclonal antibodies in two different *in vivo* mouse models. Additionally, we found that the agonists were also able to stimulate CD 8 T cells, which was indicative of an early adaptive immune response. This was particularly promising, because only a few groups have reported the development of an adaptive immune response with antibody therapeutics.[99]

Although there have been several cancer vaccines developed to stimulate an adaptive memory response in cancer patients, the cancer antigen is not necessarily personalized to the patient. Autologous vaccines utilizing patient's own tumor tissue, although personalized for the patient, are labor and time intensive and are very expensive. Monoclonal antibody therapy combined with an immune-stimulant (such as TLR7/8 agonists) can be quite advantageous considering (1) it is more cost-effective than developing a personalized vaccine for each patient (2) even though the therapy is not personalized, it is targeted (3) therapy may be initiated almost as soon as the patient is diagnosed and (4) there is evidence of an adaptive immune response with monoclonal antibodies that can be enhanced further with the combination of immune-stimulants.

The first FDA approved monoclonal antibody entered the clinic in 1985.[57] Although this class of therapeutics faced several challenges initially, today they are one of the mainstay class of drugs for cancer therapy. This thesis examined the various aspects related to antibody therapeutics, including novel targets, mechanisms of action of novel antibodies, and leveraging their mechanism of action to improve efficacy. We expect that the research presented here will help improve the treatment outcomes for patients diagnosed with cancer.

Bibliography

1. Schreiber RD, Old LJ, Smyth MJ. Cancer Immunoediting : Integrating Suppression and Promotion. 2011;331(March):1565-1571.
2. Farkona S, Diamandis EP, Blasutig IM. Cancer immunotherapy : the beginning of the end of cancer? *BMC Med*. 2016;14(73):1-18.
3. Jefferis R. Isotype and glycoform selection for antibody therapeutics. *Arch Biochem Biophys*. 2012;526(2):159-166.
4. Ecker, Dawn M; Dana Jones SLHL. The therapeutic monoclonal antibody market. *MAbs*. 2015;7:1(January-February 2015):9-14.
5. Weiner GJ. Building better monoclonal antibody-based therapeutics. *Nat Rev Cancer*. 2015;15(6):361-370.
6. Lobo ED, Hansen RJ, Balthasar JP. Antibody pharmacokinetics and pharmacodynamics. *J Pharm Sci*. 2004;93(11):2645-2668.
7. Murphy K. *Janeway's Immunobiology*.; 2012.
8. Leu J, Chen B, Schiff PB, Erlanger BF. Characterization of Polyclonal and Monoclonal Anti-Taxol Antibodies and Measurement of Taxol in Serum1. 1993.
9. Alberts B, Johnson A, Lewis J et al. *Molecular Biology of the Cell*. 4th editio. New York: Garland Science; 2002.
10. Kohler G, Milstein C. Continuous cultures of fused cells secreting antibody of predefined specificity. *Nature*. 1975;256:495-497.
11. Pirofsky, L; Casadevall, A; Rodriguez, L; Zuckeir, S; Scharff M. Current state of

the hybridoma technology. *J Clin Immunol*. 1990;10(6):5-14.

12. Brekke OH, Sandlie I. Therapeutic antibodies for human diseases at the dawn of the twenty-first century. *Nat Rev Drug Discov*. 2003;2(1):52-62.
13. Smith SL. Ten years of Orthoclone OKT3. *J Transpl Coord*. 1996;6(3):109-121.
14. Harding FA, Stickler MM, Razo J, DuBridge RB. The immunogenicity of humanized and fully human antibodies: Residual immunogenicity resides in the CDR regions. *MAbs*. 2010;2(3):256-265.
15. Wang W, Wang EQ, Balthasar JP. Monoclonal Antibody Pharmacokinetics and Pharmacodynamics. *Clin Pharmacol Ther*. 2008;84(5).
16. Genentech. Rituxan Package Insert. 2019.
17. Boyiadzis M, Foon KA. Approved monoclonal antibodies for cancer therapy. *Expert Opin Biol Ther*. 2008;8(8):1151-1158.
18. The Nobel Foundation. The Nobel Prize. Official Webpage of the Nobel Prize.
19. Abbvie. Humira Package Insert. 2019.
20. Nixon AE, Sexton DJ, Ladner RC, Nixon AE, Sexton DJ, Ladner RC. Drugs derived from phage display. *MAbs*. 2014;6(1):73-85.
21. Urquhar L. Top drugs and companies by sales in 2018. *Nat Rev Drug Discov*. 2019;18(April):245.
22. Bazan J, Całkosiñski I, Gamian A. Phage display a powerful technique for immunotherapy. *Hum Vaccines Immunother*. 2012;8(12):1817-1828.
23. Strohl WR. Current progress in innovative engineered antibodies. *Protein Cell*. 2018;9(1):86-120.

24. Kanyavuz A, Marey-Jarossay A, Lacroix-Desmazes S, Dimitrov JD. Breaking the law: unconventional strategies for antibody diversification. *Nat Rev Immunol*. 2019.

25. Salfeld JG. Isotype selection in antibody engineering. *Nat Biotechnol*. 2007;25(12):1369-1372.

26. Vidarsson G, Dekkers G, Rispens T. IgG subclasses and allotypes : from structure to effector functions. 2014;5(October):1-17.

27. Genentech. Herceptin Package Insert. 2018.

28. Bristol-Myers Squibb, Eli Lilly. Erbitux Package Insert. 2012:1-31.

29. Amgen. Vectibix Package Insert. 2017.

30. Merck. Keytruda Package Insert. 2019.

31. Topalian SL, Drake CG, Pardoll DM. Targeting the PD-1/B7-H1 (PD-L1) pathway to activate anti-tumor immunity. *Curr Opin Immunol*. 2011;24(2):207-212.

32. Bristol-Myers Squibb. Yervoy Package Insert. 2019.

33. Bristol-Myers Squibb. Opdivo Package Insert. 2019.

34. Genentech. Herceptin Hylecta Package Insert. 2019.

35. Regeneron, Sanofi Genzyme. Dupixent Package Insert. 2019.

36. Vaishnaw AK, Tenhoor CN. Pharmacokinetics, biologic activity, tolerability of lefacept by intravenous and intramuscular administration. *J Pharmacokinet Pharmacodyn*. 2003;29(5):415-426.

37. Lin YS, Nguyen C, Mendoza J, et al. Preclinical Pharmacokinetics , Interspecies

Scaling , and Tissue Distribution of a Humanized Monoclonal Antibody against Vascular Endothelial Growth Factor. 1999;288(1):371-378.

38. Richter WF, Bhansali SG, Morris ME. Mechanistic Determinants of Biotherapeutics Absorption Following SC Administration. 2012;14(3).

39. Richter WF, Jacobsen B. Subcutaneous Absorption of Biotherapeutics : Knowns and Unknowns. *Drug Metab Dispos*. 2014;42(November):1881-1889.

40. Bareford LM, Swaan PW. Endocytic mechanisms for targeted drug delivery. 2007;59(8):748-758.

41. Roopenian DC, Akilesh S. FcRn: the neonatal Fc receptor comes of age. *Nat Rev Immunol*. 2007;7(9):715-725.

42. Sethu S, Govindappa K, Park K, Sathish J. Immunogenicity to Biologics : Mechanisms , Prediction and Reduction. 2012:331-344.

43. Baxter LT, Zhu H, Mackensen DG, Jain R. Physiologically based pharmacokinetic model for specific and nonspecific monoclonal antibodies and fragments in normal tissues and human tumor xenografts in nude mice. *Cancer Res*. 1994;54(March):1517-1528.

44. Tzaban S, Massol RH, Yen E, et al. The recycling and transcytotic pathways for IgG transport by FcRn are distinct and display an inherent polarity. *J Cell Biol*. 2009;185(4):673-684.

45. Kim K, Fandy TE, Lee VHL, et al. Net absorption of IgG via FcRn-mediated transcytosis across rat alveolar epithelial cell monolayers. *Am J Physiol lung, Cell Mol Physiol*. 2004;287:616-622.

46. Junghans RP. Finally! The Brambell Receptor (FcRB). *Immunol Res*. 1997;16(1):29-57.

47. Xiao JJ. Pharmacokinetic Models for FcRn-Mediated IgG Disposition. 2012;2012.

48. Benjamin RJ, Cobbold SP, Clark MR, Waldmann C. Tolerance to rat monoclonal antibodies. *J Exp Med*. 1986;163(June):1539-1552.

49. Brliggemann BYM, Winter G, Waldmann H, Neubergert MS. The immunogenicity of chimeric antibodies. *J Exp Med*. 1989;170(December):2153-2157.

50. Harding FA, Stickler MM, Razo J, et al. The immunogenicity of humanized and fully human antibodies The immunogenicity of humanized and fully human antibodies Residual immunogenicity resides in the CDR regions. 2010;0862(May).

51. Presta LG. Engineering of therapeutic antibodies to minimize immunogenicity and optimize function B. 2006;58:640-656.

52. Sievers EL, Senter PD. Antibody-Drug Conjugates in Cancer Therapy. *Annu Rev Med*. 2013;64:15-29.

53. Seattle Genetics. Adcetris Package Insert. 2018.

54. Genentech. Kadcycla Package Insert. 2019.

55. Pfizer. Mylotarg Package Insert. 2018.

56. Pfizer. Besponsa Package Insert. 2018.

57. Liu JKH. The history of monoclonal antibody development e Progress , remaining challenges and future innovations. *Ann Med Surg*. 2014;3(4):113-116.

58. Sgro C. Side-effects of a monoclonal antibody , muromonab CD3 / orthoclone

OKT3 : bibliographic review. *Toxicology*. 1995;105:23-29.

59. Amoroso A, Hafsi S, Militello L, et al. Understanding rituximab function and resistance: implications for tailored therapy Alfredo. *Front Biosci*. 2011;16:770-782.

60. Li S, Schmitz KR, Jeffrey PD, Wiltzius JJW, Kussie P, Ferguson KM. Structural basis for inhibition of the epidermal growth factor receptor by cetuximab. *Cancer Cell*. 2005;7(April):301-311.

61. Nahta R, Esteva FJ. Herceptin : mechanisms of action and resistance. *Cancer Lett*. 2006;232:123-138.

62. Dong H, Strome S, Salomao D, et al. Tumor-associated B7-H1 promotes T-cell apoptosis : A potential mechanism of immune evasion. *Nat Med*. 2002;8(8):793-800.

63. Pardoll DM. The blockade of immune checkpoints in cancer immunotherapy. *Nat Rev Cancer*. 2012;12(April):252-264.

64. EMD Serono. Bavencio Package Insert. 2019:1-31.

65. Wang C, Thudium KB, Han M, et al. In Vitro Characterization of the Anti-PD-1 Antibody Nivolumab , BMS-936558 , and In Vivo Toxicology in Non-Human Primates. *Cancer Immunol Res*. 2014;2(September):20-22.

66. Donahue RN, Lepone LM, Grenga I, et al. Analyses of the peripheral immunome following multiple administrations of avelumab , a human IgG1 anti-PD-L1 monoclonal antibody. *J Immunother Cancer*. 2017;5(20):1-16.

67. Desjarlais JR, Lazar GA. Modulation of antibody effector function. *Exp Cell Res*.

2011;317(9):1278-1285.

68. Arnould L, Gelly M, Penault-Llorca F, et al. Trastuzumab-based treatment of HER2-positive breast cancer: An antibody-dependent cellular cytotoxicity mechanism? *Br J Cancer*. 2006;94(2):259-267.

69. Kurai J, Chikumi H, Hashimoto K, et al. Antibody-dependent cellular cytotoxicity mediated by cetuximab against lung cancer cell lines. *Clin Cancer Res*. 2007;13(5):1552-1561.

70. Brand TM, Iida M, Wheeler DL. Molecular mechanisms of resistance to the EGFR monoclonal antibody cetuximab. *Cancer Biol Ther*. 2011;11(9):777-792.

71. Hsu YF, Ajona D, Corrales L, et al. Complement activation mediates cetuximab inhibition of non-small cell lung cancer tumor growth in vivo. *Mol Cancer*. 2010;9:1-8.

72. Vargas FA, Furness AJS, Litchfield K, et al. Fc Effector Function Contributes to the Activity of Human Anti-CTLA-4 Antibodies. *Cancer Cell*. 2018;33(4):649-663.e4.

73. Morvan MG, Lanier LL. NK cells and cancer: you can teach innate cells new tricks. *Nat Rev Cancer*. 2016;16(1):7-19.

74. Smyth MJ, Hayakawa Y, Takeda K, Yagita H. New aspects of Natural-Killer-Cell Surveillance and Therapy of Cancer. *Nat Rev Cancer*. 2002;2(November):850-861.

75. Degli-Esposti MA, Smyth MJ. Close encounters of different kinds: Dendritic cells and NK cells take centre stage. *Nat Rev Immunol*. 2005;5(2):112-124.

76. Bruhns P, Iannascoli B, England P, Mancardi D a, Fernandez N, Jorieux S. Specificity and affinity of human FcG receptors and their polymorphic variants for human IgG subclasses. *Blood*. 2009;113(16):3716-3725.

77. Heiken JEGH, Schmidt ATRE. The IgG Fc receptor family. *Ann Hamatology*. 1998;76:231-248.

78. Shields RL, Namenuk AK, Hong K, et al. High Resolution Mapping of the Binding Site on Human IgG1 for FcGRI , FcGRII , FcGRIII , and FcRn and Design of IgG1 Variants with Improved Binding to the FcGR. *J Biol Chem*. 2001;276(9):6591-6604.

79. Mellor JD, Brown MP, Irving HR, Zalcberg JR, Dobrovic A. A critical review of the role of Fc gamma receptor polymorphisms in the response to monoclonal antibodies in cancer. *J Hematol Oncol*. 2013;6(1):1.

80. Cartron G, Dacheux L, Salles G, et al. Therapeutic activity of humanized anti-CD20 monoclonal antibody and polymorphism in IgG Fc receptor FcgammaRIIIa gene. *Blood*. 2002;99(3):754-758.

81. Treated P, Cetu WS. FCGR2A and FCGR3A Polymorphisms Associated With Clinical Outcome of Epidermal Growth Factor Receptor – Expressing Metastatic Colorectal Cancer FCGR2A and FCGR3A Polymorphisms Associated With Clinical Outcome of Epidermal Growth Factor Receptor – Expressin. 2007;(September).

82. Krzewski K, Coligan JE. Human NK cell lytic granules and regulation of their exocytosis. *Front Immunol*. 2012;3(November):1-16.

83. Orange JS. Formation and function of the lytic NK - cell immunological synapse. *Nat Rev Immunol*. 2008;8(August).

84. Tang Y, Lou J, Alpaugh RK, Robinson MK, Marks JD, Weiner LM. Regulation of Antibody-Dependent Cellular Cytotoxicity by IgG Intrinsic and Apparent Affinity for Target Antigen. *J Immunol*. 2007;179(5):2815-2823.

85. Hsieh Y Te, Aggarwal P, Cirelli D, Gu L, Surowy T, Mozier NM. Characterization of FcγRIIIA effector cells used in in vitro ADCC bioassay: Comparison of primary NK cells with engineered NK-92 and Jurkat T cells. *J Immunol Methods*. 2017;441:56-66.

86. Shimizu C, Mogushi K, Morioka MS, et al. Fc-Gamma receptor polymorphism and gene expression of peripheral blood mononuclear cells in patients with HER2-positive metastatic breast cancer receiving single-agent trastuzumab. *Breast Cancer*. 2016;23(4):624-632.

87. Hurvitz SA, Betting DJ, Stern HM, et al. Analysis of Fcγ receptor IIIa and IIa polymorphisms: Lack of correlation with outcome in trastuzumab-treated breast cancer patients. *Clin Cancer Res*. 2012;18(12):3478-3486.

88. Mahaweni NM, Olieslagers TI, Rivas IO, Molenbroeck SJJ, Wieten L. A comprehensive overview of FCGR3A gene variability by full- length gene sequencing including the identification of V158F polymorphism. *Sci Rep*. 2018;8(15983):1-11.

89. Chong KT, Ho WF, Koo SH, Thompson P, Lee EJD. Distribution of the Fc γ RIIIa 176 F / V polymorphism amongst healthy Chinese , Malays and Asian Indians in

Singapore. *Br J Clin Pharmacol*. 2006;63(3):328-332.

90. Pol L van der, Jansen M, Sluiter W, et al. Evidence for non-random distribution of FcG receptor genotype combinations. *Immunogenetics*. 2003;55:240-246.

91. Garrido F, Ruiz-cabello F, Cabrera T, et al. Implications for immunosurveillance of altered HLA class I phenotypes in human tumours. *Immunol Today*. 1997;18(2):89-95.

92. Sottile R, Pangigadde PN, Tan T, et al. HLA class I downregulation is associated with enhanced NK-cell killing of melanoma cells with acquired drug resistance to BRAF inhibitors. *Eur J Immunol*. 2016;46:409-419.

93. Coca S, Perez-Piqueras J, Martinez D, et al. The prognostic significance of intratumoral natural killer cells in patients with colerectal carcinoma. *Cancer*. 1997;79(12):2320-2328.

94. Natsugoe S, Tokuda K, Nakajo A, et al. Prognostic Value of Intratumoral Natural Killer Cells in Gastric Carcinoma. *Cancer*. 2000;88(3):577-583.

95. Jonker DJ, O CJ, Karapetis CS, et al. Cetuximab for the Treatment of Colorectal Cancer. *N Engl J Med*. 2007;357:2040-2048.

96. Remenar E, Kawecki A, Ph D, et al. Platinum-Based Chemotherapy plus Cetuximab in Head and Neck Cancer. 2008:1116-1127.

97. Vivier E, Raulet DH, Moretta A, et al. Innate or Adaptive Immunity ? The Example of Natural Killer Cells. *Science (80-)*. 2011;331(January):44-50.

98. Sun JC, Beilke JN, Lanier LL. Adaptive immune features of natural killer cells. *Nature*. 2009;457(7229):557-561.

99. Park S, Jiang Z, Mortenson ED, et al. The Therapeutic Effect of Anti-HER2 / neu Antibody Depends on Both Innate and Adaptive Immunity. *Cancer Cell*. 2010;18(2):160-170.

100. Yonesaka K, Zejnullahu K, Okamoto I, et al. Activation of ERBB2 Signaling Causes Resistance to the EGFR-Directed Therapeutic Antibody Cetuximab. *Sci Transl Med*. 2011;3(99):1-11.

101. Uslu R, Borsellino N, Frost P, et al. Chemosensitization of Human Cytotoxicity Prostate and Carcinoma Cell. *Clin Cancer Res*. 1997;3(June):963-972.

102. Demarest SJ, Hariharan K, Dong J, Demarest SJ, Hariharan K, Dong J. Emerging antibody combinations in oncology a. *MAbs*. 2011;34:338-351.

103. Blasius AL, Beutler B. Intracellular Toll-like Receptors. *Immunity*. 2010;32(3):305-315.

104. Kanzler H, Barrat FJ, Hessel EM, Coffman RL. Therapeutic targeting of innate immunity with Toll-like receptor agonists and antagonists. *Nat Med*. 2007;13(5):552-559.

105. Kim H, Niu L, Larson P, et al. Polymeric nanoparticles encapsulating novel TLR7/8 agonists as immunostimulatory adjuvants for enhanced cancer immunotherapy. *Biomaterials*. 2018;164:38-53.

106. Cheadle EJ, Lipowska-Bhalla G, Dovedi SJ, et al. A TLR7 agonist enhances the antitumor efficacy of obinutuzumab in murine lymphoma models via NK cells and CD4 T cells. *Leukemia*. 2017;31(7):1611-1621.

107. Lu H, Dietsch GN, Matthews MAH, et al. VTX-2337 is a novel TLR8 agonist that

activates NK cells and augments ADCC. *Clin Cancer Res*. 2012;18(2):499-509.

108. Lu H, Yang Y, Gad E, et al. TLR2 Agonist PSK Activates Human NK Cells and Enhances the Antitumor Effect of HER2-Targeted Monoclonal Antibody Therapy. *Clin Cancer Res*. 2011;17(21):6742-6753.
109. American Cancer Society. Cancer facts and figures. 2019.
110. American Cancer Society. Breast Cancer Facts Figures. *Breast Cancer Facts Fig 2017-2018*.:1-44.
111. Weinberg R. The Biology of Cancer. *Yale J Biol Med*. 2007;80(2):91.
112. Mani SA, Guo W, Liao MJ, et al. The Epithelial-Mesenchymal Transition Generates Cells with Properties of Stem Cells. *Cell*. 2008;133(4):704-715.
113. Kalscheuer S. Humanized antibody development using phage display:Applications to solid tumor metastasis. *UMN Conserv*. 2016;(July).
114. Datta MW, Hernandez AM, Schlicht MJ, et al. Perlecan, a candidate gene for the CAPB locus, regulates prostate cancer cell growth via the Sonic Hedgehog pathway. *Mol Cancer*. 2006;5:1-15.
115. Savorè C, Zhang C, Muir C, et al. Perlecan knockdown in metastatic prostate cancer cells reduces heparin-binding growth factor responses in vitro and tumor growth in vivo. *Clin Exp Metastasis*. 2005;22(5):377-390.
116. Kazanskaya GM, Tsidulko AY, Volkov AM, et al. Heparan sulfate accumulation and perlecan/HSPG2 up-regulation in tumour tissue predict low relapse-free survival for patients with glioblastoma. *Histochem Cell Biol*. 2018;0(0):1-10.
117. Sharma B, Handler M, Eichstetter I, Whitelock JM, Nugent MA, Iozzo R V.

Antisense targeting of perlecan blocks tumor growth and angiogenesis in vivo. *J Clin Invest*. 1998;102(8):1599-1608.

118. Hu H, Li S, Cui X, et al. The overexpression of hypomethylated miR-663 induces chemotherapy resistance in human breast cancer cells by targeting heparin sulfate proteoglycan 2 (HSPG2). *J Biol Chem*. 2013;288(16):10973-10985.
119. Gomes AM, Stelling MP, Pavão MSG. Heparan sulfate and heparanase as modulators of breast cancer progression. *Biomed Res Int*. 2013;2013.
120. Guelstein VI, Tchypysheva TA, Ermilova VD, Ljubimov A V. Myoepithelial and basement membrane antigens in benign and malignant human breast tumors. *Int J Cancer*. 1993;53(2):269-277.
121. Lehmann BDB, Bauer J a J, Chen X, et al. Identification of human triple-negative breast cancer subtypes and preclinical models for selection of targeted therapies. *J Clin Invest*. 2011;121(7):2750-2767.
122. Jiang G, Zhang S, Yazdanparast A, et al. Comprehensive comparison of molecular portraits between cell lines and tumors in breast cancer. *BMC Genomics*. 2016;17(Suppl 7):281-325.
123. Luo X, Mitra D, Sullivan RJ, et al. Report Isolation and Molecular Characterization of Circulating Melanoma Cells. *CELREP*. 2014;7(3):645-653.
124. Corkery B, Crown J, Clynes M, O'Donovan N. Epidermal growth factor receptor as a potential therapeutic target in triple-negative breast cancer. *Ann Oncol*. 2009;20(5):862-867.
125. Carey LA, Rugo HS, Marcom PK, et al. TBCRC 001: Randomized phase II study

of cetuximab in combination with carboplatin in stage IV triple-negative breast cancer. *J Clin Oncol*. 2012;30(21):2615-2623.

126. Ferraro DA, Gaborit N, Maron R, et al. Inhibition of triple-negative breast cancer models by combinations of antibodies to EGFR. *Proc Natl Acad Sci*. 2013;110(5):1815-1820.

127. Celgene. Abraxane Package Insert. 2018:1-23.

128. Untch M, Jackisch C, Schneeweiss A, et al. Nab-paclitaxel versus solvent-based paclitaxel in neoadjuvant chemotherapy for early breast cancer (GeparSepto-GBG 69): a randomised, phase 3 trial. *Lancet Oncol*. 2016;17(3):345-356.

129. Mego M, Mani SA, Lee B-N, et al. Expression of epithelial-mesenchymal transition-inducing transcription factors in primary breast cancer: The effect of neoadjuvant therapy. *Int J cancer*. 2012;130(4):808-816.

130. Raimondi C, Gradilone A, Naso G, et al. Epithelial-mesenchymal transition and stemness features in circulating tumor cells from breast cancer patients. *Breast Cancer Res Treat*. 2011;130(2):449-455.

131. Higgins MJ, Baselga J, Higgins MJ, Baselga J. Targeted therapies for breast cancer. *J Clin Invest*. 2011;121(10):3797-3803.

132. Perez EA, Romond EH, Suman VJ, et al. Trastuzumab plus adjuvant chemotherapy for human epidermal growth factor receptor 2-positive breast cancer: planned joint analysis of overall survival from NSABP B-31 and NCCTG N9831. *J Clin Oncol*. 2014;32(33):3744-3752.

133. Lee A, Djamgoz MBA. Triple negative breast cancer : Emerging therapeutic

modalities and novel combination therapies. *Cancer Treat Rev*. 2018;62:110-122.

134. Olsen BR. Life without perlecan has its problems. *J Cell Biol*. 1999;147(5):909-911.

135. Aviezer D, Hecht D, Safran M, Eisinger M, David G, Yayon A. Perlecan, basal lamina proteoglycan, promotes basic fibroblast growth factor-receptor binding, mitogenesis, and angiogenesis. *Cell*. 1994;79(6):1005-1013.

136. Corkery B, Crown J, Clynes M, O'Donovan N. Epidermal growth factor receptor as a potential therapeutic target in triple-negative breast cancer. *Ann Oncol*. 2009;20(5):862-867.

137. Nakai K, Hung MC, Yamaguchi H. A perspective on anti-EGFR therapies targeting triple-negative breast cancer. *Am J Cancer Res*. 2016;6(8):1609-1623.

138. Zoeller JJ, Whitelock JM, Iozzo R V. Perlecan regulates developmental angiogenesis by modulating the VEGF-VEGFR2 axis. *Matrix Biol*. 2009;28(5):284-291.

139. Ishiharasb M, Tyrrells DJ, Stauberll GB, et al. Preparation of Affinity-fractionated , Heparin-derived Oligosaccharides and Their Effects on Selected Biological Activities Mediated by Basic Fibroblast Growth Factor *. *J Biol Chem*. 1993;268(7):4675-4683.

140. Cohen IR, Murdoch AD, Naso MF, et al. Abnormal Expression of Perlecan Proteoglycan in Metastatic Melanomas Advances in Brief Abnormal Expression of Perlecan Proteoglycan in Metastatic Melanomas1. 1994;(5):5771-5774.

141. Steinhauser I, Spänkuch B, Strebhardt K, Langer K. Trastuzumab-modified

nanoparticles: Optimisation of preparation and uptake in cancer cells. *Biomaterials*. 2006;27(28):4975-4983.

142. Swaminathan SK, Roger E, Toti U, Niu L, Ohlfest JR, Panyam J. CD133-targeted paclitaxel delivery inhibits local tumor recurrence in amousemodel of breast cancer. *J Control Release*. 2013;171(3):280-287.

143. Khanna V, Kalscheuer S, Kirtane A, Zhang W. Perlecan-targeted nanoparticles for drug delivery to triple-negative breast cancer. *Futur Drug Disovery*. 2019.

144. Swaminathan SK, Roger E, Toti U, Niu L, Ohlfest JR, Panyam J. CD133-targeted paclitaxel delivery inhibits local tumor recurrence in a mouse model of breast cancer. *J Control Release*. 2013;171(3):280-287.

145. Overdijk MB, Verploegen S, Ortiz Buijsse A, et al. Crosstalk between human IgG isotypes and murine effector cells. *J Immunol*. 2012;189(7):3430-3438.

146. Shultz LD, Lyons BL, Burzenski LM, et al. Human lymphoid and myeloid cell development in NOD/LtSz-scid IL2R gamma null mice engrafted with mobilized human hemopoietic stem cells. *J Immunol*. 2005;174(10):6477-6489.

147. Li C, Iida M, Dunn EF, Ghia AJ, Wheeler DL. Nuclear EGFR contributes to acquired resistance to cetuximab. *Oncogene*. 2009;28:3801-3813.

148. Manches O, Lui G, Chaperot L, et al. In vitro mechanisms of action of rituximab on primary non-Hodgkin lymphomas. *Immunobiology*. 2003;101(3):949-954.

149. Toma A, Otsuji E, Kuriu Y, et al. Monoclonal antibody A7-superparamagnetic iron oxide as contrast agent of MR imaging of rectal carcinoma. *Br J Cancer*. 2005;93(1):131-136.

150. Takashima H, Tsuji AB, Saga T, et al. Molecular imaging using an anti-human tissue factor monoclonal antibody in an orthotopic glioma xenograft model. *Sci Rep*. 2017;7(1):4-9.

151. Murakami M, Cabral H, Matsumoto Y, et al. Improving drug potency and efficacy by nanocarrier-mediated subcellular targeting. *Sci Transl Med*. 2011;3(64):1-11.

152. Bartlett DW, Su H, Hildebrandt IJ, Weber WA, Davis ME. Impact of tumor-specific targeting on the biodistribution and efficacy of siRNA nanoparticles measured by multimodality in vivo imaging Derek. *Proc Natl Acad Sci*. 2007;104(39):15549-15554.

153. Kirpotin DB, Drummond DC, Shao Y, et al. Antibody targeting of long-circulating lipidic nanoparticles does not increase tumor localization but does increase internalization in animal models. *Cancer Res*. 2006;66(13):6732-6740.

154. Liedtke C, Mazouni C, Hess KR, et al. Response to neoadjuvant therapy and long-term survival in patients with triple-negative breast cancer. *J Clin Oncol*. 2008;26(8):1275-1281.

155. Kim H. TLR7/8 agonist encapsulating polymeric nanoparticles for cancer immunotherapy. 2018;(October).

156. Larson P, Kucaba TA, Xiong Z, Olin M, Griffith TS, Ferguson DM. Design and Synthesis of N1-Modified Imidazoquinoline Agonists for Selective Activation of Toll-like Receptors 7 and 8. *ACS Med Chem Lett*. 2017;8(11):1148-1152.

157. Kim H, Khanna V, Kucaba TA, et al. Combination of Sunitinib and PD-L1 Blockade Enhances Anticancer Efficacy of TLR7/8 Agonist-Based Nanovaccine.

Mol Pharm. 2019.

158. Wendel M, Galani IE, Suri-Payer E, Cerwenka A. Natural killer cell accumulation in tumors is dependent on IFN-γ and CXCR3 ligands. *Cancer Res*. 2008;68(20):8437-8445.

159. Livak KJ, Schmittgen TD. Analysis of relative gene expression data using real-time quantitative PCR and the 2-ΔΔCT method. *Methods*. 2001;25(4):402-408.

160. Kurai J, Chikumi H, Hashimoto K, et al. Antibody-Dependent Cellular Cytotoxicity Mediated by Cetuximab against Lung Cancer Cell Lines. *Cancer Ther Preclin*. 2007;13(5):1552-1562.

161. Steiner P, Bassi R, Wang S, Tonra JR, Hadari YR, Hicklin DJ. Tumor Growth Inhibition with Cetuximab and Chemotherapy in Non - Small Cell Lung Cancer Xenografts Expressing Wild-type and Mutated Epidermal Growth Factor Receptor. *Cancer Ther Preclin*. 2007;13(5):1540-1552.

162. Kim H, Sehgal D, Kucaba TA, Ferguson DM, Griffith TS, Panyam J. Acidic pH-responsive polymer nanoparticles as a TLR7/8 agonist delivery platform for cancer immunotherapy. *Nanoscale*. 2018;10(44):20851-20862.

163. Kasai M, Yoneda T, Habut S, Maruyama Y, Tokunaga T. In vivo effect of anti-asialo GMl antibody on natural killer activity. *Nature*. 1981;291(May):334-335.

164. Wendel M, Galani IE, Suri-payer E, Cerwenka A. Natural Killer Cell Accumulation in Tumors Is Dependent on IFN-G and CXCR3 Ligands. *Cancer Res*. 2008;9(20):8437-8446.

165. Sun JC, Beilke JN, Lanier LL. Immune memory redefined: characterizing the

longevity of natural killer cells. *Immunol Rev*. 2010;236(July):83-94.

166. Cooper MA, Elliott JM, Keyel PA, Yang L, Carrero JA, Yokoyama WM. Cytokine-induced memory-like natural killer cells. *Proc Natl Acad Sci*. 2009;106(6):1915-1919.

167. Demaria S, Golden EB, Formenti SC. Role of Local Radiation Therapy in Cancer Immunotherapy. *JAMA Oncol*. 2015;1(9):1325-1332.

168. Villamor N, Colomer D. Mechanism of Action and Resistance to Monoclonal Antibody Therapy. *Semin Oncol*. 2003;30(4):424-433.

169. Iwasaki A, Medzhitov R. Toll-like receptor control of the adaptive immune responses. *Nat Immunol*. 2004;5(10):987-995.

170. Frenzel A, Schirrmann T, Hust M. Phage display-derived human antibodies in clinical development and therapy. *MAbs*. 2016;8(7):1177-1194.

171. Lee CMY, Iorno N, Sierro F, Christ D. Selection of human antibody fragments by phage display. *Nat Protoc*. 2007;2(11):3001-3008.

172. Loi S, Giobbie-hurder A, Gombos A, et al. Pembrolizumab plus trastuzumab in trastuzumab-resistant , advanced , HER2-positive breast cancer (PANACEA): a single-arm, multicentre, phase 1b – 2 trial. *Lancet Oncol*. 2019;20(March):371-382.

173. Bauml J, Seiwert TY, David GP, et al. Pembrolizumab for Platinum- and Cetuximab-Refractory Head and Neck Cancer : Results From a Single-Arm , Phase II Study. *J Clin Oncol*. 2017;35(14):1542-1549.